ENGINEERING BEHAVIOR OF LATERITIC SOIL-RECYCLED ASPHALT PAVEMENT (RAP) BLENDS IMPROVED BY CEMENT AS STONE COLUMN AGGREGATE

ANIROOT SUKSAN

A Thesis Submitted in Partial Fulfillment of the Requirements for
the Degree of Doctor of Philosophy in Civil, Transportation
and Geo-resources Engineering
Suranaree University of Technology
Academic Year 2023

พฤติกรรมทางวิศวกรรมของดินลูกรังผสมผิวทางแอสฟัลต์รีไซเคิลปรับปรุง ด้วยซีเมนต์เพื่อใช้เป็นมวลรวมของเสาหิน

นายอนิรุทธิ์ สุขแสน

วิทยานิพนธ์นี้เป็นส่วนหนึ่งของการศึกษาตามหลักสูตรปริญญาวิศวกรรมศาสตรดุษฎีบัณฑิต
สาขาวิชาวิศวกรรมโยธา ขนส่ง และทรัพยากรธรณี
มหาวิทยาลัยเทคโนโลยีสุรนารี
ปีการศึกษา 2566

ENGINEERING BEHAVIOR OF LATERITIC SOIL-RECYCLED ASPHALT PAVEMENT (RAP) BLENDS IMPROVED BY CEMENT AS STONE COLUMN AGGREGATE

Suranaree University of Technology has approved this thesis submitted in partial fulfillment of the requirements for the Degree of Doctor of Philosophy.

Thesis Examining Committee

(Prof. Dr. Panich Voottipruex)

Chairperson

(Prof. Dr. Suksun Horpibulsuk)

Member (Thesis Advisor)

(Prof. Dr. Avirut Chinkulkijniwat)

Member

(Assoc. Prof. Dr. Menglim Hoy)

Member

(Asst. Prof. Dr. Pornpot Tanseng)

Member

(Assoc. Prof. Dr. Yupaporn Ruksakulpiwat)

Vice Rector for Academic Affairs

and Quality Assurance

(Assoc. Prof. Dr. Pornsiri Jongkol)

Dean of Institute of Engineering

อนิรุทธิ์ สุขแสน : พฤติกรรมทางวิศวกรรมของดินลูกรังผสมผิวทางแอสฟัลต์รีไซเคิลปรับปรุงด้วยซีเมนต์เพื่อใช้เป็นมวลรวมของเสาหิน (ENGINEERING BEHAVIOR OF LATERITIC SOIL-RECYCLED ASPHALT PAVEMENT (RAP) BLENDS IMPROVED BY CEMENT AS STONE COLUMN AGGREGATE).
อาจารย์ที่ปรึกษา ศาสตราจารย์ ดร. สุขสันติ์ หอพิบูลสุข, 131 หน้า.

คำสำคัญ : ผิวทางแอสฟัลต์รีไซต์เคิล, ดินซีมนต์, เสาเข็มหิน, การทดสอบกำลังอัดสามแกน

วิทยานิพน์นี้ศึกษาความเป็นไปได้ในการนำผิวทางแอสฟัลต์รีเคิลผสมดินลูกรังปรับปรุงด้วยซีเมนต์ สำหรับใช้เป็นมวลลรวมของเสาเข็มหิน ความสำคัญและวัตถุประสงค์หลักของวิทยานิพนธ์นี้ได้นำเสนอไว้ในบทที่ 1 เทคนิคการปรับปรุงดินและสมบัติโดยทั่วไปของผิวทางแอสฟัลต์รรีไซเคิล รวมทั้งงานวิจัยในอดีตที่สำคัญและเกี่ยวข้องกับวิทยานินิพนธ์นี้ ได้รวบรวมไว้ในบทที่ 2

พฤติกรรมแบบไม่ระบายน้ำของผิวทางแอสฟัลต์รีไซเคิลผสมดินลูกรังปรับปรุงด้วยซีเมนต์ที่ได้รับผลกระทบจากปริมาณผิวทางแอสฟัลต์รีไซเคิลและปริมาณซีเมนต์ต่อพฤติกรรมทางวิศวกรรมได้นำเสนอในบทที่ 3 ดินลูกรังถูกแทนที่ด้วยผิวทางแอสฟัลต์รีไซเคิลที่อัตราส่วน 10% และ 30% และ 50% ผสมกับปอร์ตแลนด์ซีเมนต์ประเภทที่ 1 ที่ปริมาณ 1% และ 3% ปริมาณผิวทางแอสฟัลต์รีไซเคิลที่เพิ่มขึ้นทำให้หน่วยน้ำหนักสูงขึ้น และช่วยให้การเสียรูปในหนึ่งมิติลดลง ความเค้นเบี่ยงเบนไม่ระบายน้ำของตัวอย่างทดสอบเพิ่มขึ้นเมื่อปริมาณผิวทางแอสฟัลต์รีไซต์เคิลและปริมาณซีเมนต์เพิ่มขึ้น ความสัมพันธ์ระหว่างความเค้นและความเครียดแสดงให้เห็นถึงการตอบสนองแบบวัสดุเปราะเมื่อปริมาณซีเมนต์เพิ่มขึ้น นอกจากนี้ความดันน้ำส่วนเกินมีค่าลดลงจนมีค่าเป็นลบเมื่อปริมาณซีเมนต์มีค่าเพิ่มขึ้น ปริมาณผิวทางแอสฟัลต์รีไซเคิลที่เพิ่มขึ้นทำให้กำลังต้านทานนแรงเฉือนของดินผสมซีเมนต์เกิดขึ้นที่ความเครียดสูงขึ้น ความแกร่งของดินลูกรังที่ไม่ปรับปรุงด้วยซีเมนต์มีค่าเพิ่มขึ้นตามปริมาณผิวทางแอสฟัลต์รีไซเคิลต์ ในทางตรงกันข้ามความแกร่งมีค่าลดลงตามปริมาณผิวทางแอสฟัลต์สำหรับตัวอย่างที่ปรับปรุงด้วยซีเมนต์

บทที่ 4 นำเสนอพฤติกรรมต้านทานแรงเฉือนในสภาวะระบายน้ำของผิวทางแอสฟัลต์ผสมดินลูกรัง เงื่อนไขตัวอย่างทดสอบคล้ายกับตัวอย่างที่ทำการทดสอบโดยวิธีไม่ระบายน้ำ การทดสอบกำลังอัดสามแกนดำเนินการด้วยอัตราการเฉือนที่ช้าจนไม่เกิดความดันน้ำส่วนเกิน กำลังต้านทานแรงเฉือนในสภาวะระบายน้ำของตัวอย่างทดสอบมีค่าสูงขึ้นตามปริมาณผิวทางแอสฟัลต์รีไซเคิลและซีเมนต์

เช่นเดียวกับผลที่ได้จากการทดสอบแบบไม่ระบายน้ำ การตอบสนองแบบวัสดุเปราะสำหรับตัวอย่างที่ปรับปรุงด้วยซีเมนต์สังเกตเห็นได้จากความสัมพันธ์ระหว่างความเค้นและความเครียด โดยเห็นได้อย่างชัดเจนเมื่อปริมาณซีเมนต์มีค่าสูง ในขณะเดียวกันเมื่อปริมาณผิวทางแอสฟัลต์รีไซเคิลเพิ่มขึ้น ดัชนีความเปราะมีค่าลดลง ปริมาณผิวทางแอสฟัลต์ที่เกินกว่าค่าเหมาะสมเป็นสาเหตุทำให้แรงยึดเหนี่ยวลดลงและทำให้กำลังต้านทานแรงเฉือนมีค่าลดลง ความสัมพันธ์ระหว่างความเครียดและการขยายตัวของผิวทางแอสฟัลต์รีไซเคิลผสมดินลูกรังมีลักษณะเช่นเดียวกับดินเม็ดหยาบทั่วไป สมการความสัมพันธ์ระหว่างความเค้นและอัตราการขยายตัวที่นำเสนอโดย Rowe สามารถทำนายอัตราส่วนความเค้นสูงสุดของตัวอย่างแบบปรับปรุงและไม่ปรับปรุงด้วยซีเมนต์ได้แม่นยำ

ผลการทดสอบกำลังแบกทานของชั้นดินเหนียวอ่อนเสริมแรงด้วยเสาเข็มหินผิวทางแอสฟัลต์รีไซเคิลผสมดินลูกรังปรับปรุงด้วยซีเมนต์นำเสนอในบทที่ 5 แบบจำลองเสาเข็มหินเดี่ยวชนิดแบกทานที่ปลายเข็มถูกติดตั้ง ณ ตำแหน่งกึ่งกลางแบบจำลองชั้นดินเหนียวอ่อนในท่อ PVC ผิวทางแอสฟัลต์รีไซเคิลแทนที่ดินลูกรังที่อัตราส่วนคงที่ 30% เสาเข็มหินผิวทางแอสฟัลต์รีไซเคิลผสมดินลูกรังถูกปรับปรุงด้วยปอร์ตแลนด์ซีเมนต์ที่ 1% และ 3% ความสัมพันธ์ระหว่างความเค้นแบกทานและการทรุดตัวของชั้นดินเหนียวที่เสริมแรงด้วยเสาเข็มหินปรับปรุงด้วยซีเมนต์แสดงให้เห็นถึงการลดลงของกำลังแบกทาน หลังจากพัฒนากำลังไปจนถึงสูงสุด ซึ่งเป็นผลมาจากเสียหายของพันธะเชื่อมประสานจากซีเมนต์ กำลังแบกทานสูงสุดของขั้นดินเหนียวอ่อนขึ้นอยู่กับกำลังอัดแกนเดียวของวัสดุเสาเข็มหินอย่างมีนัยสำคัญ และสามารถทำนายได้โดยสมการที่นำเสนอในงานวิจัยนี้

สาขาวิชา วิศวกรรมโยธา
ปีการศึกษา 2566

ลายมือชื่อนักศึกษา
ลายมือชื่ออาจารย์ที่ปรึกษา

ANIROOT SUKSAN : ENGINEERING BEHAVIOR OF LATERITIC SOIL-RECYCLED ASPHALT PAVEMENT (RAP) BLENDS IMPROVED BY CEMENT AS STONE COLUMN AGGREGATE.

THESIS ADVISOR : PROFESSOR SUKSUN HORPIBULSUK, Ph.D., 131 PP.

Keywords: Recycled Asphalt Pavement/RAP/cement stabilized/lateritic soil/triaxial compression test.

This thesis study investigated the feasibility of Recycled Asphalt Pavement (RAP)-Lateritic soil blends improved by cement as a stone column aggregate. The state of the problems and the main objectives of this study are provided in Chapter 1. The background of the stone column technique, the typical basic properties of RAP and essential literature reviews of previous research relevant to this study are detailed in Chapter 2.

The undrained shear behavior of RAP-soil blends improved by cement is presented in Chapter 3. The RAP replaced the lateritic soil at 10%, 30%, and 50% by dry weight. The Portland cement at 1% and 3% were used to stabilize RAP-soil blends. The compaction tests were performed to determine the compaction characteristic and compressibility of RAP-soil blends. The consolidated undrained triaxial tests were performed at confining pressures of 50, 100, and 200 kPa which are associated with the in-situ effective pressure of the stone column. The result showed that the strength of RAP-soil blends increased with RAP replacement ratio and cement content. The strength improvement indicated the strength of RAP-soil blends of cement stabilized specimens is mobilized at large strain due to the compressibility of RAP. The stiffness of unstabilized RAP-soil blends increased the RAP replacement ratio. On the other hand, the compressible asphalt binder coating surrounding the surface is attributed to the significantly decreased stiffness of cement stabilized RAP-soil blends.

Chapter 4 presents the drained shear response of RAP-soil blends. The consolidated drained triaxial compression tests were performed in the RAP-soil blends at the same specimen condition as the consolidated undrained triaxial compression test. The slow rate of shearing was carried out to allow the water to drain out while the confining pressure was maintained constant. The result indicated that the shear strength of RAP-soil blends increased when RAP replacement ratio and cement content increased similar to that found in the undrained condition. Higher RAP replacement ratio and cement contents caused the denser packing of the blends and increased cohesion resulting in higher shear strength. The excess RAP replacement ratio decreased shear strength due to the cohesion decrease. The stress-dilatancy of RAP-soil blends exhibited similar to those of natural granular soil. The Rowe's stress-dilatancy can model the maximum dilatancy of unstabilized and stabilized RAP-soil blends.

The load-settlement relationship of soft clay reinforced by compacted RAP-soil stone column is presented in Chapter 5. The isolated end-bearing type of compacted stone column was installed at the center soil model. The soft clay layer was prepared identically in PVC mold while the stone column contained various cement contents. The lateritic soil was replaced by RAP at 30% by dry weight. The load-settlement response of the composite ground reinforced by the cement stabilized column showed peak bearing strength before dropping to a lower value due to the destruction of cementation. The load-bearing capacity highly depended upon the unconfined compressive strength of the stone column and was predicted satisfactorily by the proposed equation.

School of Civil Engineering Student's Signature........

Academic Year 2023 Advisor's Signature........

ACKNOWLEDGMENT

I would like to express my deep gratitude to Professor Dr. Suksun Horpibulsuk, my research advisor for his worth guidance, endless encouragement, kindness, enthusiasm, and useful suggestion throughout my study.

I wish to thank Assistant Professor Dr. Pornpot Tangseng and Professor Dr. Avirut Chinkulkijniwat for their useful lectures on Geotechnical Engineering. I would also like to thank other lecturers at the School of Civil Engineering, Suranaree University of Technology for their useful and contractive recommendation.

I would like to thank Associate Professor Dr. Jirayut Suebsuk and the Department of Civil Engineering, Rajamangkala University of Technology Isan for their support in the equipment testing.

My grateful thanks are also extended to my friend Mrs. Suphapit Jungkonklang and all staff members of the School of Civil Engineering for their assistance.

Finally, I wish to thank my parents for their encouragement, perspective, and support throughout my study.

ANIROOT SUKSAN

TABLE OF CONTENTS

TABLE OF CONTENTS (CONTINUED)

LIST OF TABLES

LIST OF FIGURES

LIST OF FIGURES (CONTINUED)

Figure **Page**

LIST OF FIGURES (CONTINUED)

Figure **Page**

LIST OF ABBREVIATIONS

ACV	Aggregate Crushing Value
AIV	Aggregate Impact Value
AASHTO	American Association of State Highway and Transportation Officials
AS	Asphalt Binder Content
BAC	Bottom Ash Column
C&D	Construction and demolition
CB	Crushed Brick
CBR	California Bearing Ratio
CC	Recycled Crushed Concrete
CR	Crushed Rock
FDR	Full-Depth Reclamation
DGABC	Dense-Grade Aggregate Base Course
MDD	Maximum dry density
LL	Liquid limit
MSE	Mechanically Stabilized Earth
OCR	Over-consolidation Ratio
OMC	Optimum moisture content
PI	Plasticity Index
PL	Plastic Limit
QA	Quality Assurance
RAP	Recycled asphalt pavement
RCA	Recycled Concrete Aggregate
SRB	Spent railway track ballast
SEM	Scanning Electro Microscopic

LIST OF ABBREVIATIONS (CONTINUED)

UCS	Unconfined Compressive Strength
USCS	Unified Soil Classification System
XRD	X-ray diffraction
XRF	X-ray fluorescence

CHAPTER I

INTRODUCTION

1.1 Statement of the problems

The stone column inclusion is a ground improvement technique to improve the engineering performance of impermissible ground layer. The partial functions of the stone column are densifying and strengthening the ground. The stone column is also used to accelerate the consolidation. There are many installation methods for stone columns provided for various ground conditions. All of these installation methods form unbound backfill aggregate into columns by densification.

The load capacity of the ground reinforced by the stone column depends on backfill performance and confining stress surrounding the soil (Han, 2015). The selected backfill aggregate should be clean, hard, and uncontaminated with organic and toxic matter (Elias et al., 2004). Typically, the conventional stone quarry has been selected for stone column backfill. For the past decade, due to the environmental impact and sustainability, engineers and researchers are encouraged to seek for alternative materials such as recycled, solid waste, and industrial by-products to the conventional stone backfill. Crushed concrete, steel slag, artificial cemented soil, and other waste materials were investigated to demonstrate their potential as stone column backfill (Juran & Riccobono, 1991; MacKay; Shahverdi & Haddad, 2019; Zukri & Nazir, 2018).

Installing stone columns in very soft ground (undrained shear strength < 15 kPa) is inapplicable due to the lack of bonding of aggregate and low strength of surrounding soil, causing bugling failure (Han, 2015). Stabilized aggregate with chemical agent has been considered to solve this problem.

Several researchers proposed the stabilization of fill aggregate to increase their cohesion and extended their potential to withstand bugling failure when installing in the soft ground (Y. S. Golait & Padade, 2017; Y.S. Golait, Satyanarayana, & Raju, 2009; Juran & Riccobono, 1991; Zhou, Yin, & Ming, 2002).

Recycled Asphalt Pavement (RAP) is one of by-product materials form rehabilitation and demolition of asphalt pavement. RAP is composed of aggregate and binder coating surround surface (Chesner, Collins, & MacKay, 2008). RAP increasing annually side by side pavement construction activity. The large quantity of solid volume of RAP required the large area to disposal. Following the last surveying reported in 2018 by National Asphalt Pavement Association (2019) amount of RAP 82.1 million tons in U.S.A. was reused in the new pavement which it is nearly increase 46.8 % increase form 2009. The remaining RAP approximately 3% or 6.4 million tons was used in other applications such as aggregate or backfill. RAP also has been successfully reused in highway and pavement applications (Bennert, Papp, Maher, & Gucunski, 2000). Utilization of RAP in highway work in particular base course achieved by blending with conventional aggregate (i.e., crushed rock, lateritic soil) in properly fraction to replace volume of raw material (Taha, Al-Harthy, Al-shamsi, & Al-Zubeidi, 2002). RAP can also improve the properties of marginal soil to meet standard specification for stabilized base course (Suebsuk et al., 2017). RAP/lateritic soil blends improved by cement provided the satisfy result for using in the highway application (Guthrie, Cooley, & Eggett, 2007; Suebsuk, Suksan, & Horpibulsuk. S., 2014; Taha et al., 2002). Beside the highway and applications, RAP can be used as stone column backfill due to its strength, stiffness and permeability when compare to soft clay.

Thus, this thesis investigates the shear response and shear strength of RAP/lateritic soil blend, which are a vital information required for the composite clay ground. Triaxial compression tests were conducted on the cement stabilized RAP/lateritic soil blends at various RAP contents from 0-50% and Portland cement contents from 1-3%. The soft clay improve by stone column were modeled to investigate load-settlement behavior.

1.2 Research object and scope

1.2.1 To investigate undrained shear behavior of lateritic soil/ RAP blend improved by cement.

1.2.2 To investigate drained shear behavior of lateritic soil/ RAP improved by cement.

1.2.3 To study bearing capacity of soft clay improved by stone column made by soil/RAP aggregate.

1.3 Organization of the dissertation

The six chapters incorporated in this thesis including as follow:

Chapter 1 presents the introduction, object of the study and organization of the thesis.

Chapter 2 present the literature review of recent research and study of utilization of recycled material for stone column, the engineering characteristic of recycled asphalt pavement and the utilization of RAP in civil engineering works.

Chapter 3 presents the investigation of the undrained behavior of lateritic soil improved by recycled asphalt pavement and cement under consolided undrained triaxial test. The basic properties of lateritic soil and recycled asphalt pavement, compaction and compressibility characteristics are presented. The effect of cement and RAP replacement ratio on the strength and stiffness of the samples are discussed in this chapter.

Chapter 4 presents the drained shear response of lateritic soil/RAP improved by cement. The result of consolidated drained triaxial test is presented in this chapter. The effect of effective confining pressure, cement level and RAP replacement ratio were discussed in this chapter.

Chapter 5 presents investigation results of modeled stone column made of compacted lateritic soil/RAP improved by cement. The soft clay improved by stone column were modeled to investigate load-settlement behavior.

Chapter 6 conclude the present work in this thesis and suggests topic for further study.

CHAPTER II

LITERATURE REVIEW

2.1 Introduction

This chapter presents the literature review of alternative materials used for stone column aggregate. This chapter is divided into three main parts. Firstly, the literature review deals with the recent construction technology of stone columns. Many installations of stone column methods are available for various soil conditions. Installing stone columns in very soft clay is challenging due to soil stability and the duration of a composite foundation made from the unbound granular aggregate.

The second part focuses on the recycled materials from construction or demolition activity to aggregate stone columns. The environmental impact and the lack of natural resources are the main reasons engineers and researchers seek alternative materials. Recycled materials are used to replace raw materials.

Typically, stabilization with a chemical agent produces the cementation bond and is a traditional technique to improve the soil which can be expected to strengthen aggregate quickly. Thus, the final part of this chapter presents the literature review of the engineering behavior of cement or chemically stabilized aggregate.

2.2 Stone column

The stone column is a ground improvement technique for stabilizing the improper soil layer for construction. Stone columns are widely used to stabilize soft soil by increasing bearing capacity, mitigating differential settlement, and accelerating consolidation. Generally, the stone columns support embankments or other shallow foundations of superstructure construction in soft ground.

The installations of stone columns carry out by forming the columnar densified unbound aggregate into the ground. There is a great number of installation methods for stone columns which depend on the available equipment, suit condition, and cost. The installations of the stone column can be divided into two categories as follow: 1) the excavation method, which aims to make the hole into the soil by injecting water or drilling 2) the aggregate replacement method, which can be done by diving the steel casing into the ground or diving reverse flight auger to make the hole. The various type of installation of the stone column is illustrated in Figure 2.1. The densification of the stone column aggregate can be carried out by deep compaction in many ways. Since the column is formed by densification, the strength and stiffness of fill materials are higher than surrounding soil. As a result, their load capacity depends on the strength of compacted fill performance and the level of confining pressure (Han, 2015). Several installation methods of stone columns provide for various soil conditions. The proper undrained shear strength of the ground stabilized by the stone column range from 15-60 kPa.

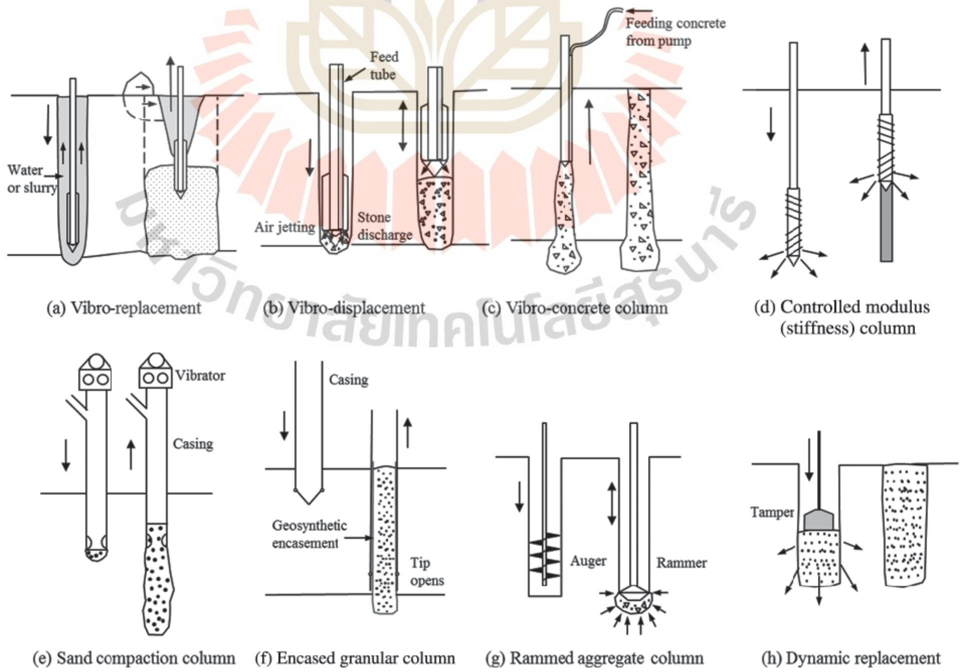

Figure 2.1 Various installation methods of stone column (Han, 2015)

2.2.1 Stone columns backfill

The selected aggregate used for stone column backfill should be hard, clean, and uncontaminated with toxic suggested by Barksdale and Bachus (1983). Brown (1977) proposed the index indicating the suitability of aggregate in use for vibro-stone columns. The index that defined as follows.

$$S_N = \sqrt{\frac{3}{(D_{50})^2} + \frac{1}{(D_{20})^2} + \frac{1}{(D_{10})^2}} \quad (2.1)$$

where D_{50}, D_{20} and D_{10} are the particle size of 50%, 20% and 10% passing respectively.

Table 2.1 Suitability of backfill for stone column (Brown, 1977)

Suitability number, S_N	0-10	10-20	20-30	30-40	>50
Rating	Excellent	Good	Fair	Poor	Unsuitable

Building Researched Establishment (BRE., 2000) standard suggested aggregate index tests of vibro-stone columns, including aggregate crushing value (ACV) and aggregate impact value (AIV) for the evaluation of aggregates in stone columns. The AIV gives a relative measure of the resistance of an aggregate to a sudden shock or impact, and the ACV provides comparable measure of the resistance of an aggregate to crushing under a gradually applied load. Both tests can be obtained as follows:

$$\text{AIV or ACV} = \frac{M2}{M1} \times 100 \quad (2.2)$$

where *M1* is the mass of the test specimen, and M2 is the mass of the material after testing passing the 2.36 mm sieve. The standard recommends that a maximum AIV or ACV does not exceed 30% for the materials of stone columns in the UK.

2.2.2 Alternative aggregate for stone column backfills

The previous studies of using recycled aggregate as stone column backfill can be categorized into two manners: 1) the potential of the material and 2) the behavior of the stone column (Shahverdi & Haddad, 2019). Regarding materials performance, the strength of the materials was evaluated through the comprehensive laboratories that investigated stone column backfill. Meanwhile, the model test was performed to examine the behavior of the ground improved by stone columns made of recycled aggregate.

Juran and Riccobono (1991) reported the result of an experimental on study load -settlement response of artificial cemented compacted-sand column. The cohesive soft soil was reinforced by cemented compacted-sand columns isolated and a group of column patterns. Triaxial compression tests were performed to investigate the load-settlement and load-bearing capacity behavior of composite reinforced soil samples and unreinforced samples. The result shows that intergranular cementation increases column's stiffness with cement. The load-bearing capacity of composite clay reinforced by cemented columns increased the cement level. The low level of cement caused the composite clay to exhibit a brittle response. When cementation completely deteriorates, a rapid decrease in shear resistance can be observed. The ultimate state of composite clay approached the shear resistance of untreated clay. Using low cement levels can be extended the range of using sand columns.

The vibro-stone column has used primary quarried aggregate, but in recent years recycled materials have been considered as an alternative due to the developments in sustainable practice; recycled materials can be classified as Recycled

Aggregate (RA) from the processing of waste construction materials or Secondary Aggregates (SA) from by-products of industrial processes. These aggregates have been used historically in lower-grade applications, which require low levels of specification (e.g. grading, strength or leachate potential). However, after processing, recycled aggregate materials could be utilized for higher-grade applications with more stringent requirements, e.g., vibro-stone columns (Tranter et al., 2008). Serridge (2005) considers that these crushed concretes and recycled (spent) railway ballast offer the greatest potential for use in vibro-stone columns.

Crushed Concrete is the material by processing construction and demolition. Due to the source material's variable historical nature of the source material various contaminants may exist and need to be removed, as these control aggregate properties. Mckelvey et al. (2002) and Steels (2004) performed a large direct shear test on crushed concrete. The internal friction angle ranges from 35° to 42°, tested in a large direct shear box under normal stresses of between 60 kPa to 300 kPa. The result indicated that these materials meet the requirement for use in the Vibro-stone column (Serridge, 2005).

Mckelvey et al. (2002) also investigated the effects of fines content on the performance of the vibro-stone column. The observation showed a dramatically decreased friction angle when kaolin slurry was present. They further showed that this would result in a potential increase in settlements of some 30%, which were too high for most applications. In addition, McKelvey et al. (2002) further observed that the shearing behavior of crushed concrete changed as vertical stress increased, changing from a dilatant to a compression material in shear, corresponding to an increased fine content with stress. This indicates that a minimal number of compaction passes should be used to control fines and reduce the impact on the overall field performance of the Vibro-stone column made from crushed concrete. In addition, certain restrictions with the soil type to be treated should be observed, where soils high in sulfates or from organic/acidic environments should be avoided due to deleterious effects.

Crushed concrete has been used successfully on a post-industrial site (made up of ash, slag, and brick) to mitigate the need to import primary aggregate (Serridge, 2005). This was achieved with careful monitoring with the resulting settlement reductions being well within specified limits.

Spent railway track ballast (SRB) is a high-quality aggregate (typically granite or limestone) taken from beneath railway tracks when excessive fines occur after continued attrition under repeated railway carriage loads. In addition, a suite of contaminants (hydrocarbon) is also contained within the aggregate matrix, so these often require solvent cleaning. Thus, a grading suitable for vibro-stone column specifications can be met with careful cleaning and screening. Serridge (2005) reported a friction angle of SRB excess of 43° when SRB aggregate was used for a vibro-stone column on an old derelict industrial site in the West Midlands of England. Unfortunately, no details of costing were given. Values of friction angle were obtained as part of a detailed quality assurance testing program. On completion, vibro-stone column SC using SRB proved very effective, achieving settlements of less than 10 mm when tested. The reports also showed that SRB's successful use on other UK sites provides a sustainable solution.

A wide variety of SA is available in vibro-stone columns, including slags and rock waste. SA can often be weaker than RA and thus have greater potential for a breakdown during vibro-stone column installation. Serridge (2005) considered that given SA's potential for breakage, especially underwater, a greater number of vibro-stone columns would be required to achieve satisfactory result. However, inconsistency of supply, stability and general fitness for use in the take-up of SA in vibro-stone column applications.

The model test of stone columns installed in soft clay made of recycled aggregate can be done by static load test. Differences between recycled and by-product aggregate were compared to their behavior. Shahverdi and Haddad (2019) reported performance of floating stone columns constructed of recycled aggregates from demolition waste. A single stone column with three types of materials, including recycled crushed brick (CB), recycled crushed concrete (CC) and gravel as natural aggregates was modeled. Aggregate index tests evaluated the quality of the recycled aggregates used were carried out according to Building Research Establishment BRE. (2000). The crushing and impact value test results have demonstrated that gravel and CC can be used as fillers of stone column material. Meanwhile, CB has not achieved the criterion to be considered for the filler. The steel plate was employed to carry plate load tests for both delivered recycled aggregate and a combination of several types of aggregate. Static loading results indicated that the bearing capacities of the clay beds reinforced with the columns constructed with CB, CC, and gravel were the same and approximately five times the unreinforced clay bed.

The bottom ash is a by-product of coal-burning activity to support the power plant. Marto et al. (2014) evaluated the shear strength parameters of clay improved by single and group of bottom ash stone columns. A series of undrained triaxial tests were performed. The bottom ash column (BAC) installed in the clay to form a composite specimen. The influence parameter studied includes the diameter and height of the column. The result indicated that the bottom ash column in clay specimens effectively acts as a vertical drain during consolidation. The confining pressure played an important role in the consolidation of soft clay reinforced with BAC at low confining pressure. The clay cohesion increased significantly, and the group pattern showed a higher cohesion than single column. However, the friction angle did not show a significant difference.

Ayothiraman and Soumya (2011) used type chips of size 10 mm and stone aggregates as stone column aggregate. Different mix proportions of stone aggregates and type chips were studied. Triaxial tests were conducted on samples of 50 mm diameter—the aggregate insert in the Kaolinite clay bed. The result clearly showed that waste-type chips can partially replace stone aggregates up to about 60% in stone columns.

Xueyi et al. (2009) investigated the behavior of stone columns under a confined compression state oriented mainly towards the determination of stress concentration ratio (*n*) of the stone column system and to understand the mechanism of load transfer between the stone and surrounding soil. The crushed stone was examined separately and mixed with sand, lime, or cement in different percentages. The modifications of the backfill martial and their effect on the stress concentration ratio were also investigated. The model test of the stone column was performed to investigate bearing capacity. Figure 2.3 shows the model test schematically of the test setup.

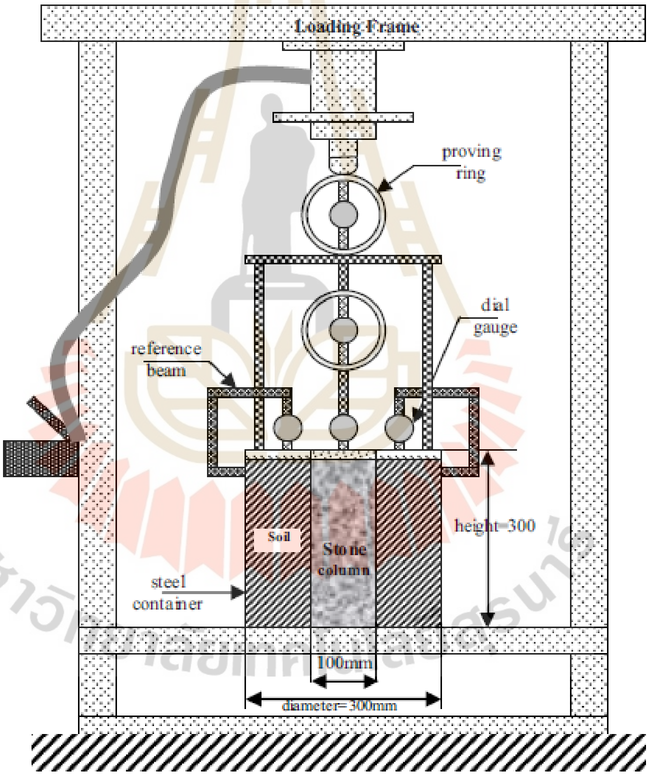

Figure 2.2. Schematically of stone column testing in clay bed (Xueyi et al., 2009)

The backfill materials used are crushed stone with 50% sand, crushed stone with 5 and 10 % dry lime, and crushed stone with 2.5 and 5 % cement. Cement content increases the stress concentration ratio (n) values, defined as the ratio of elastic increment stress of column and surrounding soil. On the other hand, the presence of dry lime did not show any significant increase in the stress concentration. It was found that the value of stress concentration ratio (*n*) increased with decreasing the shear strength of the surrounding soil. It was also found that the stress concentration ratio (*n*) increased when the total stress is held constant and increased with the time at different rates depending on the type of the backfill material.

2.3 Recycled asphalt pavement (RAP)

Recycled asphalt pavement (RAP) is a by-product of the rehabilitation or demolition of distressed asphalt pavement. RAP consists of coarse aggregate and binder partially coating on the surface (W. H. Chesner et al., 1998). Typically, RAP is reused for asphalt pavement to replace a raw material. In the United States in 2019, the survey revealed that 89.2 million tons of RAP were reused in asphalt mixture, saving 4.5 million tons of asphalt binder and 84 million tons of aggregate. However, the critical RAP content is limited to 15-20% in many counties (Tarsi et al., 2020). RAP is also used as base course aggregate, i.e., full-depth reclamation and cold in-place recycling.

2.3.1 Material properties

RAP's engineering properties differ in different sources, design standards and ages. The typical physical and mechanical properties of RAP can be summarized in Table 2.3

Table 2.2 Typical physical and mechanical properties of RAP (W. H. Chesner et al., 1998)

Physical properties	
Unit weighs	19 -23 kN/m^3
Moisture content	Normal: up to 5 % Maximum: 7-8 %
Asphalt content	4.5-6 %
Asphalt penetration	10-80 % (at 25 C°)
Absolute viscosity	4000-25000 poises (at 60 C°)
Mechanical Properties	
Compacted unit weigh	15-20 kN/m^3
California bearing ratio (CBR)	20-25%

2.3.2 Gradation

During removing process, the removing machine pulverized existing asphalt concrete pavement and turn into a small aggregate. The gradation of RAP depends on the speed spacing of the teeth milling machine and the source of asphalt pavement. Figure 2.3 shows the variation of RAP gradation from different sources-the grain-size distribution curve of RAP shows that it falls similarly in the narrow band. The scarcity fine fraction can be found for about 5-8%. The gradation of RAP is finer than virgin aggregate such as crushed rock, but RAP's gradation exhibits coarse aggregate with a low fine fraction compared with lateritic soil. The gradation also depends on the types of equipment used to remove RAP in the field. Kallas (1984) performed a sieve analysis of RAP before and after milling. The result shows that the percent passing of sieve number 8 (2.36 mm) increase ranged from 41-69 percent to 52-72, and the 200 (0.075 mm) increases ranged from 6-10 percent to 8-12 percent after milling RAP. According to the Unified Soil Classification System (USCS), most of the RAP in this literature are classified as (Gravel with well-grade, GW) and A-1-a group for the AASHTO system.

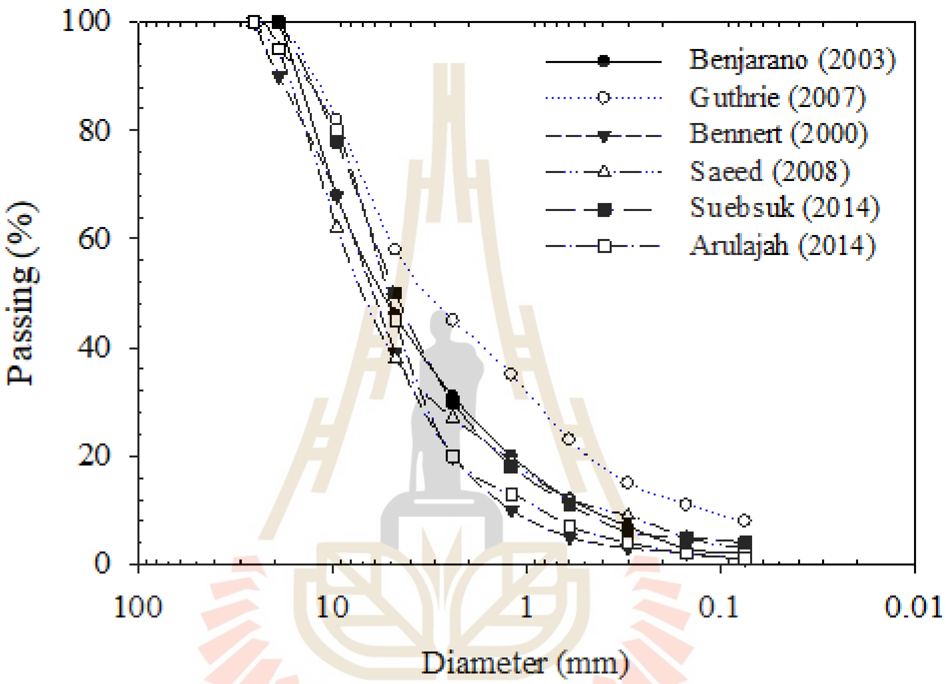

Figure 2.3. The typical range gradation of RAP (Arulrajah et al., 2014; Bejarano & Harvey, 2003; Bennert et al., 2000; W. S. Guthrie et al., 2007; Suebsuk et al., 2017)

2.3.3 Compaction characteristics

The dry density-water content relationship of RAP is compilated in Figure 2.4. The result shows that compaction characteristics of RAP are insensitive to water content, indicated by the dry density insignificantly increased with water content. The flat compaction cure of RAP may contribute to low water absorption of RAP (Arulrajah et al., 2014), the higher compaction energy causes dry density to increase. Table 2.1 presents the range of maximum dry density of RAP from different sources. The range of OMC of RAP is within 5-8 percent, and the maximum dry density is 1870

– 2085 kg/cm^3. The particles of RAP partial coating with asphalt binder which lower specific gravity led to low compaction ability. Moreover, low water absorption of RAP aggregate required low water content at the maximum dry unit weight (W. S. Guthrie et al., 2007)

Table 2.3 The typical compaction characteristics of RAP

Authors	Proctor Effort	OWC (%)	MDD (kg/cm^3)
Bennert et al. (2000)	Standard	5.0	1,872
Ramzi Taha et al. (2002)	Modified	7.0	1,885
W. Spencer Guthrie et al. (2007)	Modified	5.6	2,083
Jirayut et al. (2014)	Modified	6.2	1,785
Arulrajah et al. (2014)	Modified	8.2	2,038

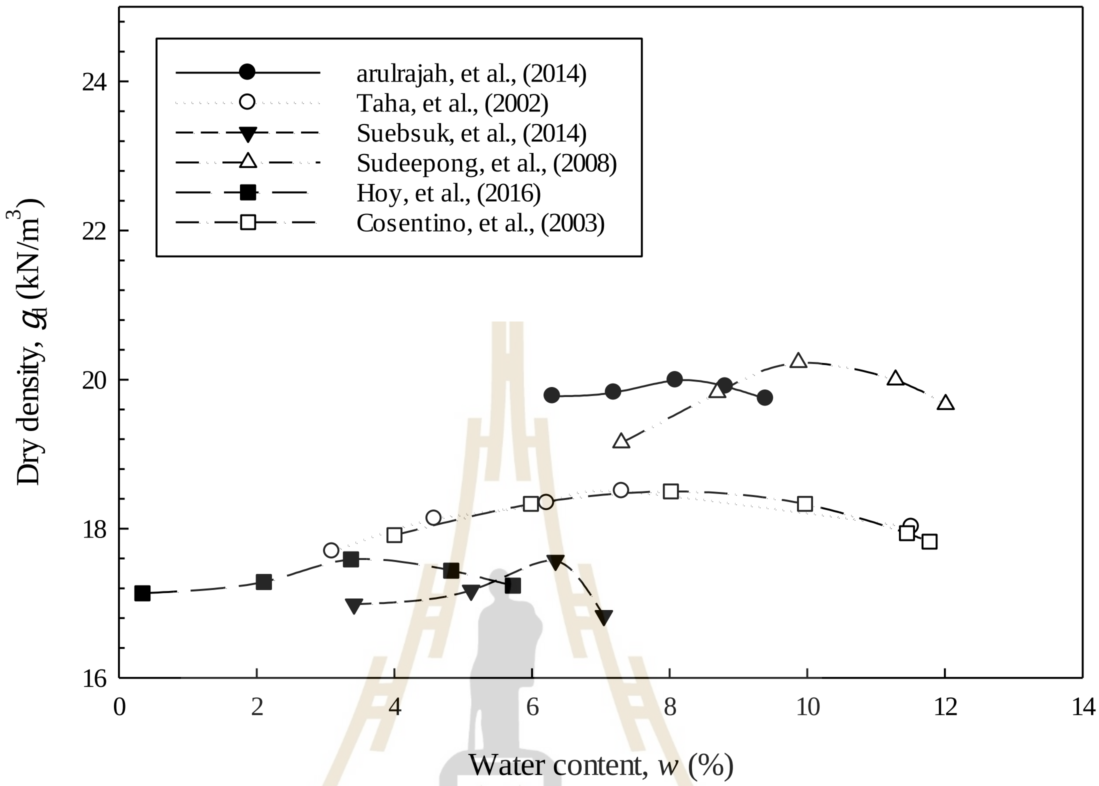

Figure 2.4 The summary of the compaction curve of RAP from various sources

2.3.4 Chemical properties

RAP consists of mostly aggregate and partially hardened asphalt binder coating the surface (3-7 percent by dry weight). The primary chemical componence of RAP is similar to the original aggregate that RAP made (Warren H. Chesner et al., 2002).

Hoy et al. (2016) investigated RAP's mineral and chemical constituents. X-ray diffraction (XRD) and X-ray fluorescence (XRF) were used to identify RAP minerals' quantity and chemical composition. It was found that the predominant mineral components in RAP were calcite-magnesium and dolomite (Figures 2.5-2.6). The main chemical compositions detected in RAP were 41.93% CaO and 36.11% MgO, according to the mineral aggregate of the original RAP.

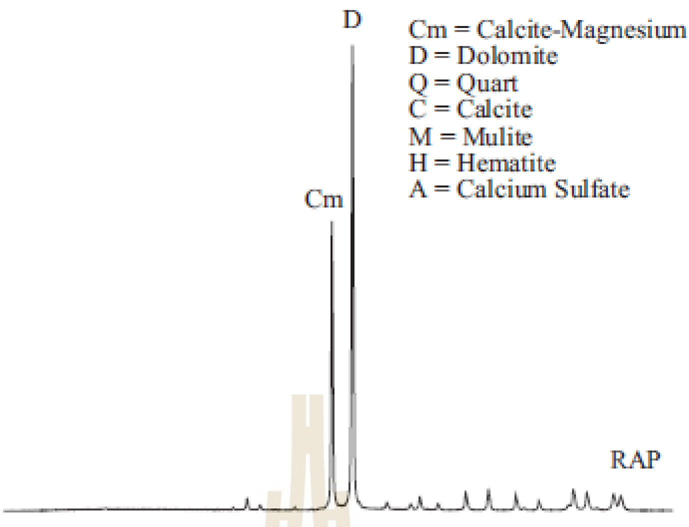

Figure 2.5 The result of XRD of RAP (Hoy et al., 2016)

Figure 2.6 Scanning Electron Microscopic photo of RAP (Hoy et al., 2016).

During service, asphalt binder ages, and hardens through various mechanisms. The hardening of RAP has been associated with six major mechanisms (Karlsson & Isaacsson, 2006; Roberts et al., 1996; Tyrion, 2000):

1) Oxidation through a diffusive reaction between the binder and oxygen in the air
2) Volatilization through evaporation of the lighter components especially during construction
3) Polymerization through the chemical reaction of molecular components
4) Thixotropy due to the formation of a structure within the asphalt binder over a long period
5) Syneresis due to the exudation of thin oily components
6) Separation through removing oily constituents, resins, and asphaltenes by absorptive aggregates.

The senior level that asphalts binder experiences during production and service depends on the void content of the original asphalt pavement. Recovered binder from porous asphalt pavement has shown significantly greater stiffness than regular asphalt pavement (Kemp & Predoehl, 1981). In addition, the properties of aged binders depend on the damage to the recycled pavement (Smilikanic et al., 1993). Stockpiling also accelerates binder aging as the material is more prone to air exposure and oxidation (McMillan & Palsat, 1985). As the asphalt binder reacts and loses some components during aging, its rheological behavior will naturally differ from virgin materials.

2.3.5 Shear strength

The shear strength of RAP was generally evaluated by triaxial compression or direct shear tests. Arulrajah et al. (2014) reported direct shear test results and drained triaxial test on various types of recycled aggregate obtained from construction and demolition (C&D). They revealed that the shear response of RAP exhibited strain-hardening in the shear stress-displacement relationship followed by strongly dilated afterward at low normal stress and compressive when normal stress is higher (figure 2.7 (a)). The result from the drained triaxial test exhibited similar to that from the direct shear test—the strain-hardening behavior in the stress-strain curve (figure 2.7 (b)). The contractive-dilative behavior in volumetric strain versus axial strain relationship can be found for low effective confining pressure, while contractive behavior exhibited at higher effective confining pressure. A similar shear response of RAP from a triaxial drained test was also reported by Cosentino et al. (2003).

Due to the nature of the coarse-grained aggregate of RAP, it results in high friction angle. In this literature, the friction angle of RAP reported from previous studies indicated that the friction angle ranges from 43-45° (Table 2.4). RAP generally blends with aggregate to replace the virgin materials. The increased proportion of virgin aggregate among composted fine fractions may decrease the friction angle of the blends (Bennert & Maher, 2005).

Table 2.4 The typical range of strength parameter of RAP

Authors	Friction angle (degree)	Cohesion (kPa)
Arulrajah et al. (2014)	43	0
Cosentino et al. (2003)	44	33
Bennert and Maher (2005)	44.5	25

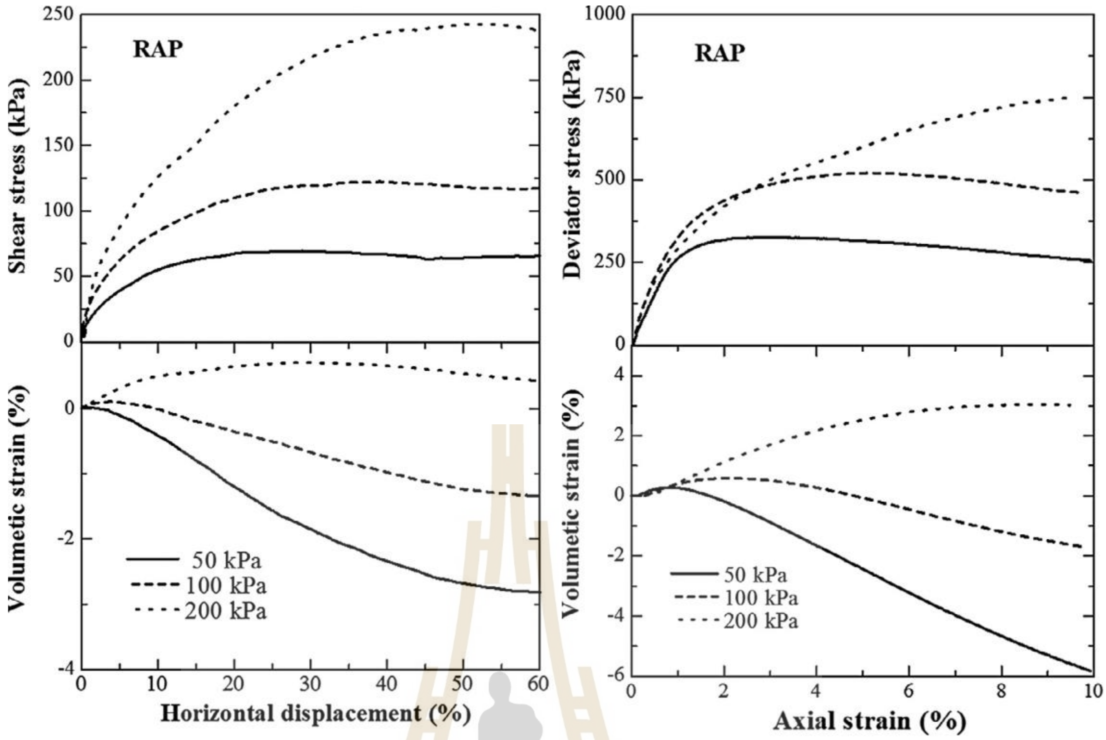

(a) (b)

Figure 2.7 Shear behavior of RAP (a) Direct shear test result (b) Triaxial drained test result.

2.3.6 Aggregate blends

The large volume of RAP annually increases. By mixing with the traditional aggregate, RAP can be replaced a million tons of aggregate. The aggregate mixing can reduce the amount of virgin aggregate or improve the physical properties of marginal aggregate for highway applications. The full-depth reclamation (FDR) method is extensively used to maintain damaged asphalt pavement. In this process, the existing asphalt pavement and base course underneath the pavement will be removed together and turn into coarse aggregate. Simultaneously, RAP and base course are blended and injected with cement slurry and water to improve the strength of the mixture. Consequently, RAP/ aggregate blends will pave by compaction machines. The procedure of FDR is illustrated in Figure 2.8.

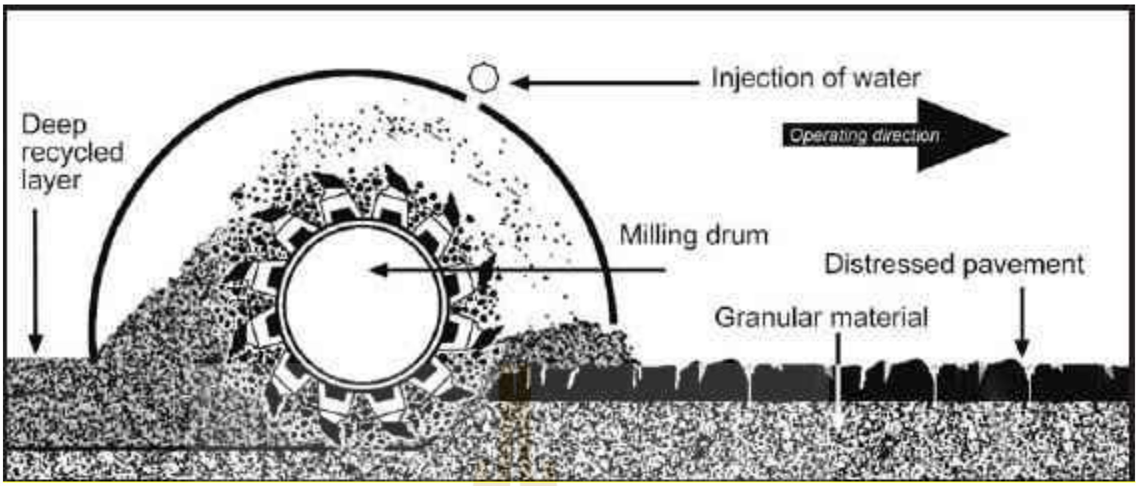

Figure. 2.8. The procedure of Full-depth reclamations (Luhr et al., 2005)

Over the two past decade, several researchers have evaluated the engineering properties of RAP/aggregate blends to meet the standard highway specification. R. Taha et al. (2002) performed unconfined compressive strength and compaction to evaluate the strength of RAP-aggregate blends in various proportions ranging from 0-100% of RAP. Portland cement was used to stabilize the mixture. The results indicated that increased RAP content decreases optimum moisture content, maximum dry density, and strength of RAP/aggregate blends. The specimens stabilized with cement yielded higher strength with a long curing time.

Suebsuk et al. (2014) proposed the generalized strength equation of RAP-lateritic soil mixture for the mixture containing RAP lower than the fixation point (RAP/Soil 50/50) and stated that within the active zone of stabilization (1-5% cement content). The unconfined compressive strength of the specimens after 28 days of curing can be assessed by the strength at an early period of curing.

The durability of cement-stabilized course-based materials can be determined by loss in weight when experiencing the cyclic wetting and drying. Suddeepong et al. (2018) investigated the durability of cement-stabilized RAP-crushed rock (CR) blends. They revealed that the unconfined compressive strength of RAP/CR blends increased with the cement content. The weight loss of cement-stabilized RAP/CR increased with the number of cycles of wetting-drying associated with the decrease of unconfined compressive strength.

Bennert et al. (2000) investigated the engineering properties of construction and demolition material, including recycled concrete aggregate (RCA) and recycled asphalt pavement (RAP) blended with the dense-grade aggregate base course (DGABC) at various percentages of RAP and RCA. The materials were evaluated under a traffic-type loading scheme, including resilient modulus and permanent deformation via cyclic triaxial testing. Laboratory tests indicated that the RAP, RCA, and DGABC blended materials obtained higher resilient modulus values than the currently used DGABC. The permanent deformation testing on RAP mixed samples resulted in the highest permanent deformation at 100,000 cycles.

Bleakley et al. (2014) have compared the performance of traditional mechanically stabilized earth (MSE) wall backfill material to the performance of 100% RAP and 50% RAP/50% sand blends to determine the suitability of RAP or RAP–sand blends as MSE wall backfill. Vertical creep was compared with one-dimensional oedometer compression tests at three stress levels to simulate different depths behind an MSE wall. Large-scale test was performed to determine reinforcing strip's pullout strength; pullout creep at 25%, 50%, and 75% of top pullout; and vertical creep at the three overburden stress levels. The test results indicated that RAP–sand blends had higher density, friction angle factors, and pullout strength and developed ultimate pullout strength at lower displacements than either 100% sand or 100% RAP. The RAP–sand blends exhibited more horizontal and vertical creep than 100% sand but significantly less creep than 100% RAP.

Stolle et al. (2014) evaluated RAP-natural aggregate blends for base and subbase materials. They revealed that the mechanical properties of RAP- group A aggregate combination are similar to those of group A granular aggregate. The result of CBR on RAP-aggregate blends highly depends on the constituent aggregate and compaction effort that specimens were prepared. The static triaxial test result indicated that when RAP content increases, the shear strength slightly decreases but the accumulated strain increases for the repetitive loading triaxial test.

Besides the cement stabilized RAP as base materials, Hoy et al. (2016) proposed a novel RAP-fly ash geopolymer for road construction material. The liquid alkaline activator is the mixute of sodium hydroxide solution (NaOH) and Sodium silicate solution (Na_2SiO_3). The results of the unconfined compressive strength of RAP-FA geopolymer confirmed that it meets standard strength requirements for road base application. The microstructurale analysis of the RAP-FA geopolymer was carried out by X-ray Diffraction (XRD) and scanning electron microscopic (SEM) examination. The major cement products, which are Calcium Silicate Hydrate (C-S-H), and Calcium Aluminate Hydrate (C-H-A) were detected.

Yuan et al. (2010) evaluated the feasibility of using high RAP content mixed with aggregate for base course applications. RAP content at 50%, 75%, and 100% were evaluated through the comprehensive laboratory. The cement content, RAP content, and fine content significantly affect the properties of the RAP mixture. The presence of cementation compounds enhancing the mixture’s strength after chemical treatment was confirmed by SEM photo (figure 2.9 (a-b)).

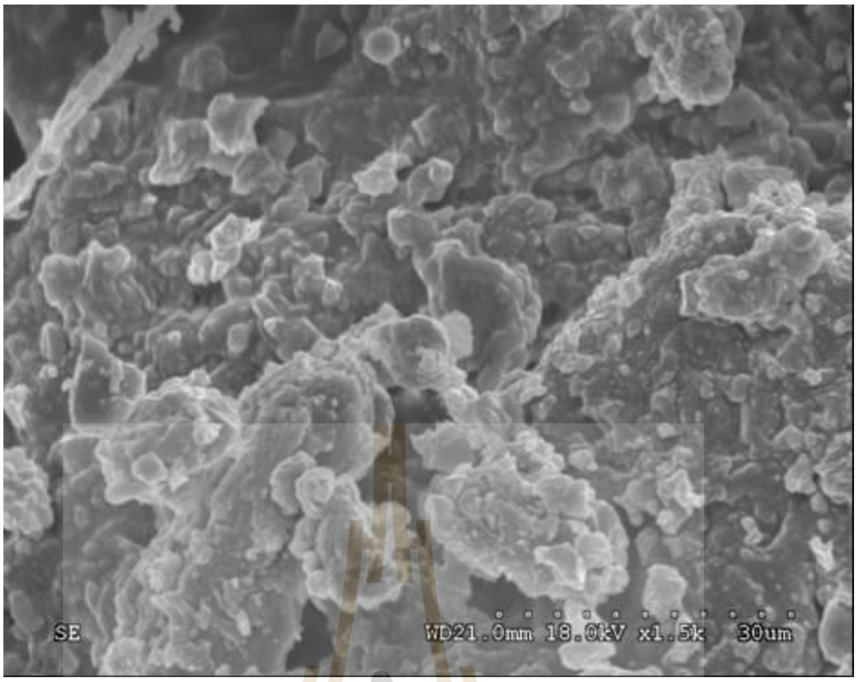

(a)

(b)

Figure 2.9 SEM image (a) untreated RAP (b) cement treated RAP (Yuan et al., 2010)

2.4 Hardening of soil cement

The major constituents of cement consist of tricalcium silicate ($3CaO.SiO_2$), dicalcium silicate ($2CaO.SiO_2$), tricalcium aluminate ($3CaO.Al_2O_3$), tetra calcium silicate aluminoferrite ($4CaO.Al_2O_3.Fe_2O_3$). Generally, abbreviated notation in the literature, these cement compounds are designed as C_3S, C_2S, C_3A, and C_4AF, respectively. When water adds dry cement powder, a reaction between each combination occurs. The equation of the hydration of tricalcium silicate and dicalcium silicate is given by

$$3CaO \cdot SiO_2 + nH_2O \rightarrow 2CaO \cdot SiO_2(aq) + Ca(OH)_2 \tag{2.3}$$

$$2CaO \cdot SiO_2(aq) \rightarrow 3CaO \cdot SiO_2(aq) + Ca(OH)_2 \tag{2.4}$$

Soon after cement mixes with water, tricalcium silicate reacts with water rapidly $Ca(OH)_2$ and calcium silicate hydrate (CSH) is produced. At the same time, dicalcium silicate co-occurs at a lower rate. Tricalcium silicate is responsible for early strength, while dicalcium silicate is much slower and contributes to long-term strength. Although C_3A also contributes to strength gain, it has a high heat of hydration. To render C_3A inert during early cement hydration, gypsum ($CaSO_4.2H_2O$) is added (Laguros, 1962).

For cemented soil, the cement particles would bind adjacent soil grains together during hardening and form a more or less continuous skeleton of a hard, strong material enclosing a matrix of unaltered soil. This skeleton could also be expected to "plug" some of the voids of the soil, reducing permeability and swelling and increasing the resistance of soil cement to the deleterious effects of changes in ambient moisture conditions. The cementation is to weld the particle together as shown in Figure 2.10. The investigation of thin sections by Price (1988) revealed that light cementing appeared only around the fringes of the particles and at particle contract. On the other hand, heavier cementing causes the void spaces to be filled with a cement matrix. The additional cementitious material could be generated, strengthening the bonds between the soil grains and soil and cement particles (Herzog & Mitchell, 1963).

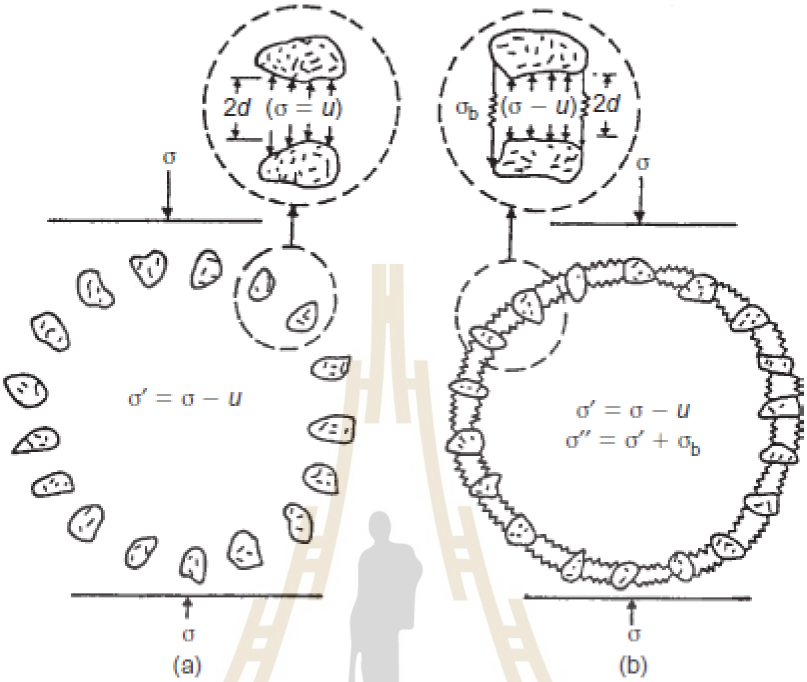

Figure 2.10 Schemically of clay structure (a) microfabric of uncemented clay (b) structure of induced cemented clay (Horpibulsuk et al., 2003)

2.5 Cemented soil behavior

The improvement of soil by cement has been widespread over the past decades. The addition of cement especially ordinary Portland cement is usually employed to improve the mechanical properties of soil. Utilization of cement promotes the strength, bearing capacity and workability of soil in the early period. Moreover, the economics of this technique is also accepted. Several researchers investigate the engineering properties of cemented soil in both coarse-grained and fine-grained soil. Comprehensive laboratories were performed to evaluate cemented soil's strength, including unconfined compressive strength, California bearing ratio, Indirect tensile test, direct shear test, and triaxial compression test. In addition, the microstructure of cemented soil has been considered to understand the interaction of soil particles and cementation bond, which provided the vital formation to understand the behavior of the soil improved by cement.

Leroeil and Vaughan (1990) detailed the pattern of naturally and artificially cemented soils, which depends on their initial state, position in the yield curve and the critical state line of the non-structured remolded soil. A conceptual described the stress-strain behavior of soils was also proposed. The effects of structure on soil behavior are identical to those emerging from over-consolidation in clays. It comprises an initial stiff behavior followed by increasing plastic deformation as the soil approaches failure.

G.W. Clough et al. (1981) conducted a triaxial drained compression test on the cemented soil. Natural cemented soil and artificial cemented soil by varying cemented levels and density were used to identify the effect of cement level. The results show that the behavior of natural cemented and artificial cement sand depends on the amount of cement agent, density, confining pressure, and grain size distribution. In addition, the cemented soil's failure mode also varied with confining pressure, cement level and density. The peak strength of artificial cemented soil was identical, but the cohesion significantly increased with cement content (figure 2.11).

Airey (1993) investigated the effect of cementation on the shear behavior of carbonate sand cored from North West Shelf of Australia. The result showed that natural calcarenite was similar to artificially cemented sand. The effect of cementation on soil’s behavior can be catalogized into two parts 1) increased the size of yield loci and 2) increased soil shear modulus.

T. and W. (1998) tested artificially cemented sand to investigate the effect of density and degree of cementation. The artificial cemented soil was prepared by varying the density and degree of cementation. The result shows that cementation's impact is only significant when the state of stress is lower than the yield stress. As expected, cementation increased the strength and stiffness of artificial cemented soil, but the effect of cement decreased as the densities of specimens increased.

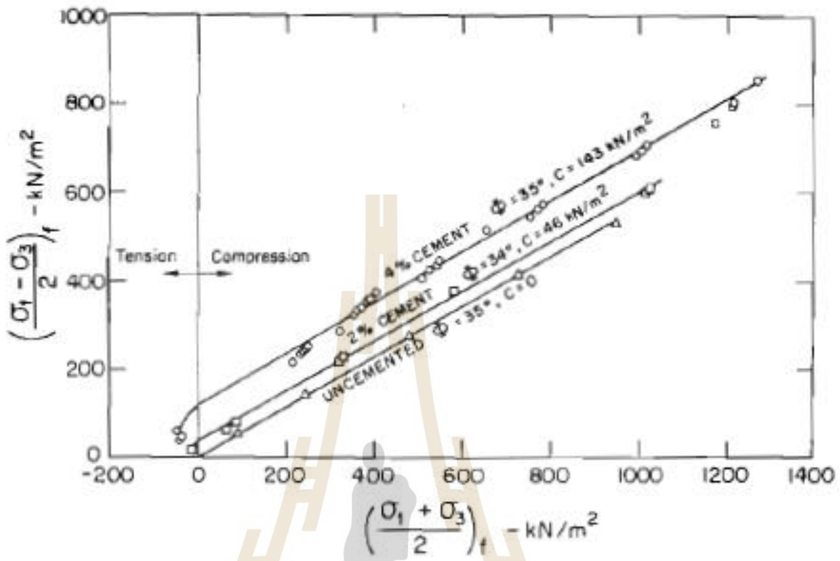

Figure 2.11 The peak strength of artificial cement and uncemented sand (G. Wayne Clough et al., 1981)

Coop and Akinson (1993) conducted triaxial tests to investigate artificially cemented carbonate behavior. The results show that an essential effect of cementation is a reduction in specific volume resulting from increased fines content. This influences stress-strain behavior and the peak strength at strains beyond those required to fracture the cementation bond. For cemented samples, it is possible to identify a yield curve outside the state boundary surface of the uncemented soil. Moreover, a framework for the behavior has been defined, which depends on the relative magnitudes of the confining pressure and cementation bond strength. The idealized stress-strain curve for cemented soil is illustrated in Figure 2.12. The first class (1 in figure 2.12.) of behavior occurs where the sample has passed its yield point during isotropic compression; subsequent shearing should produce behavior similar to that of an initially uncemented soil with no yield point. The second class (2 in Figure 2.6) occurs at intermediate confining stresses so that although the cementation bonds are intact at the start of the test, they yield during shearing and the peak state is governed by the frictional behavior of the uncemented soil. The stress-strain curve for this type of test might be expected to show a distinct yield point after an initial elastic section. For the third class the sample is sheared at low confining stresses relative to the strength of the cementation bond. A peak state occurs at low strains well outside the state boundary surface of the uncemented soil.

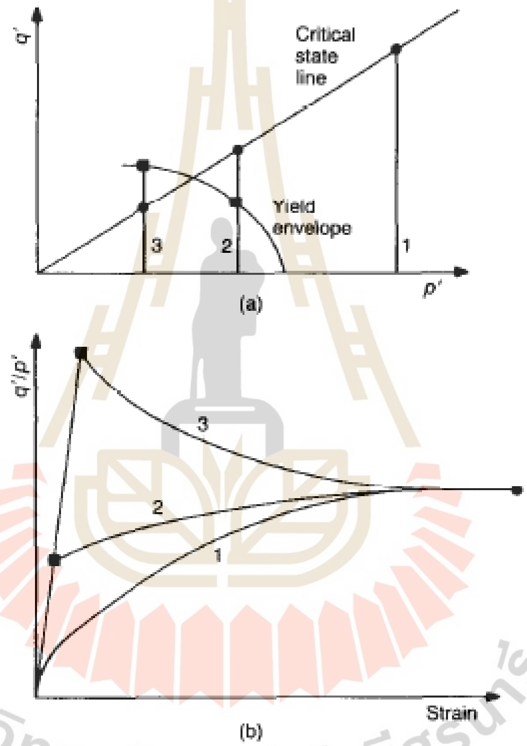

Figure 2.12 Idealized behavior of cemented soils: (a) stress paths; (b) stress-strain behavior (Coop & Akinson, 1993)

Schnaid et al. (2001) proposed the stress- strain- strength behavior of an artificially cemented sandy soil produced by adding Portland cement. Triaxial compression drained test and unconfined compressive strength were performed on uncemented and cemented soil. For cemented sandy soils, it was concluded that the unconfined compression resistance is a direct measurement of the degree of cementation. Consequently, the triaxial shear strength can be expressed as a function of only two variables: (1) the internal shear angle of the non-structured material; and (2) the unconfined compression resistance. The deformation secant modulus of the cemented soil is not significantly affected by the initial mean effective stress. The change in the secant deformation modulus of cemented soils with the axial strain can be qualitatively represented by mathematical expressions initially proposed for uncemented granular materials.

Lo and Wardani (2002) studied the mechanical behavior of weakly cemented silt—the cementing agent comprising cement and fly ash. The behavior of natural sandy silt and cemented silty sand were compared. The triaxial compression test was performed under both drained and undrained condition on saturated specimens. They reveal that the cemented soil was initially less dilatant than uncemented sandy silt, but eventually, the cemented soil became more dilatant. The shear strength data show the curvature of the failure envelope and can be modeled by the failure function.

Baxter et al. (2011) have proposed different failure criteria for weakly cemented sands to explain the uncertainty in determining effective strength parameters from undrained tests. A series of consolidated triaxial tests were conducted on artificially cemented silty sand improved by ordinary Portland cement. Maximum principal stress ratio, maximum excess pore pressure, and Skempton's pore pressure parameter $\bar{A} = 0$ were evaluated, and a criterion that reduces the variability in the strength of weakly cemented soils is proposed. The use of $\bar{A} = 0$ as a failure criterion of cemented ground agrees with the Morh-Coulumb failure envelope for undrained conditions.

The effect of cement type on the shear behavior of cemented sand was reported by Ismail et al. (2002). The three cement agents were used to investigate the specific effect on shear behavior. The result showed that despite the specimen's control density and the unconfined compressive strength identically, the undrained shear response exhibited differently. The specimens prepared by Portland cement exhibited ductile response accompanied by strongly dilate. Meanwhile, calcite and gypsum-cemented samples showed more brittle responses, followed by contractive behavior. They revealed the different shear responses of various cement-type samples due to the volumetric response during shearing.

CHAPTER III

EVALUATION OF CEMENT STABILIZED RECYCLED ASPHALT PAVEMENT/LATERITIC SOIL BLENDS FOR SOFT SOIL IMPROVEMENT

3.1 Sate of problems

Stone column inclusion is a ground improvement technique to improve the impermissible soft soil layer. The main function of stone column is densifying and strengthening of the soft ground. Stone column is also used to accelerate consolidation process of soft soil. There are many installation methods of stone column for various ground condition. These installation methods form unbound backfill aggregate into the composite ground by densification.

The load capacity of the ground reinforced by stone column depends on backfill performance and confining stress (Han, 2015). Typically, the quarried stone has been selected as stone column backfill. For the past decades, the environmental impact and sustainable reasons encourage the usage of the alternative materials such as construction and demolition (C&D) materials and industrial by-products as a stone column backfill. Many researchers have ascertained the potential of the crushed concrete, steel slag and artificial cemented soil as a stone column backfill (Juran & Riccobono, 1991; Mckelvey, Sivakumar, Bell, & Mclaverty, 2002; Shahverdi & Haddad, 2019; Zukri & Nazir, 2018).

In addition, installing stone columns in very soft ground (undrained shear strength < 15 kPa) is not applicable due to the lack of bonding of aggregates and low shear strength of surrounding soil, causing bugling failure (Han, 2015). Stabilized aggregates with chemical agents have been applied to overcome this problem.

Many researchers proposed the stabilization of fill aggregates to increase their cohesion to withstand bugling failure when installed in the soft ground (Golait & Padade, 2017; Golait, Satyanarayana, & Raju, 2009; Juran & Riccobono, 1991; Zhou, Yin, & Ming, 2002). Recycled Asphalt Pavement (RAP) is one of C&D materials from rehabilitation of asphalt concrete pavements. RAP is composed of aggregates and binder coating their surface (Chesner, Collins, & MacKay, 2008). The amount of RAP has been increasing annually due to the economical growth worldwide, which is generally disposed of to landfill. National Asphalt Pavement Association (2019) reported that the total RAP in U.S.A. was about 101.3 million tons in 2018. The estimated 82.2 million tons of RAP were used to construct new asphalt pavements to reduce amount of natural materials. The amount of RAP used for infrastructure construction in 2018 was approximately 46.8% higher than that used in 2009.

RAP has been successfully used in highway and pavement applications (Bennert, Papp, Maher, & Gucunski, 2000). Utilization of RAP in highway construction in particular base curses was achieved by blending it with conventional aggregates (i.e., crushed rock, lateritic soil) at proper replacement ratio (Taha, Al-Harthy, Al-shamsi, & Al-Zubeidi, 2002). RAP can also improve the properties of marginal lateritic soil to meet standard specification for stabilized base course (Suebsuk et al., 2017). RAP/lateritic soil blends improved by cement provided the satisfactory properties for highway applications (Guthrie, Cooley, & Eggett, 2007; Suebsuk, Suksan, & Horpibulsuk, 2014; Taha et al., 2002).

The marginal lateritic soil, which is sub-standard for highway application but is abundant in topical counties including Thailand can be improved by RAP to be used as a stone column backfill. This study investigates the possibility of using RAP/marginal lateritic soil blends as stone column aggregate instead of the traditional quarry aggregate. The samples have been evaluated through undrained triaxial compression loading at various RAP replacement and effective confining pressure. The effect of RAP on undrained shear strength characteristic and stiffness of the blended materials in which significant for the design of composite ground was focused in this research.

3.2 Materials

Lateritic soil sample was collected from a borrow pit in Nakhon Ratchasima, Thailand. The lateritic soil was composed of 15% gravel, 62% sand and 23% fine particle. Following unified soil classification system (USCS), the lateritic soil was classified as clayey sand (SC). The fine content of aggregates for highway applications must be less than 20% (Department of Highway, 1989). Therefore, this lateritic soil was classified as a marginal material, which cannot be used in highway application.

Recycled asphalt pavement (RAP) was obtained from Bureau of Nakhon Ractchasima, Department of Highways, Thailand. RAP was composed of 60-70 penetration grade asphalt binder at approximately 7% by dry weight. RAP was classified as well-graded sand with gravel (SW). Basic and geotechnical properties of the lateritic soil and RAP are summarized in table 3.1.

Table 3.1 Basic properties of lateritic soil and RAP

Properties	Soil	RAP
Liquid limit, *LL* (%)	32	N/A
Plastic limit, *PL* (%)	16	N/A
Plastic index, *PI* (%)	16	N/A
Gravel (%)	15	45
Sand (%)	62	43
Fine content (%)	23	1.4
Specific gravity, G_s	2.58	2.35
Soil classification	SC	SW
Asphalt binder, *AS* (%)	-	7

3.3 Experimental methodology

Extensive laboratory tests were conducted on cement stabilized RAP-soil blends to evaluate the effect of RAP replacement ratio and cement content on their undrained shear behavior. The lateritic soil was replaced by RAP contents at 10, 30 and 50% by dry weight of lateritic soil to minimize the fine contents (interparticle contact prior to cement stabilization). RAP10, RAP30 and RAP50 herein represented the lateritic soil blended with 10%, 30% and 50% replacement ratio, respectively. Ordinary Portland cement (Type I) was used to stabilize RAP-soil blends at 1% and 3% in this research, which is commonly used for soil stabilization in practice (Suksun Horpibulsuk, Katkan, Sirilerdwattana, & Rachan, 2006).

The compaction test was conducted on RAP-soil blends in order to determine the maximum dry unit weight (MMD) and optimum moisture content (OWC) under modified compaction energy (ASTM D1557). Both lateritic soil and RAP were sieved through sieve No. 4 (4.75 mm) and No. 3/8 (9.5 mm), respectively to remove larger particles. The lateritic soil and RAP were air-dried for at least 3 days prior to compaction test. The lateritic soil was replaced by RAP at the target RAP replacement ratios. The RAP-lateritic soil blend was thoroughly mixed and then water was sprayed into the blend for compaction. The sample was compacted in five layers with 25 blows per layer in a standard mold with dimensions of 101.6 mm diameter and 110.68 mm height. In order to obtain complete compaction curve, at least five compaction data points were required

The compressibility of RAP-soil samples was evaluated via one-dimensional consolidation test following ASTM D2435. The samples were prepared by tamping RAP-soil blends in three layers in a floating-type consolidation ring with dimensions of 20 mm height and 75 mm diameter at MDD and OWC. The sample was submerged under water in a consolidation cell for over 24 hours to ensure saturation before testing. The maximum effective vertical stress applied was 1500 kPa. Due to very high yield stress of cement stabilized RAP-soil and limitation of equipment, the test was limited to only unstabilized samples.

The cement stabilized RAP-soil samples for triaxial tests were prepared by compaction method suggested by Ladd (1978). The air-dried lateritic soil, RAP and cement were thoroughly mixed by hand to attain uniform mixture prior to mixing with water at the desired quantity. The lateritic soil-RAP-cement mixture was then compacted in a steel mold with dimension of 50 mm diameters and 100 mm height at MDD and OMC predetermined from the compaction test. After 24 hours, the samples were extruded and sealed by plastic sheet. The unstabilized samples were tested after extrusion while the cement stabilized samples were tested after 28 days of curing to avoid effect of strength development due to hydration during consolidation and shearing processes. The undrained triaxial compression tests were conducted following the procedure suggested by Head and Epps (2014). The method consists of three stages of testing namely saturation, consolidation and shearing. The saturation stage is the process allowing the water through the sample to fill the void by the incremental back pressure technique. The cell pressure and back pressure were increased while the effective stress held constant about 10 kPa until B values reached 0.95 and 0.90 for unstabilized and cemented stabilized samples, respectively. The samples were then subjected to consolidation stage. The desired effective stresses of 50, 100 and 200 kPa were then applied on the samples until the end of consolidation. Finally, the samples were sheared with a rate of 0.1 mm/min while the back pressure valve was closed and excess pore pressure was measured during shear. The stress-strain variants in this study were calculated as follows:

$$q = \sigma'_1 - \sigma'_3 \tag{3.1}$$

$$p' = \frac{\sigma'_1 + 2\sigma'_3}{3} \tag{3.2}$$

$$\varepsilon_q = \varepsilon_a = \frac{\Delta l}{l_0} \tag{3.3}$$

$$\eta = \frac{q}{p'} \tag{3.4}$$

where $\sigma'_1, \sigma'_2, \sigma'_3$ = effective principal stresses, q = deviator stress, p' = mean effective stress, η = stress ratio and ε_a = axial strain. In the undrained condition, the volume change is not allowed, thus the shear strain and axial strain are identical.

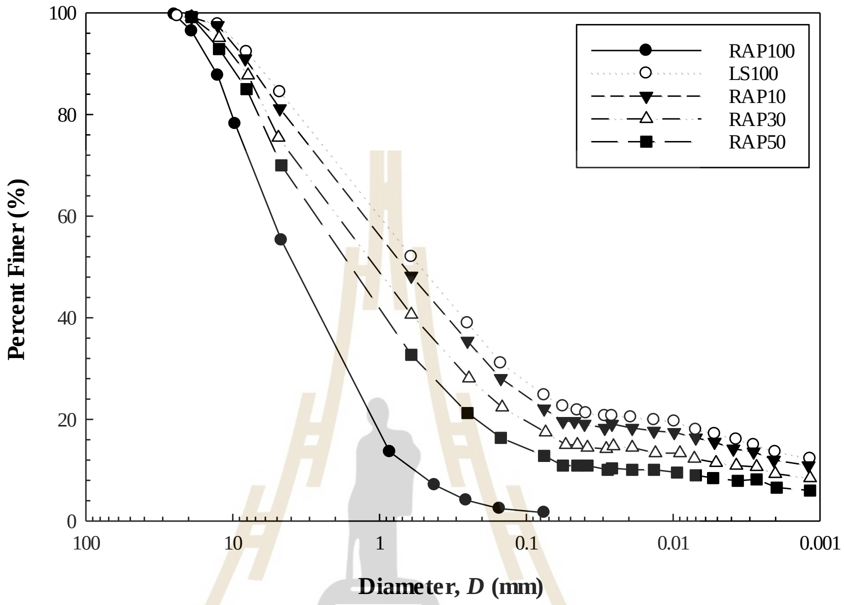

Figure 3.1. Particle size distribution of RAP-soil blends

3.4 Results and discussion

The particle size distribution curves of RAP-soil blends with various RAP replacement ratios are shown in figure 3.1. The RAP contained larger particles than the lateritic soil. The replacement of soil by RAP therefore increased the average particle size (D50) of the blends and reduced fine contents. The presence of asphalt binder with a low specific gravity of approximately 1.03 caused the RAP having lower specific gravity than the lateritic soil. The specific gravities of RAP-soil blends with different RAP replacement ratios can be approximated by using the following function:

$$G_{blend} = \frac{1}{\frac{LS}{G_s} + \frac{(1-LS)}{G_{RAP}}} \tag{3.5}$$

where G_{blend} = specific gravity of blends, G_s = specific gravity of lateritic soil, G_{RAP} = specific gravity of RAP, LS = lateritic soil content in %. The amount of asphalt binder in the blends is determined as follows:

$$AS = \frac{Wa}{Ws} * 100 \tag{3.6}$$

where W_a = weight of asphalt, W_s = weight of solid aggregates. Table 3.2 summarizes the calculated values of G_{blend} and AS. The higher RAP content results in a higher asphalt binder adherence and a lower specific gravity of the blends.

Table 3.2 Properties of RAP-soil blends

Sample identification	RAP (%)	OMC (%)	MDD (kN/m^3)	Fine fraction (%)	Void ratio	*AS* (%)
LS100	0	10.8	19	23	0.33	0
RAP10	10	10.5	19.3	21	0.29	0.7
RAP30	30	10.3	19.7	18	0.24	2.1
RAP50	50	10.3	19.7	15	0.22	3.5

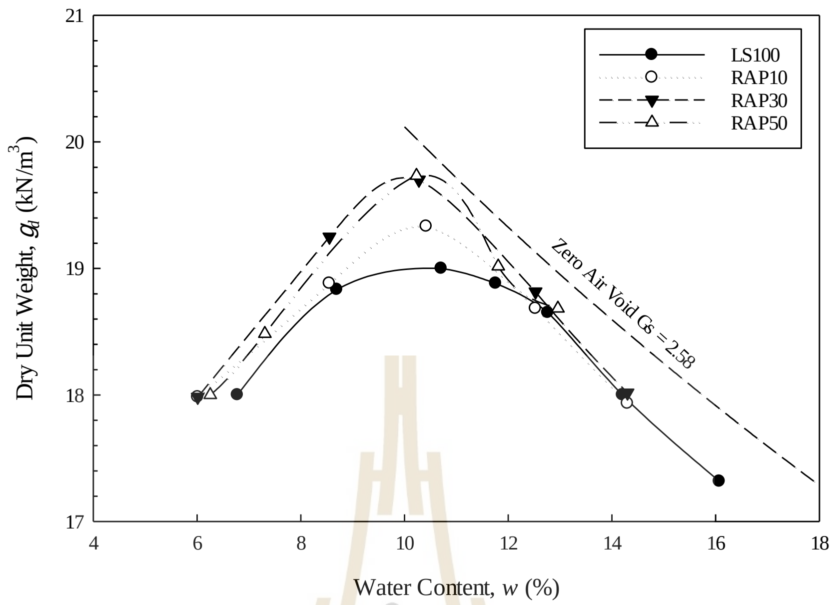

Figure 3.2 Compaction characteristic of lateritic soil and RAP blends

The results of compaction test are summarized in figure 3.2 and table 3.2. The compaction curve of lateritic soil could be represented by a bell shape, typically found in granular soil. The compaction behavior of pure RAP was found to be insensitive to water (the flat compaction curve) due to high energy absorption of RAP (Arulrajah, Disfani, Horpibulsuk, Suksiripattanapong, & Prongmanee, 2014). As such, RAP alone is not suitable as the compacted fill material and must be blended with lateritic soil; the flat compaction curve of RAP tended to diminish when blended with lateritic soil. The MDD of the blends increased with increasing the RAP replacement ratio indicating the higher compactibility of the blends. The compaction curves of RAP30 and RAP50 samples were similar. The OMC of all RAP replacement ratios changed in narrow range and was approximately 10%.

The relationship between void ratio versus effective vertical stress of RAP-soil blends is shown in figure 3.3. Compression index, Cc and swelling index, Cs remarkably decreased with the increased RAP replacement ratio particularly for RAP30 and RAP50.

The value of Cc reduced from 0.13 to 0.125, 0.071 and 0.076 while Cs reduced from 0.28 to 0.32, 0.16 and

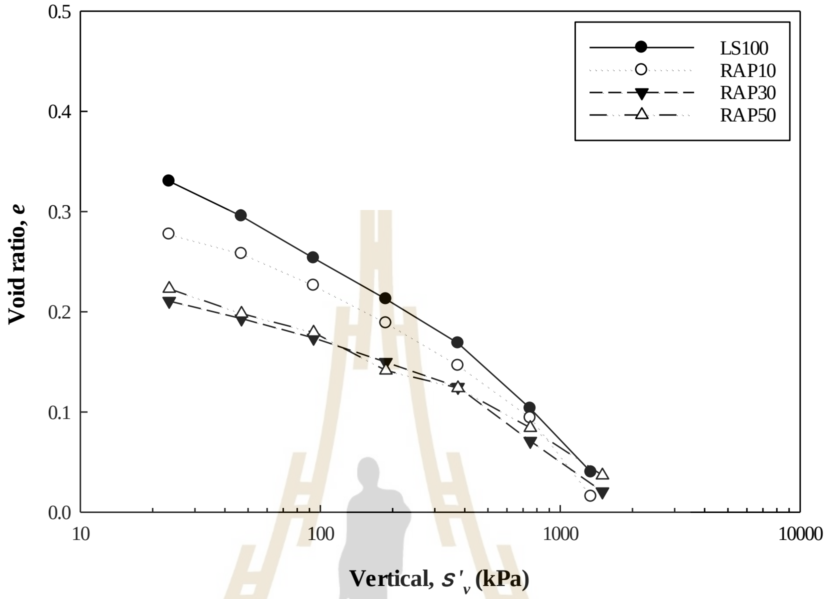

Figure 3.3 Consolidation test result of RAP-soil blends

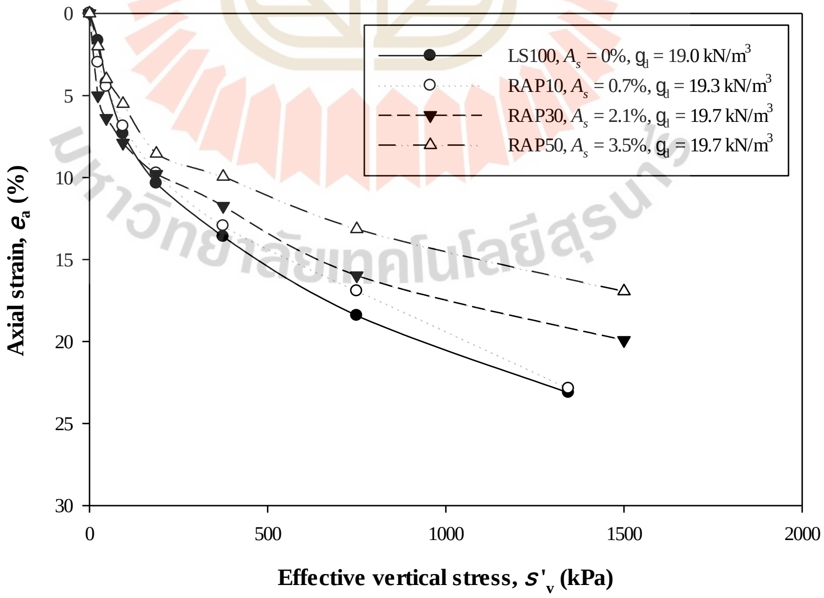

Figure 3.4 Relationship between axial strain and effective vertical stress lateritic soil and RAP-soil blends

0.177 for 10%, 20% and 30% RAP replacement ratios (RAP110, RAP20 and RAP50), respectively. However, RAP replacement ratio insignificantly affected the yield stress, whereby the yield stress varied between 400 and 500 kPa for all mixtures.

The effect of RAP replacement ratio on the deformation at the same effective vertical stress of all blends is shown in Figure 3.4. At post-yield state, the lateritic soil exhibited larger deformation while the RAP50 sample exhibited the lowest deformation at the same effective vertical stress. For example, the axial strain of the RAP50 sample was 13.2% while it was 18.4% for lateritic soil at the same effective vertical stress of 750 kPa. It was noted that the RAP10 sample exhibited the similar axial strain to the lateritic soil at high stress of 1350 kPa. The RAP replacement increased large particles and meanwhile reduced fines particles as seen by the increase in the average particle size (D_{50}). This improved the resistance to compression at post-yield stress even though the yield stress and density were practically the same.

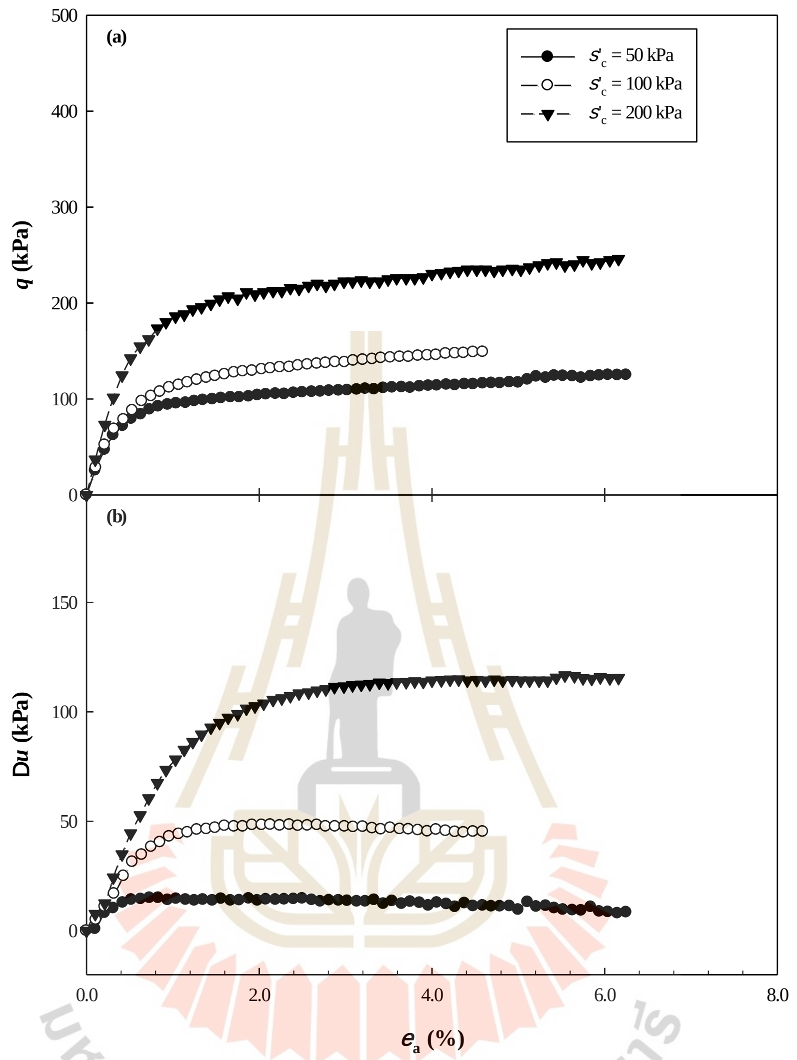

Figure 3.5 Undrained behavior of unstabilized lateritic soil

The triaxial undrained test results of both unstabilized and stabilized samples at different RAP replacement ratios are summarized in table 3.3. The undrained shear response of unstabilized lateritic soil under three confining pressures of 50, 100 and 200 kPa is presented in figure 3.5. The samples exhibited strain-hardening behavior whereby the deviator stress increased with the axial strain without clear peak. The strength and stiffness increased with the increased effective confining pressure. During shearing, the positive excess pore pressure was generated depending upon level of effective confining pressure. The higher effective confining pressure resulted in the higher excess pore pressure. Assuming that the at-rest lateral earth pressure coefficient (K0) equals 0.5, the yield mean effective stress was calculated to be 300 kPa (the 1-D yield stress was found to be 400-500 kPa from consolidation test). This yield mean effective stress was greater than the applied effective confining stresses. In other words, the samples were in over-consolidated state. Typically, over-consolidated clay exhibits negative pore pressure, which was different from the present samples. Even at low effective confining pressure of 50 kPa (the highest over-consolidation ratio, OCR), the negative pore pressure developed very little at the end of test. This might be due to the larger particles of the samples when compared with overconsolidated clay.

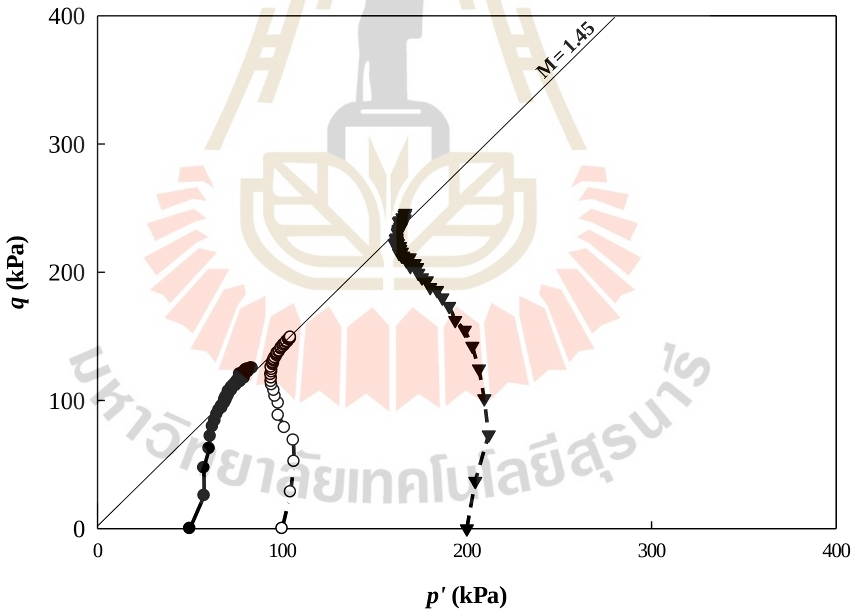

Figure 3.6 The undrained stress paths of unstabilized lateritic soil

The undrained stress paths of unstabilized lateritic soil under 50, 100 and 200 kPa effective confining pressures are shown in Figure 6. The path of the highest OCR samples (50 kPa of effective confining pressure) initially located close to applied total stress path due to little positive excess pore pressure development.

On the other hand, the lowest OCR samples (200 kPa of effective confining pressure) moved more to the left side of the applied total stress path due to high positive excess pore pressure. However, the undrained stress paths of unstabilized lateritic soil for all effective confining pressures were turned to the right side after the peak failure was attained due to the reduction in excess pore pressure.

The relationship between stress ratio (h) versus axial strain of unstabilized lateritic soil is shown in Figure 7. The h increased with the increased axial stain for all effective confining pressures tested but the slope of relationship was found to be different; i.e. the gentler slope was associated with the higher effective confining pressure. The maximum η was found to be identical for all the effective stresses tested, resulting in the unique failure envelope. This is the distinct undrained shear behavior of compacted lateritic soil which is different from that of normally and over-consolidated clay.

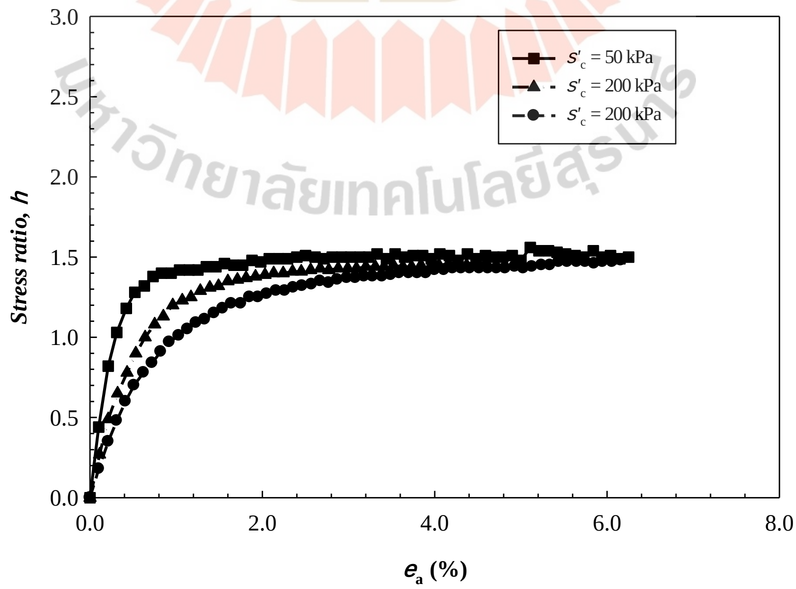

Figure 3.7 Relationship between stress ratio versus axial strain of unstabilized lateritic soil

The stress versus strain and excess pore pressure versus axial strain relationships of unstabilized RAP-soil blends are shown Figure 3.8. It is evident that the strain-hardening behavior in deviator stress versus axial stain relation is associated with the strain-softening behavior in excess pore water pressure versus axial strain relation in all RAP replacement ratios. The maximum deviator stress increased with the increased RAP replacement ratio while the maximum positive excess pore pressure was more or less the same. As such, the failure envelope of RAP-soil blends was steeper than that of the unstabilized soil as shown in figure 3.9. It was evident that the cohesion (c') was zero for both unstabilized soil and RAP-soil blends.

Table 3.3 Results of consolidation undrained triaxial compression test on unstabilized and cement stabilized RAP-soil blends

Samples identical	Cement (%)	σ'_c (kPa)	ε_a at q_{max} (%)	ε_a at Δu_{max} (%)	ε_a at η_{max} (%)	q_{max} (kPa)	Δu_{max} (kPa)	η_{max}
100/0	0	50	6.25	0.73	5.11	125.13	14.98	1.56
100/0	0	100	4.59	2.35	4.16	156.26	48.41	1.46
100/0	0	200	6.11	4.31	6.11	246.08	114.77	1.48
100/0	1	50	6.32	0.31	0.41	523.82	24.24	2.40
100/0	1	100	5.70	0.41	0.41	655.89	58.87	2.37
100/0	1	200	4.79	0.62	0.83	748.40	84.34	1.94
100/0	3	50	1.67	0.73	0.73	1722.60	37.95	2.92
100/0	3	100	1.56	0.31	0.31	1875.35	80.21	2.80
100/0	3	200	1.86	0.41	0.52	2090.75	62.04	2.33
90/10	0	50	6.20	1.14	2.31	143.70	19.14	1.56
90/10	0	100	6.39	2.73	5.03	175.91	46.84	1.51
90/10	0	200	6.13	4.97	4.97	265.91	107.33	1.45
90/10	1	50	1.86	0.41	0.52	644.71	33.15	2.68
90/10	1	100	6.32	0.52	0.62	813.41	69.01	2.49

Table 3.3 Results of consolidation undrained triaxial compression test on unstabilized and cement stabilized RAP-soil blends (Continued)

Samples identical	Cement (%)	σ_c (kPa)	ε_a at q_{max} (%)	ε_a at Δu_{max} (%)	ε_a at η_{max} (%)	q_{max} (kPa)	Δu_{max} (kPa)	η_{max}
90/10	1	200	5.39	0.52	0.62	742.69	102.48	2.04
90/10	3	50	1.45	0.52	0.52	1739.53	36.88	2.91
90/10	3	100	2.19	0.52	0.52	1934.31	60.98	2.74
90/10	3	200	1.46	0.63	0.73	2192.00	139.13	2.72
70/30	0	50	5.62	0.62	1.14	201.09	12.47	1.59
70/30	0	100	5.04	1.26	2.42	205.07	46.30	1.52
70/30	0	200	4.96	1.90	4.33	338.64	101.49	1.56
70/30	1	50	7.13	0.62	0.72	835.26	32.88	2.69
70/30	1	100	6.36	1.04	1.25	962.80	58.47	2.34
70/30	1	200	5.44	0.84	0.94	1042.79	117.15	2.17
70/30	3	50	2.71	0.52	0.62	1927.04	33.57	2.89
70/30	3	100	1.97	0.41	0.52	2368.55	80.75	2.89
70/30	3	200	2.19	0.73	0.94	2537.47	100.35	2.56
50/50	0	50	6.31	0.84	4.21	183.55	19.40	1.73
50/50	0	100	6.06	1.57	3.87	231.95	51.23	1.70
50/50	0	200	6.23	3.17	6.23	424.67	95.59	1.68
50/50	1	50	6.20	0.83	1.14	835.88	30.87	2.61
50/50	1	100	6.38	0.84	0.94	1000.68	70.04	2.57
50/50	1	200	4.91	1.36	1.67	1088.54	110.59	2.18
50/50	3	50	3.84	0.62	0.83	1775.99	37.95	2.92
50/50	3	100	4.16	0.83	0.93	1887.30	79.04	2.84
50/50	3	200	4.16	0.62	0.73	2381.92	144.47	2.69

The undrained shear behavior of cement stabilized lateritic soil at cement contents of 1% and 3% is shown in figure 3.10. Both strength and stiffness significantly increased with increasing the cement content. For the low cement content of 1%, the cement stabilized lateritic soil sample exhibited stain-hardening behavior in deviator stress versus axial strain associated with strain-softening behavior in excess pore water pressure versus axial strain relation, which was similar to unstabilized lateritic soil sample. However, with the high cement content of 3%, the strain-softening behavior was found for both deviator stress and excess pore pressure versus axial stain relation. The deviator stress increased to the peak at small axial stain and then decreased to lower value.

The excess pore pressure initially increased to the peak value at small stain (0.5-1% axial strain) and then decreased to negative value. The rate of reduction in excess pore pressures depended upon degree of cementation and level of effective confining pressures. The cementation bond increased the inter-particle forces, resulting in a higher maximum deviator stress and resistance to deformation. The higher cementation bond strength was associated with the higher negative pore pressure. The strain at peak excess pore pressure was lower than that at the peak deviator stress. The is different from the cement stabilized high water content clay in that the strain at peak excess pore pressure and peak deviator stress is almost identical (S. Horpibulsuk, Miura, & Bergado, 2004). This difference is possibly due to the compaction energy effect, which caused the dense package

The undrained stress paths of cement stabilized lateritic soil are presented in figure 3.11. The undrained stress path finally located on the left side of applied total stress path due to negative pore pressure development. The cohesion increased with the increased cement content while the friction angle was insignificantly changed. In other words, the friction angle of cement stabilized was not significantly affected by cementation bonds. This result is in agreement with previous study reported that the friction angle of cement and unstabilized soil are identical (G.W. Clough, Sitra, & Bachus, 1981; Juran & Riccobono, 1991; F. Schnaid, Predo D. M. Prietto, & N.C. Consoli, 2001).

The relationship between stress ratio versus axial strain of cement stabilized soil sample compared with that of unstabilized soil samples is shown in figure 3.12. The stress ratio of the stabilized samples increased to the peak at small strain after that tended to decrease to the critical state stress ratio of unstabilized samples. The higher cement content resulted in the higher peak stress ratio. It is of interest to mention that the axial strains at the peak of stress ratio and at the peak of positive pore water pressure were practically identical but take place before the strain at peak deviator stress (table 3.3). Coop and Atkinson (1993) revealed that the location of the breakup of the cementation bond took place at peak of stress ratio for cemented sand. S. Horpibulsuk et al. (2004) reported that the location at peak of stress ratio, peak of deviator stress and peak of excess pore pressure of cement stabilized high-water content clay was practically identical, which is different with the present study. This can be explained that the peak strength of cement stabilized lateritic soil is mainly dependent upon the cementation bond strength and interlocking due to the very low pre-shear moisture content. The cementation bond only influenced the strength until the peak of excess pore pressure.

The undrained shear behavior of cement stabilized RAP-soil blends is shown in the figure 3.13. The cement stabilized RAP-soil blends exhibited similar behavior to the cement stabilized lateritic soil. The strain-softening behavior in deviator stress and axial strain relation was found for the 3% cement stabilized RAP10

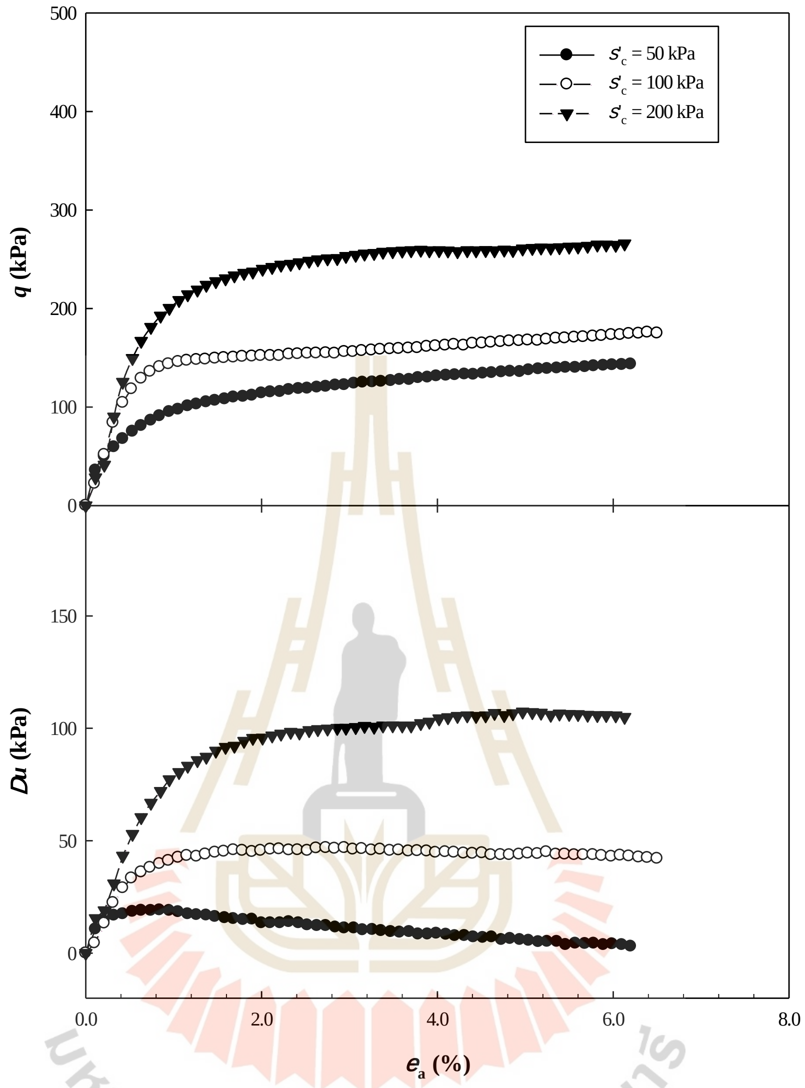

500
400
300
200
100
0
q (kPa)
150
100
50
0
Du (kPa)
0.0
2.0
4.0
6.0
8.0
e_a (%)
s'_c = 50 kPa
s'_c = 100 kPa
s'_c = 200 kPa

(a)

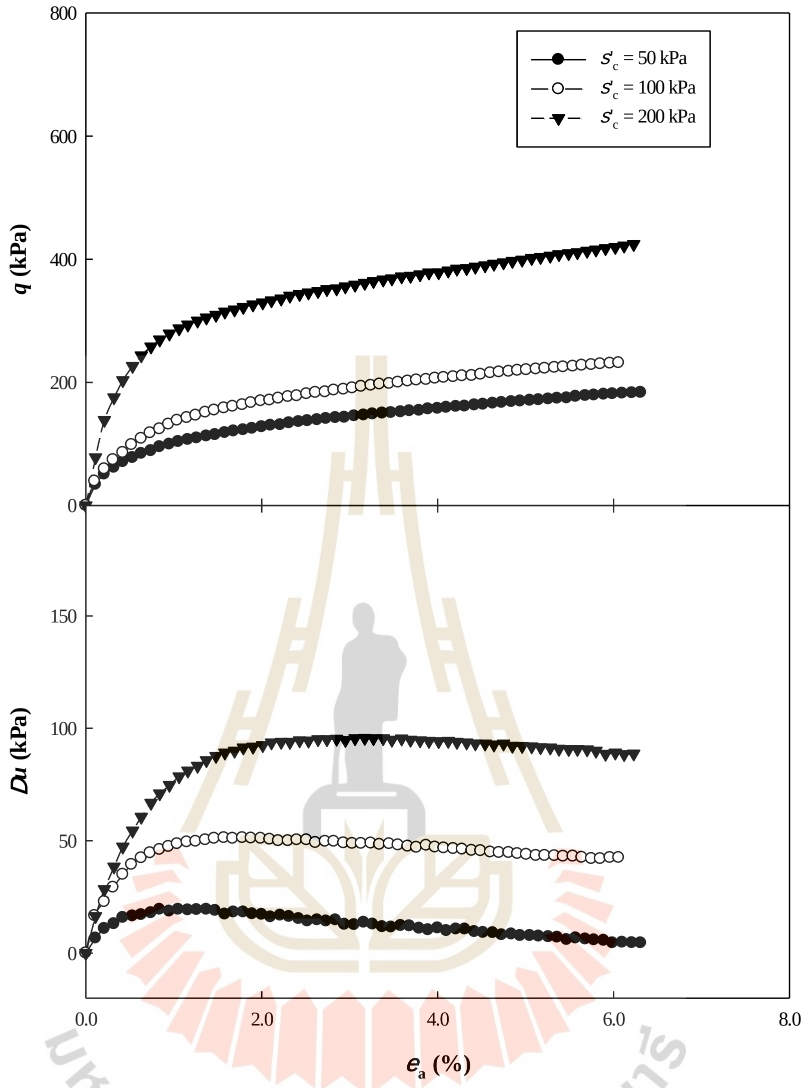

(b)

Figure 3.8 Undrained behavior of unstabilized RAP-soil blends (a) RAP10 (b) RAP 50

and RAP30 samples whereas the cement stabilized RAP50 exhibited stain-hardening behavior in deviator stress and axial strain relation. This is because RAP50 had higher energy absorption due to higher asphalt binder in the blend. However, the cement stabilized RAP10, RAP30 and RAP30 exhibited the strain-softening behavior in excess pore pressure and axial stain relation. In other words, the asphalt binder content did not affect the excess pore pressure development. Similar to the cement stabilized lateritic soil, the peak positive excess pore pressure took place at small stain, which was also observed for cement stabilized RAP-soil blends.

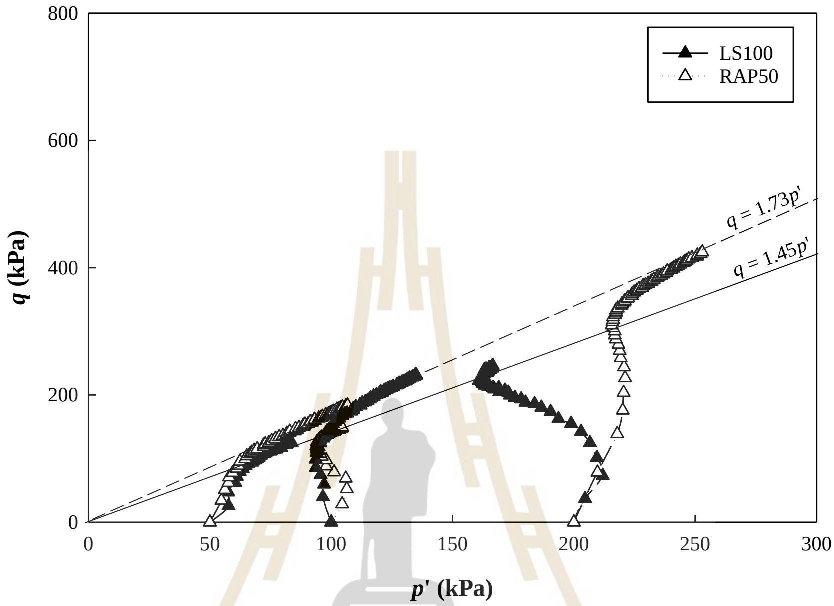

Figure 3.9 Effect of RAP replacement on effective stress paths of unstabilized samples

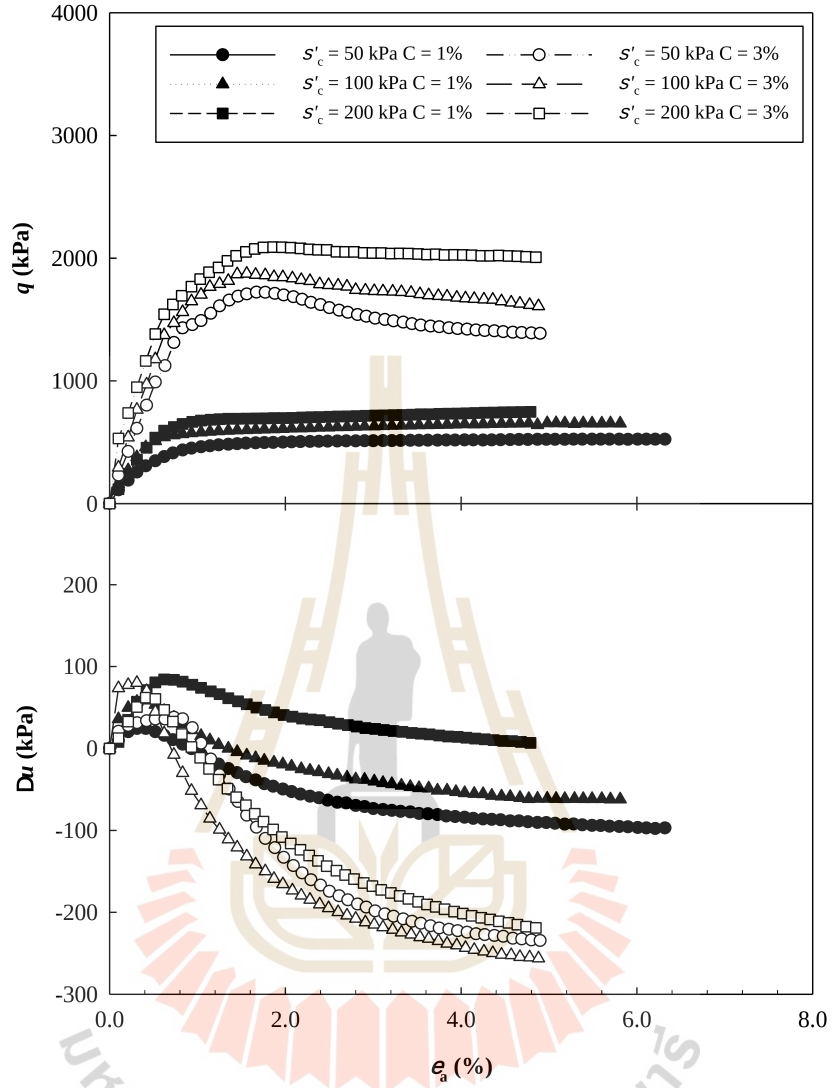

Figure 3.10 The undrained behavior of cement stabilized lateritic soil

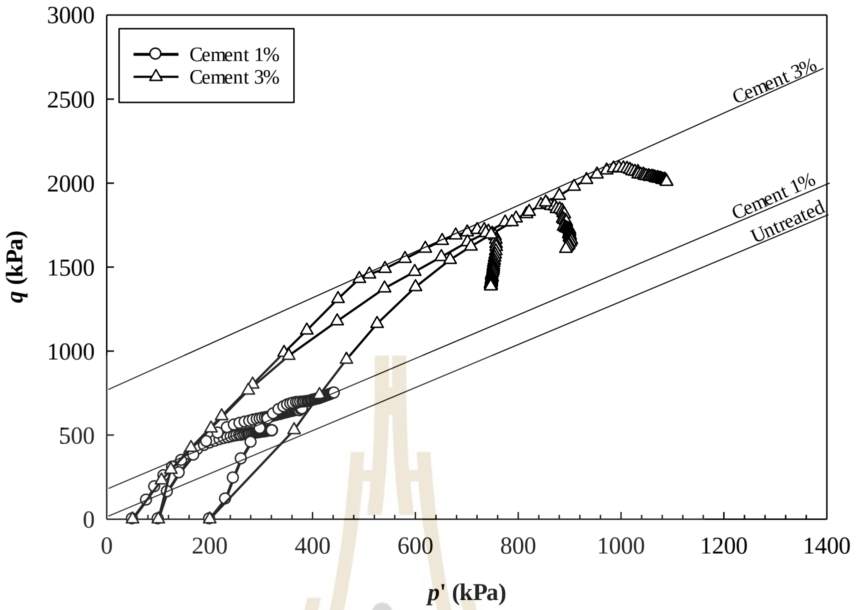

Figure 3.11 Undrained stress paths of unstabilized and cement stabilized lateritic soil

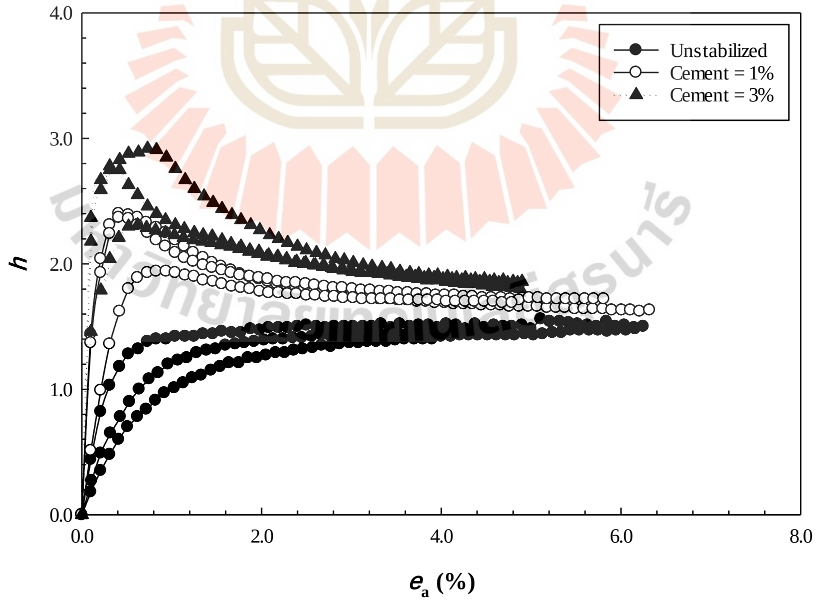

Figure 3.12 Stress ratio versus axial stain relationship of unstabilized and stabilized lateritic soil samples

The effect of RAP replacement ratio on shear strength improvement is determined as follows:

$$\Delta q = q_R - q_S \tag{3.7}$$

where q_R is the deviator stress of RAP-soil blends samples and q_S is the deviator stress of the lateritic soil at the same axial strain level in similar test condition. The relationship of Δq versus axial strain of both unstabilized and cement stabilized RAP-lateritic soil samples under 200 kPa confining pressure is shown in figure 3.14. For unstabilized samples, Δq was higher for higher RAP replacement ratio because the increased RAP replacement ratio caused denser particle package and lower void ratio. For low cement content of 1%, except RAP10 sample, Δq decreased initially to the lowest value and then increased sharply to the peak value before levelling off.

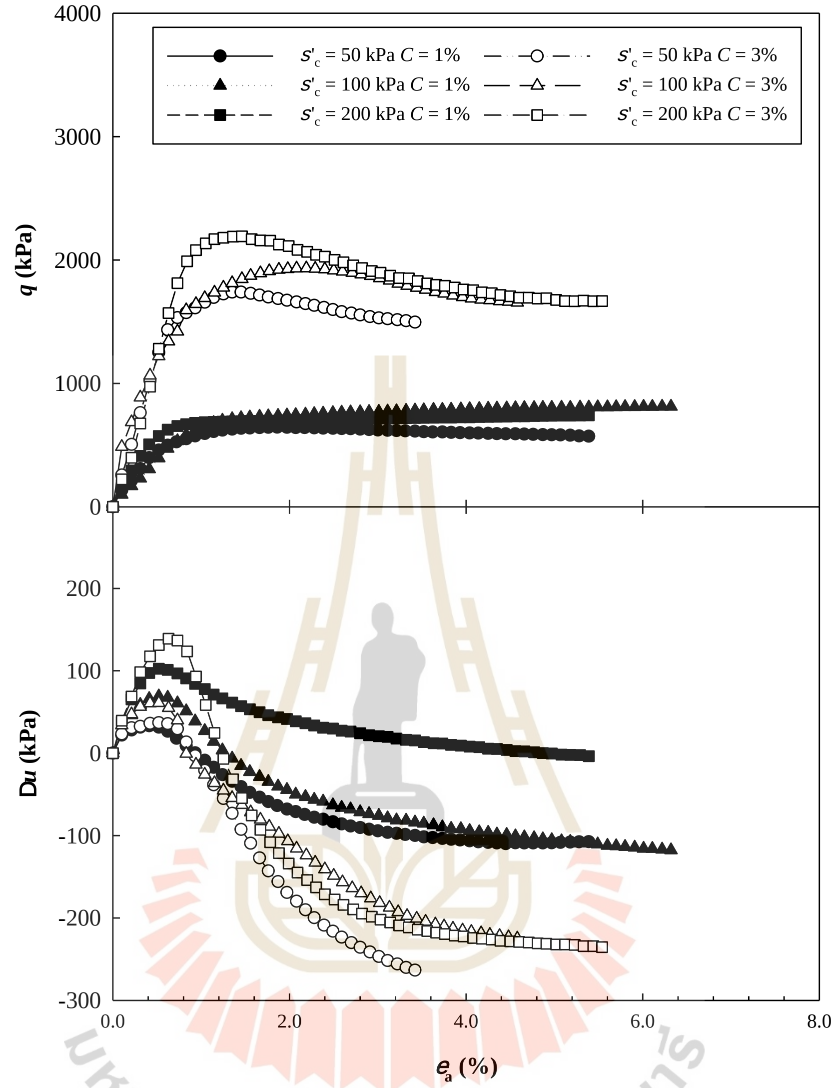

4000
3000
2000
1000
0
q (kPa)
s'c = 50 kPa C = 1%
s'c = 100 kPa C = 1%
s'c = 200 kPa C = 1%
s'c = 50 kPa C = 3%
s'c = 100 kPa C = 3%
s'c = 200 kPa C = 3%
200
100
0
-100
-200
-300
Du (kPa)
0.0
2.0
4.0
6.0
8.0
ea (%)

(a)

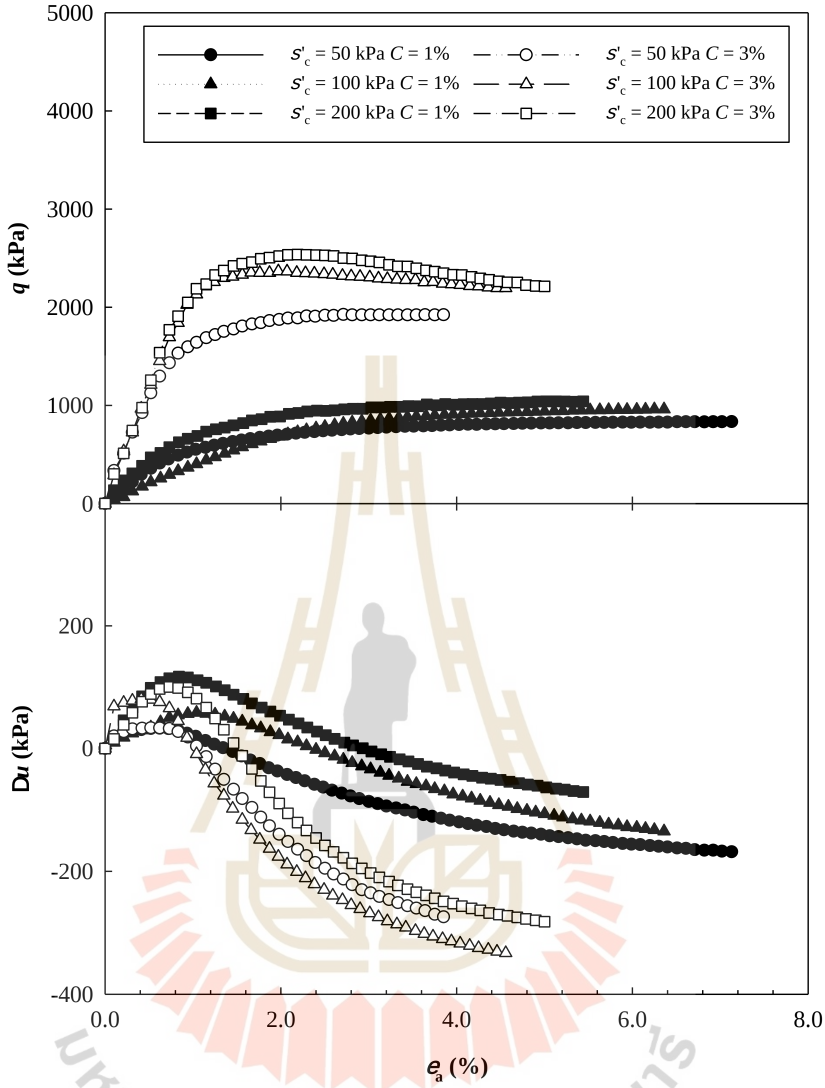

5000
4000
3000
2000
1000
0
q (kPa)
s'c = 50 kPa C = 1%
s'c = 100 kPa C = 1%
s'c = 200 kPa C = 1%
s'c = 50 kPa C = 3%
s'c = 100 kPa C = 3%
s'c = 200 kPa C = 3%
200
0
-200
-400
Du (kPa)
0.0
2.0
4.0
6.0
8.0
ea (%)

(b)

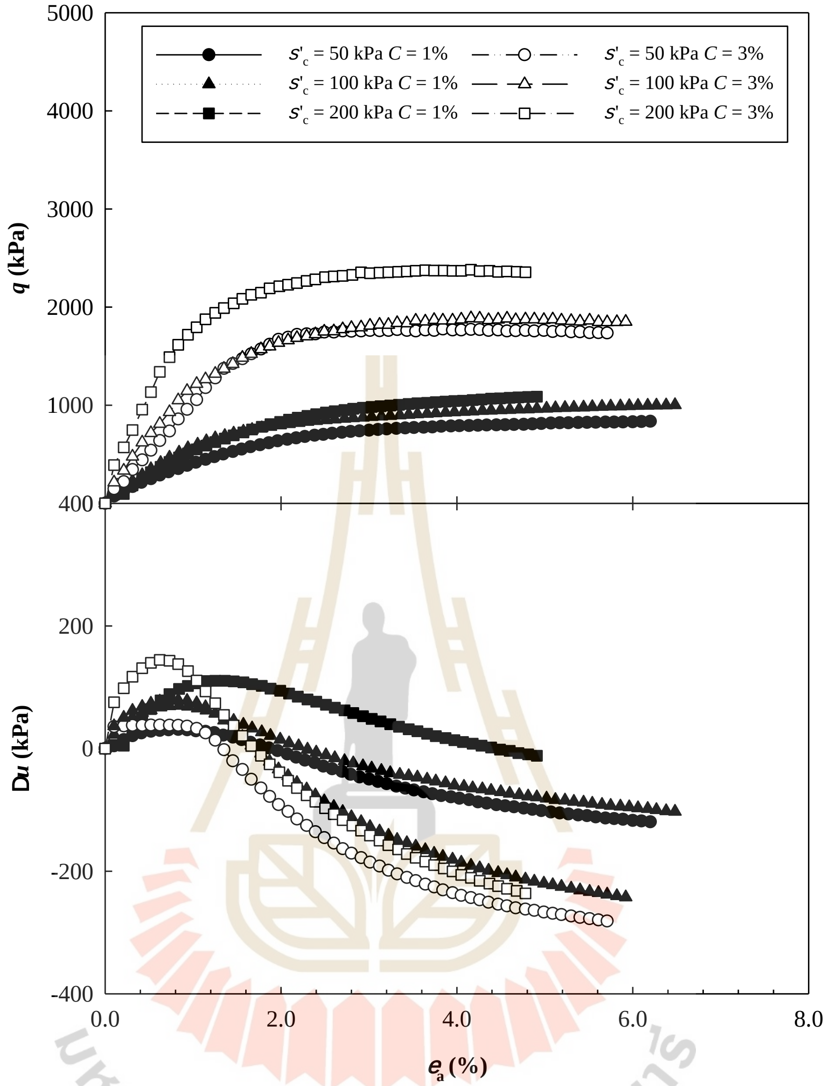

(c)

Figure 3.13 Undrained behavior of cement stabilized RAP-soil blends: (a) RAP10 (b) RAP30 (c) RAP50

The decrease of Δq at the initial stage indicated that slope of stress-stain curve of cement stabilized RAP-soil blends was lower than that of cement stabilized lateritic soil. In other words, the gentle strength development at the initial stage was found for RAP10 while the significant strength development associated with lower stiffness was found for RAP30 and RAP50 samples. The shear strength improvement at larger strain was more with the increased RAP replacement ratio for both the unstabilized and stabilized RAP-soil samples. With strain-softening behavior in deviator stress and axial strain relation for 3% cement samples, Δq of RAP10 and RAP30 samples decreased after the peak value. On the other hand, Δq of RAP50 sample increased gradually even with the increase in strain due to strain-hardening behavior. It is clear that Δq increased with the increased RAP replacement ratio for both unstabilized and cement stabilized RAP-soil blends. Due to high energy absorption of asphalt binder, the more delay in Δq of cement stabilized RAP-soil blends was found at initial stage as the RAP replacement ratio increased. Eventually, the strength development of cement stabilized RAP-soil was mobilized at larger strain due to interlocking. The result

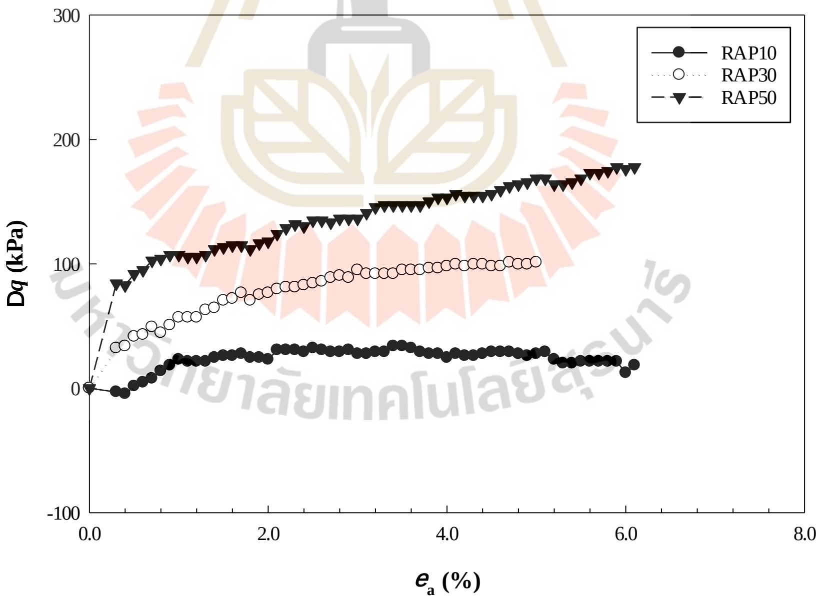

(a)

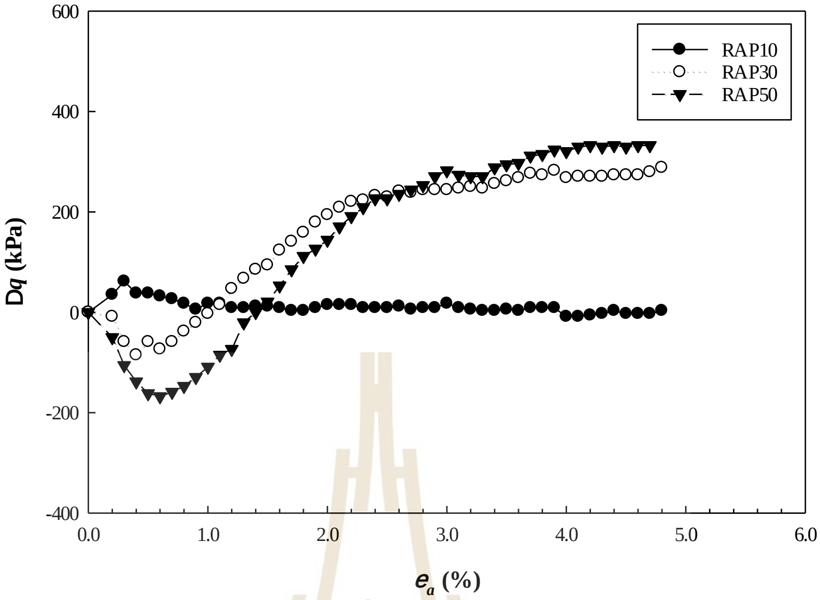

(b)

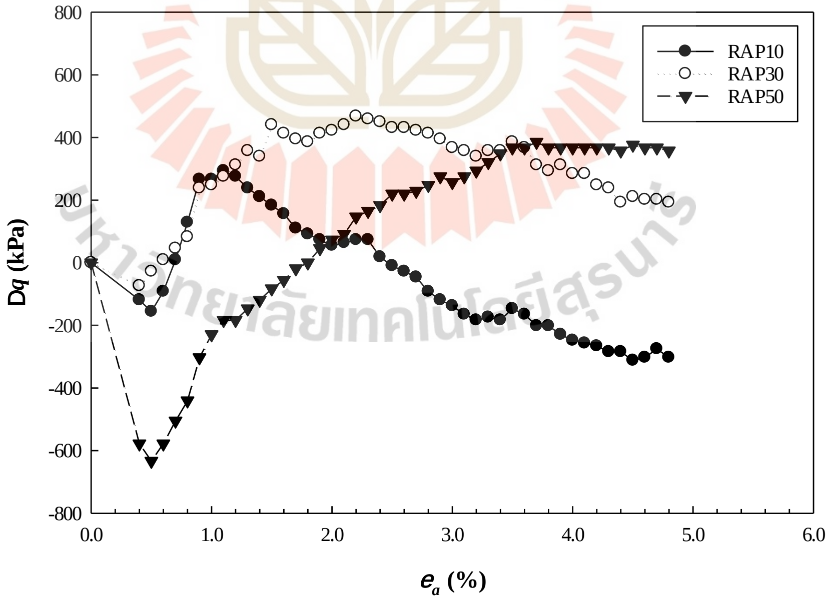

(c)

Figure 3.14 Strength improvement under 200 kPa confining pressure : (a) unstaibilized blends (b) 1% cement stabilized blends (c) 3% cement stabilized blends

The variation in shear improvement as discussed early indicated the lower slope of stress-stain curve of cement stabilized samples when RAP replacement ratio increased. To evaluate the effect of RAP replacement on stiffness of cement stabilized RAP-soil blends, the initial tangent modulus (E_i) of the blends with various RAP replacement ratios and cement contents was compared. The E_i of stabilized materials is typically steeper with an increase of confining pressure. The normalized initial tangent modulus by atmosphere pressure (P_a = 101.3 kPa) is employed to evaluate the stiffness of the cement stabilized RAP-soil blends. The relationship between E_i versus confining pressure normalized by P_a in log-log scale is shown figure 3.15 and can be expressed in term of power function (Janbu, 1963) as follows :

$$E_i = k.P_a\left(\frac{\sigma'_c}{P_a}\right)^n \tag{3.8}$$

where k is the intercept at $\frac{\sigma'_c}{P_a} = 1$ and n is slope.

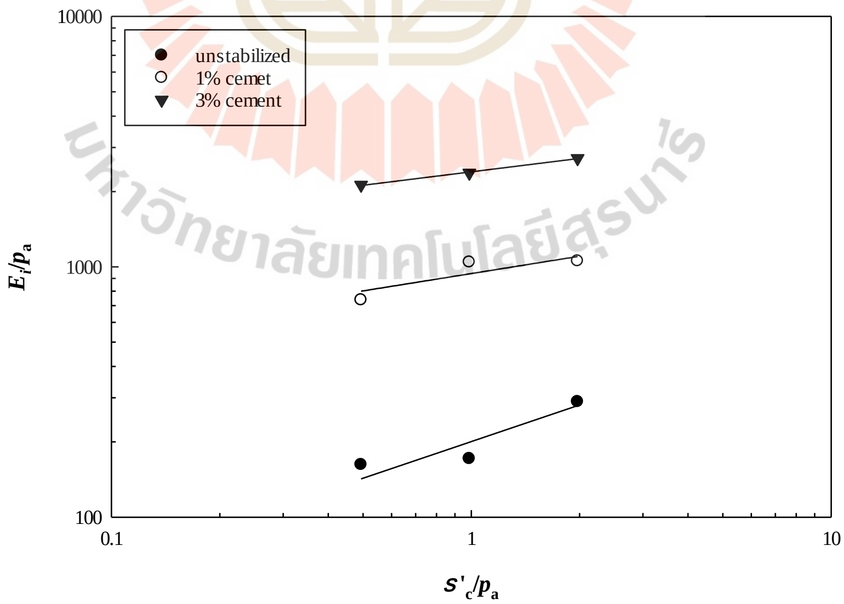

(a)

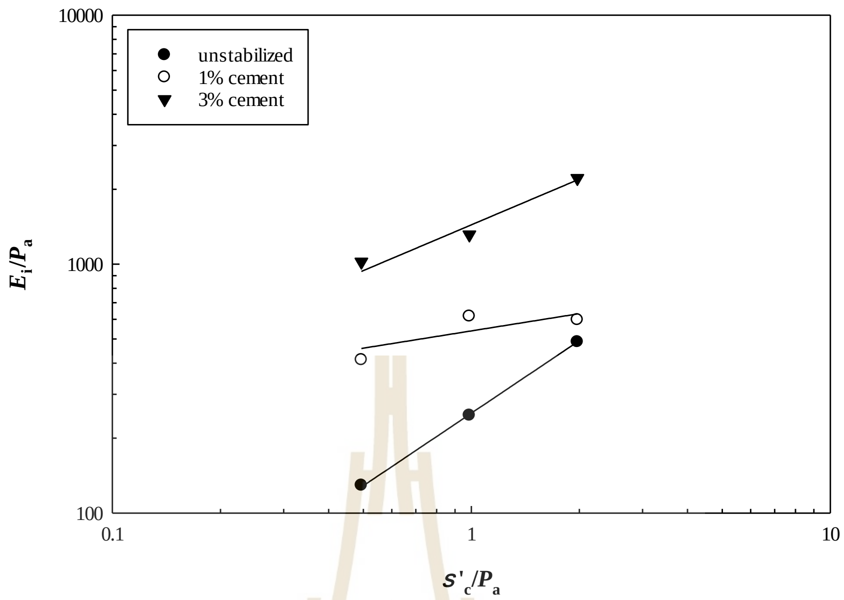

(b)

Figure 3.15 Normalized initial stiffness versus normalized effective confining pressure: (a) lateritic soil (b) RAP50

Table 3.4 summarizes result of E_i for unstabilized and cement stabilized RAP-soil blends. The relationship of coefficient of *k* versus RAP replacement ratios is shown in figure 3.16. As expected, *k* of unstabilized samples gradually increased with RAP replacement ratio associated with the increased shear improvement. With higher cement content, at the same RAP replacement ratio, *k* increased because the higher cementation bond strength induced more resistance to deformation during shear (higher slope stress-strain curve). The increase of *k* value with cement content is in agreement with the result of cement stabilized sand reported by previous studies (G. Wayne Clough, Sitar, Bachus, & Rad, 1981; Fernando Schnaid, Pedro D. M. Prietto, & Nilo C. Consoli, 2001). However, *k* of cement stabilized RAP-soil blends decreased with the increased RAP replacement ratio. Hoy, Horpibulsuk, and Arulrajah (2016) investigated the microstructure of RAP using scanning electron microscope and indicated that asphalt binder partly coated the surface of aggregate and hence resulted in lower stiffness. The reduction of stiffness associated with shear strength improvement increased at large strain when RAP replacement ratio increased for cement stabilized RAP-soil blends implied that the allowable working strain of composite ground can be extend.

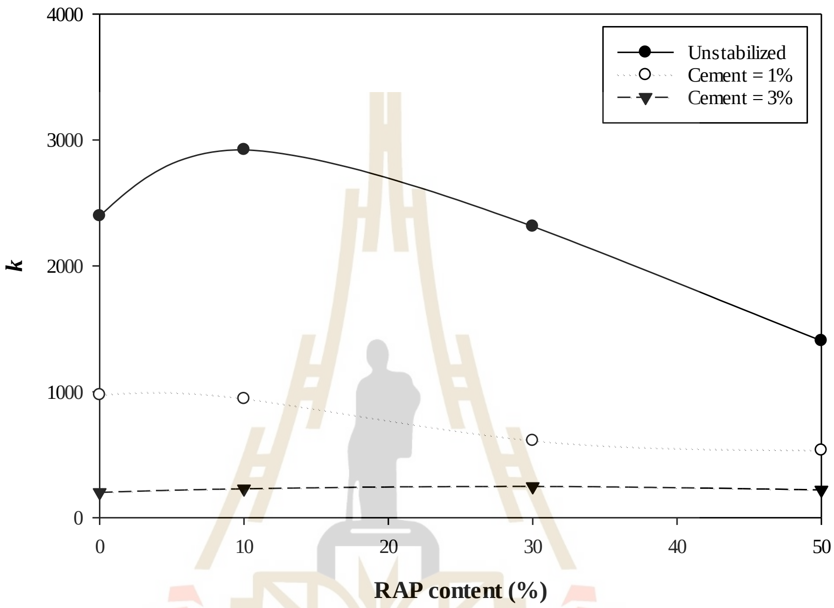

Figure 3.16 Effect of RAP on *k* value

Table 3.4. Values of stiffness parameter

Sample Name	RAP content (%)	Cement, *C* (%)	*k*	*n*
LS100	0	0	201.14	0.4181
		1	975.26	0.2581
		3	2397.1	0.1767
RAP10	10	0	229.56	0.445
		1	945.07	0.2378
		3	2922.9	0.231
RAP30	30	0	247.98	0.6753
		1	611.5	0.1481

Table 3.4. Values of stiffness parameter (Continued)

Sample Name	RAP content (%)	Cement, C (%)	k	n
		3	2315.4	0.124
RAP50	50	0	219.8	0.9679
		1	534.89	0.2677
		3	1405	0.5687

3.5 Conclusions

This study presents the evaluation of cement stabilized recycled asphalt pavement/marginal lateritic soil blends for soft clay improvement. The undrained shear response of the blended materials at various RAP replacement ratios and effective confining pressures were discussed. The conclusion of this investigation can be drawn as follow:

1) The unstabilized RAP-soil blends exhibited strain-hardening behavior in deviator stress versus axial stain relation associated strain-softening behavior in excess pore water pressure versus axial strain relation. The transitional response from strain-hardening to strain-softening behavior in deviator stress versus axial strain was found when cement contents increased.

2) The failure envelope of unstabilized RAP-soil blends was steeper with the increased RAP replacement ratio while the cohesion (c') was zero for unstabilized samples. For cement stabilized samples, the cohesion increased with the increased cement content while the friction angle was insignificantly changed.

3) The shear strength improvement increased with the increased RAP replacement ratio. The shear strength improvement of cement stabilized RAP-soil blends was more delay at initial stage as RAP replacement ratio increased. Eventually, the shear strength improvement was mobilized at larger axial strain due to interlocking.

4) Stiffness of unstabilized RAP-soil blends increased with RAP replacement ratio associated with the increased shear strength improvement. Meanwhile, stiffness decreased with increased RAP replacement ratio for cement stabilized samples. The reduction of stiffness of cement stabilized RAP-soil blends associated with delay shear strength improvement at initial and can be extended allowable working strain of composite ground.

CHAPTER IV

DRAINED SHEAR RESPONSE OF CEMENT STABILIZED RECYCLED ASPHALT PAVEMENT-LATERITIC SOIL BLENDS

4.1 Statement of problems

Over the past few years, the consumption of construction materials for infrastructure construction projects has increased with economic growth. Recently, engineers have been seeking for more natural resources to be construction materials. Extracting natural resources and manufacturing construction materials is an activity that generates carbon footprint emissions (Labaran, Mathur, Muhammad, & Musa, 2022). While, construction and deconstruction activity produces enormous waste materials, which are generally deposited in an available landfill, and directly impacted the environment. Construction and demolition (C&D) materials are defined as solid waste debris obtained from various construction and demolition activities (Response & Associates, 1998). The C&D materials are possibly reused as alternative construction materials (Vieira & Pereira, 2015). The C&D is widely reused for construction materials not only because of being environmentally friendly but also economical. Researchers and engineers have assessed the potential usage of various types of abundant C&D materials over the past two decades (Arulrajah, Disfani, Horpibulsuk, Suksiripattanapong, & Prongmanee, 2014; Chesner, Collins, MacKay, & Emery, 2002).

Recycled Asphalt Pavement (RAP) is a C&D material generated during the demolition of aged hot-mixed asphalt pavement. RAP consists of majority aggregate and partially of hardening asphalt binder. Over service life, the asphalt binder is subjected to variations of the physicochemical process and becomes stiffer. According to the National Asphalt Pavement Association (NAPA) (Williams & Willis, 2020), 89.2 million tons of RAP were reused in the USA in 2019. Using RAP in a new asphalt mixture can save greenhouse gas emissions of 2.4 million tons of CO_2e (Williams & Willis, 2020). European Asphalt Pavement Association (EAPA) reported that 46 million tons of RAP were widely reused in European countries in 2020. 64% of RAP were reused for new asphalt pavement surface, and 33% for unbound layers and the rest for other civil engineering works (European Asphalt Pavement Association, 2019).

Regarding road base construction materials, the proper percentage of RAP can mix with traditional or marginal aggregates for both unbound and bound pavement applications. Several researchers conducted a comprehensive laboratory to assess engineering properties of RAP-aggregate blends. Guthrie, Cooley, and Eggett (2007) revealed that the excessive RAP contents significantly decreased the strength and stiffness of the RAP/aggregate blends. However, the appropriate RAP content can provide the satisfied result and meet strength requirement for subbase materials (Taha, Ali, Basma, & Al-Turk, 1999).

Because of the rapid strength development and economics, cement stabilization is the traditional soil improvement technique. Jirayut, Aniroot, and Suksun (2014) evaluated effect of cement content and RAP content on unconfined compressive strength (UCS) of RAP/marginal lateritic soil mixture. They revealed that the proper amount of RAP could improve the mechanical properties of the cement stabilized marginal lateritic soil. Yang and Wu (2014) reported a similar result, revealing UCS of RAP-aggregate mixture increased at a low proportion of RAP. Increase of UCS of RAP-aggregate mixture with cement content was also reported by several previous study (Ghanizadeh, Rahrovan, & Bafghi, 2018; Taha, Al-Harthy, Al-Shamsi, & Al-Zubeidi, 2002; Yuan, Nazarian, Hoyos, & Puppala, 2011).

Aside from Portland cement stabilization, geopolymers technique can improve the geomechanical properties of RAP-soil samples. The role of fly ash content on the geomechanical properties of RAP-soil stabilized with sodium hydroxide and sodium silicate solution as a liquid alkaline activator was investigated by Adhikari, Khattak, and

Adhikari (2020). They revealed that RAP-soil geopolymer can be an alternative stabilized road base material. Hoy, Horpibulsuk, and Arulrajah (2016) reported a similar result of RAP-fly ash geopolymer. They revealed that the UCS increased as the sodium hydroxide to sodium silicate ratio decreased.

RAP can be also used as concrete aggregate as reported by Hassan, Brooks, and Erdman (2000). Even though the compressive and tensile strengths reduced as RAP increased, RAP could enhance ductility and strain absorption. The scanning electron microscopic (SEM) image showed the interfacial transition zone, which significantly affected the reduction of concrete's compressive strength and elasticity when RAP was utilized (Soltanabadi & Behfarnia, 2022). Chaidachatorn, Suebsuk, Horpibulsuk, and Arulrajah (2019) evaluated the influence of RAP on the compressive strength development of cement mortar. They revealed that using RAP as fine aggregate can increase the compressive strength of cement mortar at a low water to cement ratio (w/c). Contrary, due to high water absorption of RAP the compressive strength of cement mortar decreased at higher (w/c).

Recently, Aniroot and Suksun (2022) investigated undrained shear behavior of cement stabilized RAP-soil samples alternative to the conventional stone column aggregate. They revealed that the strength and stiffness were significantly affected by cement content and RAP replacement ratio. The results indicated that RAP increased the shear strength of lateritic soil and the maximum shear stress was mobilized at a larger strain. However, the stiffness of RAP-soil samples significantly decreased with the excessive RAP replacement ratio due to high energy absorption of asphalt binder.

This study aims to further investigate drained shear behavior of cement stabilized RAP-soil samples to obtain complete picture on shear response of cement stabilized cement stabilized RAP-soil samples when used under low to high confining stresses in pavement and ground improvement applications. The marginal lateritic soil was improved by RAP replacement at 10%, 30%, and 50% by dry weight. Portland cement type I at 1% and 3% were used to stabilize RAP-soil samples. Drained triaxial compression tests were conducted on unstabilized and cement stabilized RAP-soil samples under various effective confining pressures from 50-200 kPa.

4.2 Materials and experimental methodology

The lateritic soil was sourced from a borrow pit in Nakhon Ratchasima, Thailand. The lateritic soil contained 16% gravel, 59% sand, and 25% fine fraction. Lateritic soil's liquid and plastic limits were 32% and 16%, respectively. Recycled asphalt pavement (RAP) was collected from the rehabilitation of aged asphalt pavement from Nakhon Ratchasima, Thailand. RAP was non-plastic debris composed of aggregate coating with AC60-70 asphalt binder of about 7%. The gradation curves of lateritic soil and RAP are presented in Figure 4.1. The average grain size lateritic soil was smaller than that of RAP; RAP was composed of 45% gravel, 43% sand and 2% fine. The process of removing RAP from old asphalt pavement road, by recycling machines, results in the presence of fine particles. Associated with Unified Soil Classification System (USCS), RAP and lateritic soil were classified as well-graded sand (SW) and clayey sand (SC), respectively. The cement contents at 1% and 3% dry weight were used to stabilize the blends. RAP was used to replace the lateritic soil at the replacement ratios of 10%, 30%, and 50% by dry weight.

To determine the compaction characteristic of RAP-soil samples, the compaction test was conducted at various RAP replacement ratios. The result of the compaction test under modified Procter energy effort is shown in Figure 4.2. The results showed that maximum dry density (MDD) slightly increased while optimum water content (OWC) decreased with the increased RAP replacement ratio. This was due to fine fraction of lateritic soil filling the RAP aggregate's void space, resulting in denser packing. Moreover, RAP partially coated with asphalt binder caused low water absorption.

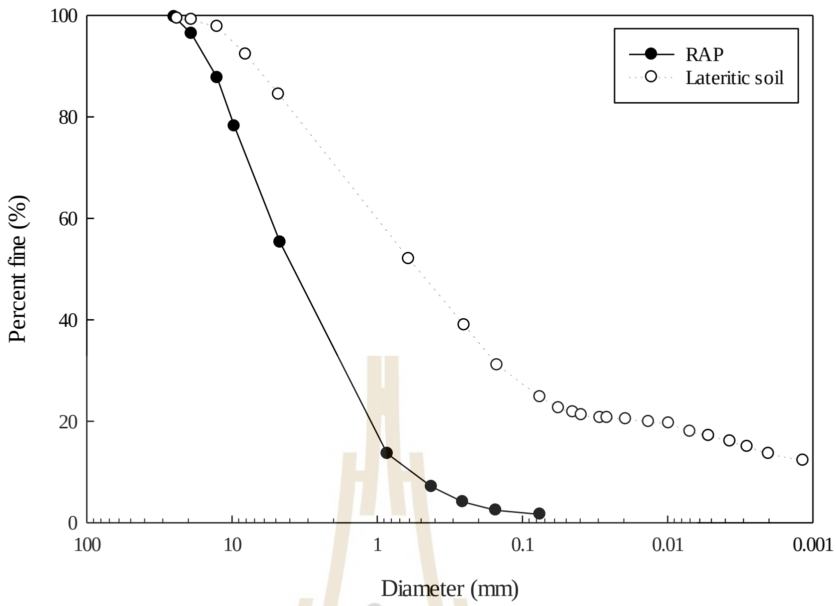

Figure 4.1 Grained sized distribution of RAP and Lateritic soil

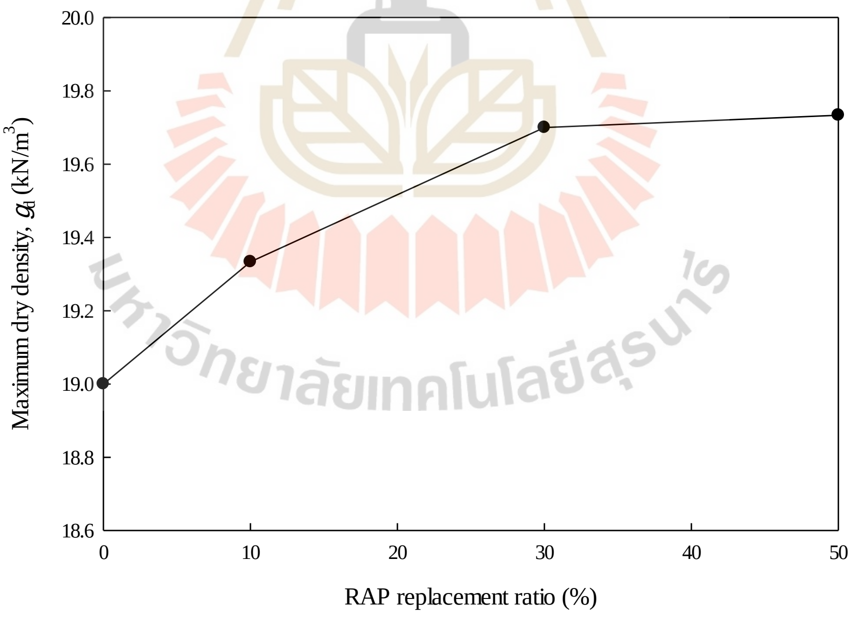

(a)

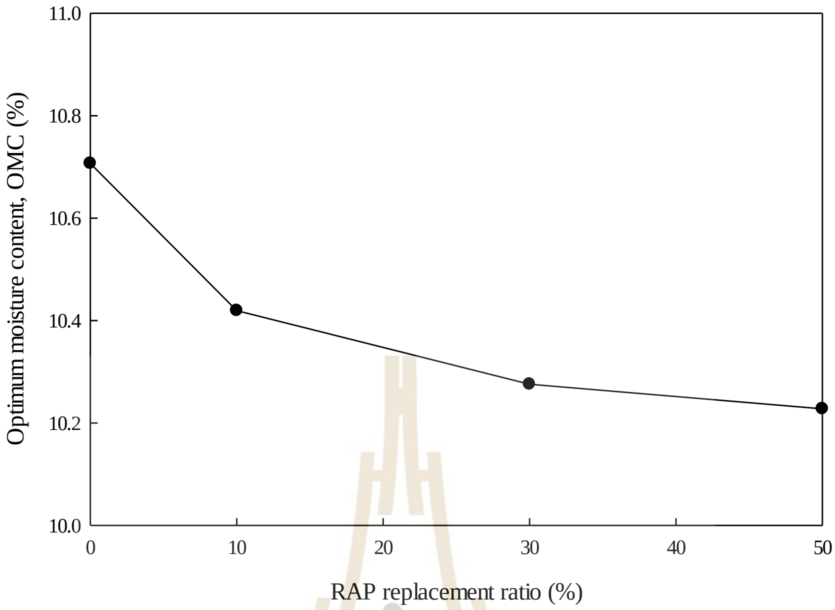

(b)

Figure 4.2 Effect of RAP replacement ratio on compaction charecterisitic (a) Maximum dry density (b) Optimum moisture content

The triaxial specimens were prepared by compacting the blends into a cylinder mold. The larger aggregates of lateritic soil and RAP were screened by sieving through standard sieves #4 and #3/4, respectively. Dry lateritic soil, RAP, and cement were first mixed thoroughly. A desired amount of water was then added into the mixture to achieve the OWC and mixed thoroughly. The mixture was filled into a steel spilled mold with a diameter of 50 mm and 100 mm high, then compacted into three layers to achieve its MDD. The specimens were then extruded, and sealed with plastic wrap immediately. The cement stabilized specimens were next cured at humid room for 28 days while the unstabilized specimens were tested after three days of curing. The triaxial consolidated drained tests were conducted on the specimens following the testing procedure in ASTM D7181. After setting up of the specimen completely done, the testing procedure was divided into three states. Firstly, the specimens were saturated by increased cell and back pressure simultaneously while effective stress was maintained at approximately 10 kPa. Skempton's parameter *B* was checked before shearing. When the *B* value was achieved of 0.95 for unstabilized and 0.90 for cement stabilized specimens, the specimens were consolidated to the desired effective stress of 50, 100, and 200 kPa. After the consolidation, the specimens were sheared with a very low constant shear rate of 0.10 mm/min. The shearing rate is sufficient to allow water to drain out of specimens during shear and ensure excess pore pressure will not generate.

4.3 Results and discussion

This study investigated the drained shear behavior on unstabilized and cement stabilized RAP-soil samples. The typical drained shear response of unstabilized stabilized RAP-soil samples is presented in Figure 4.3. The stress-strain curve of unstabilized RAP-soil samples exhibited strain-hardening behavior in the q-e_a relationship whereas the deviator stress increased with axial strain in which the peak deviator stress is unclear. Increasing effective confining pressure results in a higher deviator stress and stiffness. Compared with the same effective confining pressure, an increased RAP replacement ratio increased the deviator stress value at a given axial strain.

The relationship between the volumetric strain versus axial stain of unstabilized RAP-soil blend at various effective confining pressures is presented in Figure 3. The volumetric responses of unstabilized RAP-soil samples were dependent upon the effective confining pressure level. The result showed that at 50 kPa confining pressure, the specimens contracted initially before dilating (expanded) at a large strain. When effective confining pressure increased, the specimen sustainably contracted throughout the test. It was expected that with low effective confining pressure and the breaking of aggregate, aggregates tend to slip each other, resulting in dilation. Contrary, the dilatation was suppressed when effective confining pressure increased. The drained shear behavior of unstabilized RAP-soil samples in this study is consistent with that of the typical loose to medium granular soil (Chu, 1995; Lo & Wardani, 2002).

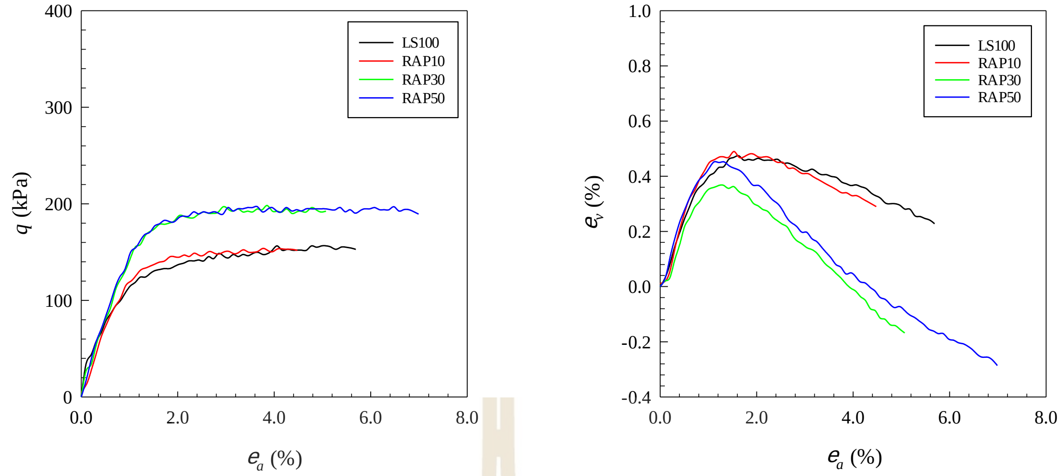
q (kPa)
e_a (%)
LS100
RAP10
RAP30
RAP50
e_v (%)
e_a (%)

(a)

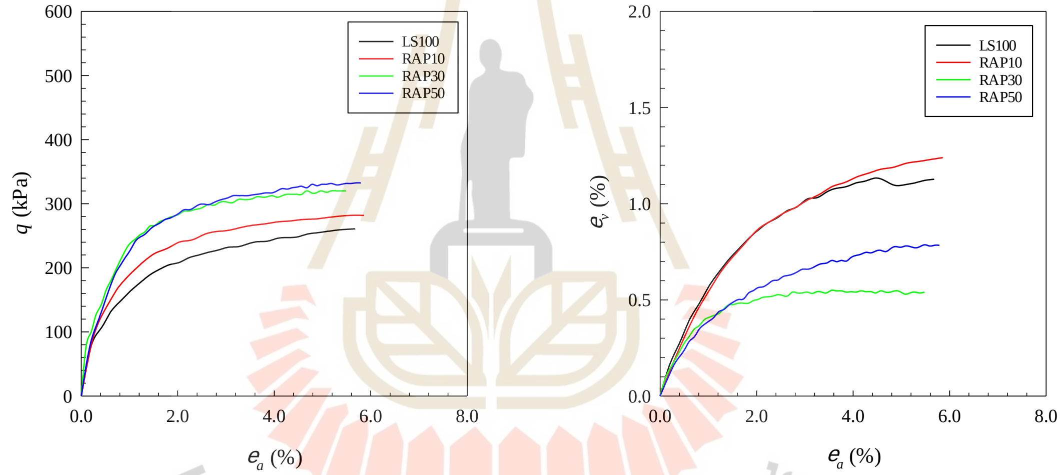
q (kPa)
e_a (%)
LS100
RAP10
RAP30
RAP50
e_v (%)
e_a (%)

(b)

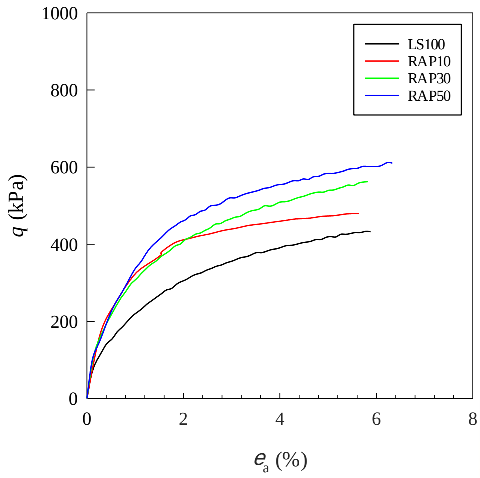

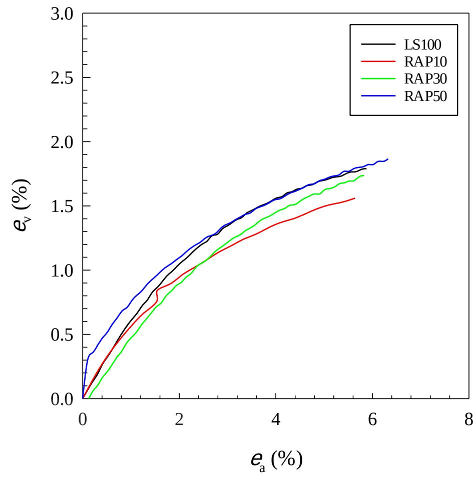

(c)

Figure 4.3 Typical drained shear behavior of unstabilized RAP-soil blends (a) 50 kPa (b) 100 kPa (c) 200 kPa

The typical drained shear response of cement stabilized RAP-soil samples is presented in Figures 4.4 and 4.5. At 1% cement content, RAP-soil samples exhibited a brittle response, indicated by strain-softening behavior in the q-e_a curve. The deviator stress increased linearly to the maximum value at a small strain then slightly decreased to a lower value. The brittle behavior approaches toward the ductile behavior when effective confining pressure increased due to the break-down of cementation bonding between soil particles (Lo & Wardani, 2002). The noticeable strain-softening behavior in q-e_a curve can be observed at higher cement content of 3% (Figure 4.5). The axial strain corresponding to the peak deviator stress was smaller than that for 1% cement samples. The deviator stress at post failure state decreased rapidly when compared with 1% cement samples. Noting that the strain-softening behavior in q vs e_a relationship can be found even at the highest effective confining pressure of 200 kPa. With stronger cementation bonds, 3% cement samples had large degree of strain-softening because of the large break-up of cementation bonds after the peak.

The volumetric response for cement stabilized RAP-soil samples is also presented in Figures 4.4 and 4.5. Unlike the unstabilized RAP-soil samples, the strain-softening behavior induced contractive-dilative behavior in e_v-e_a relationship. RAP replacement significantly increased the maximum compressive volumetric strain for the same effective confining pressure and cement level. In addition, the rate of dilation also increased with RAP replacement ratio. It was expected that the compressible asphalt binder in RAP resulted in more initial compression. At further axial strain, the interlocking effect and break-up of cementation caused a large dilatancy.

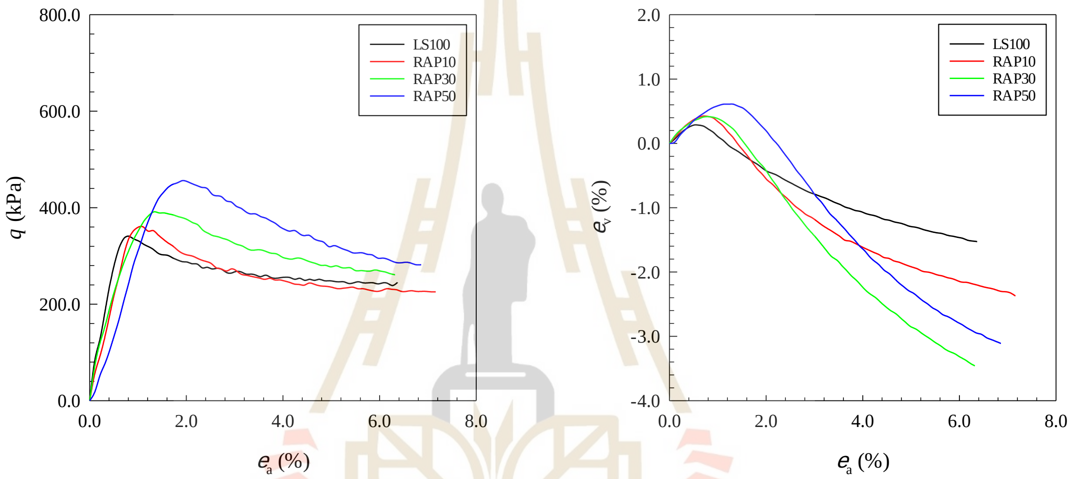

(a)

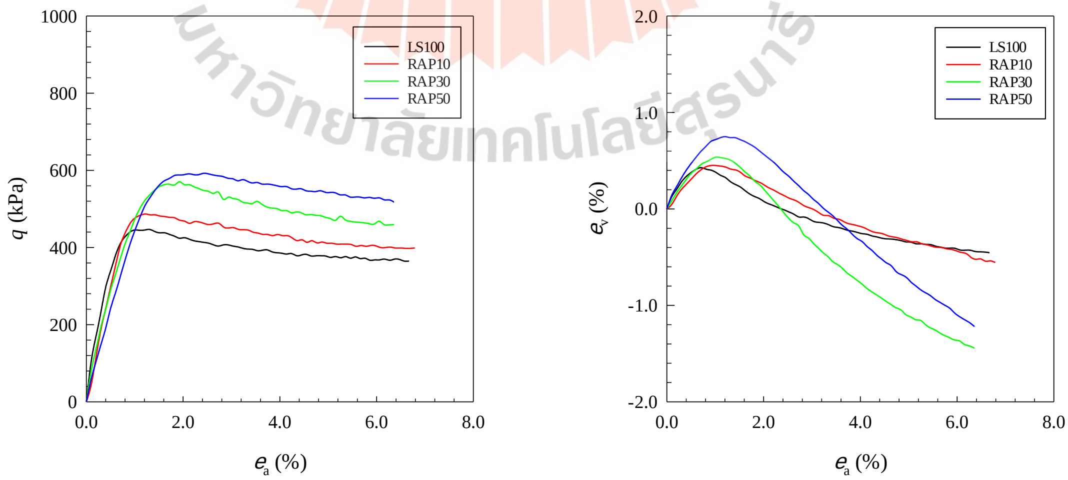

(b)

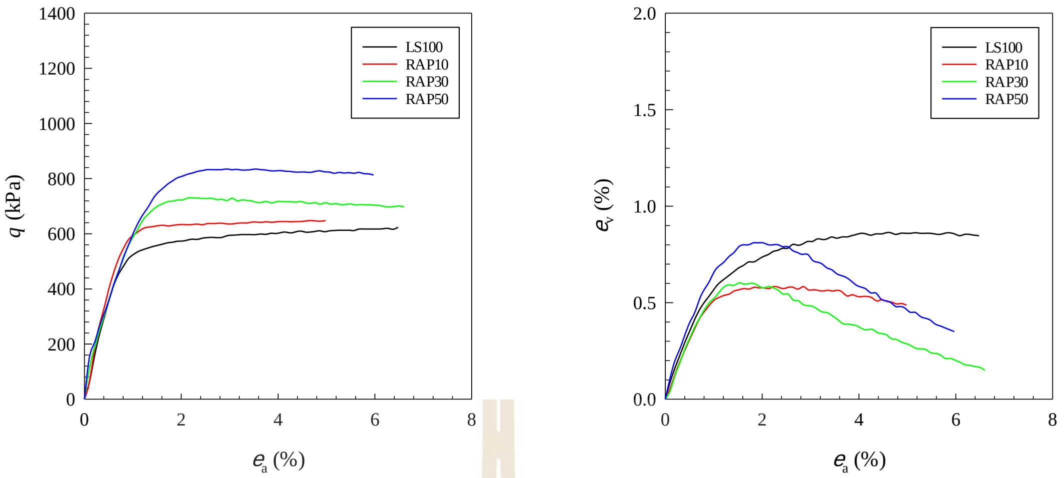

(c)

Figure 4.4 Typical drained shear behavior of 1% cement RAP-soil blends (a) 50 kPa (b) 100 kPa (c) 200 kPa

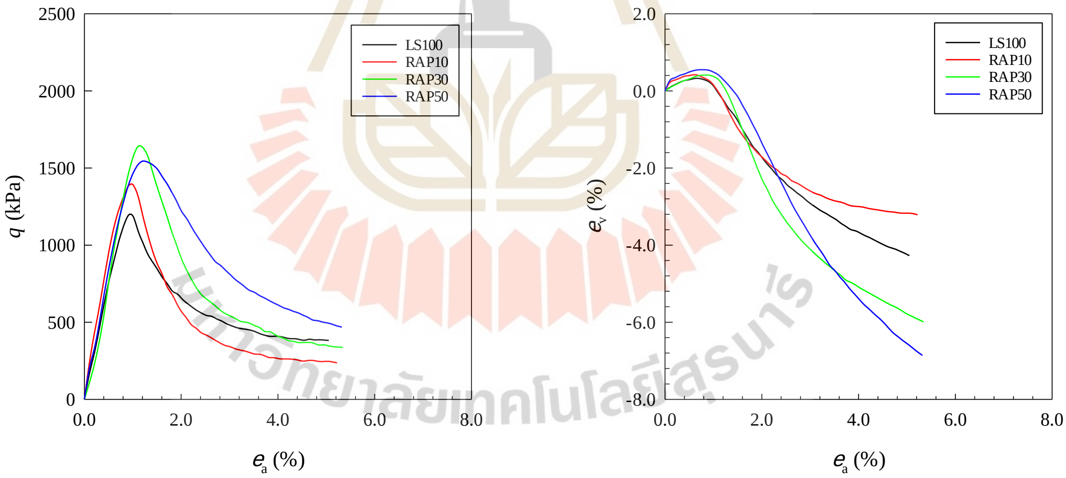

(a)

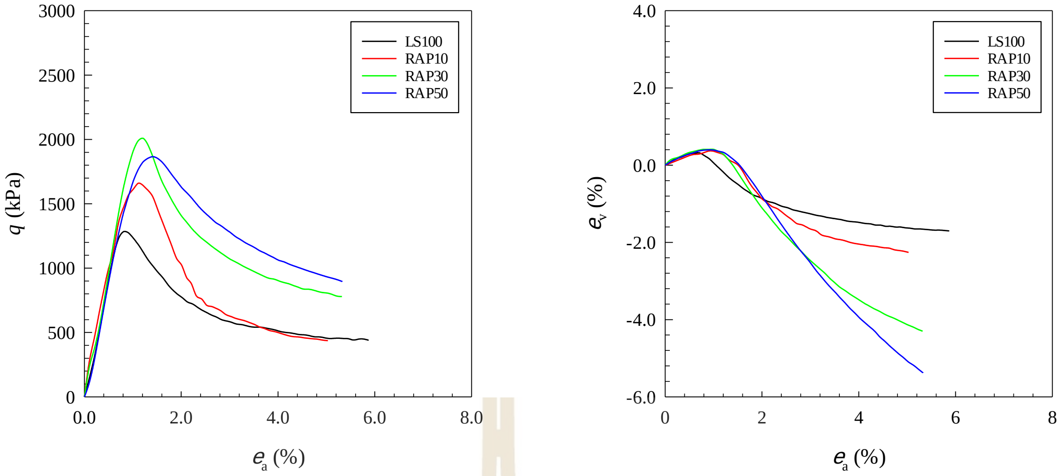

(b)

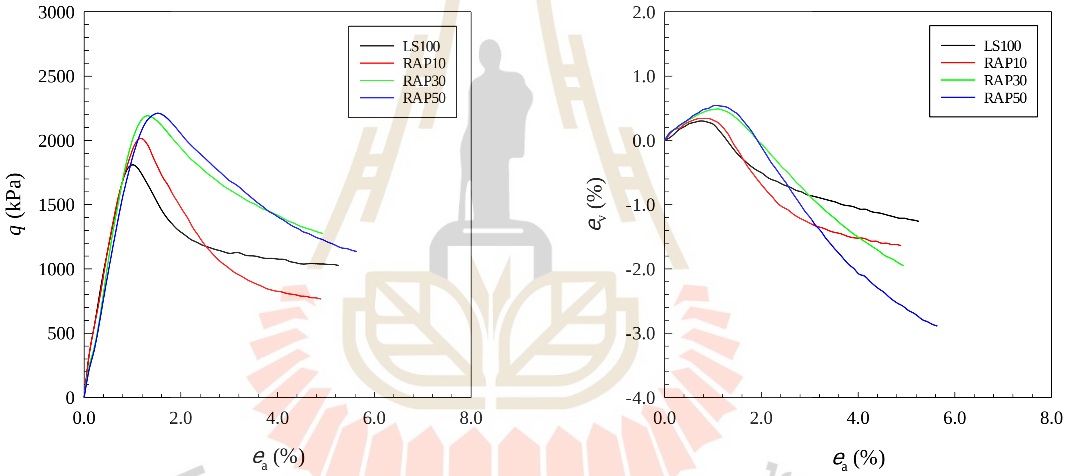

(c)

Figure 4.5 Drained shear response of 3% cement RAP-soil blends (a) 50 kPa (b) 100 kPa (c) 200 kPa

The examination of effect of RAP replacement on the stress-strain curve is presented in Figure 4.6. At the same effective confining pressure, the peak deviator stress increased with the increased RAP replacement ratio for both unstabilized and 1% cement stabilized RAP-soil samples. However, the same is not for 3% cement stabilized samples. The peak deviator stress decreased when RAP replacement ratio of 50%.

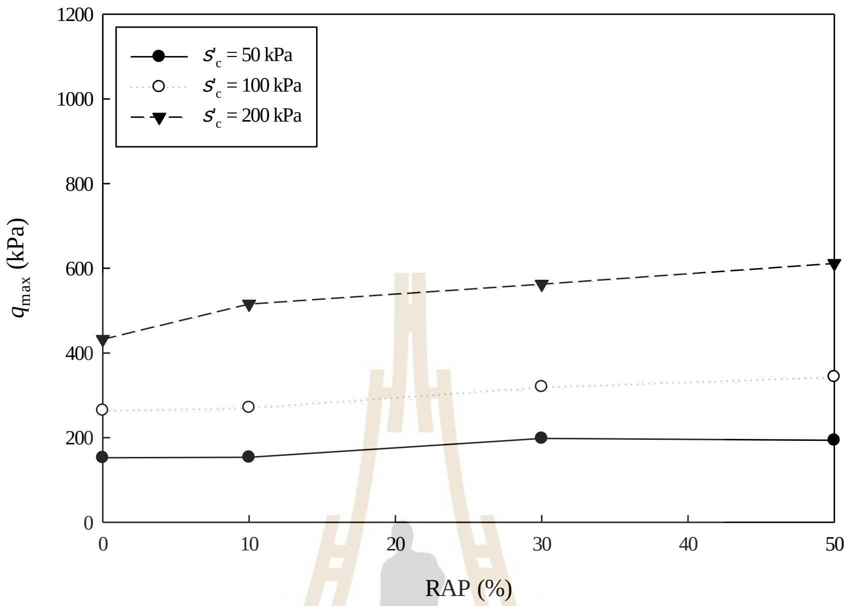
1200
1000
800
600
400
200
0
q_{max} (kPa)
s'_c = 50 kPa
s'_c = 100 kPa
s'_c = 200 kPa
0
10
20
30
40
50
RAP (%)

(a)

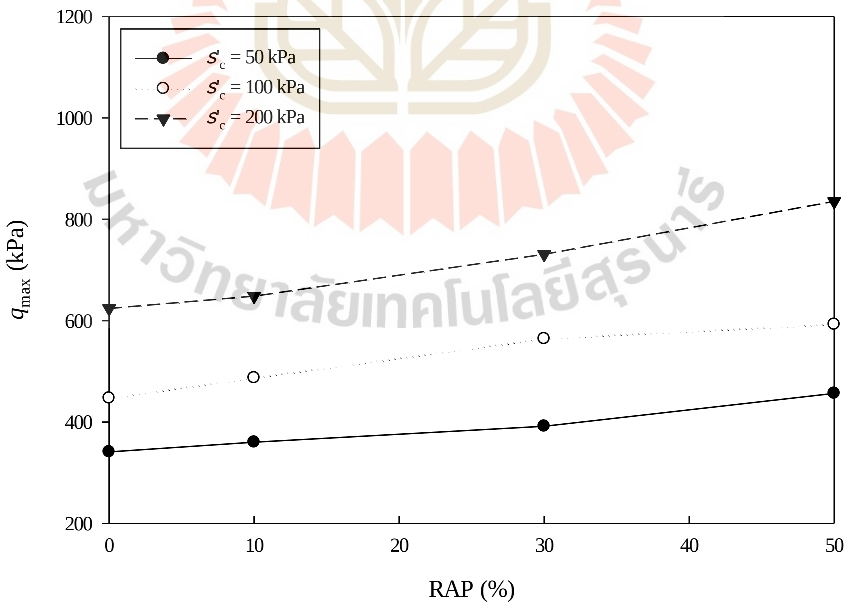
1200
1000
800
600
400
200
q_{max} (kPa)
s'_c = 50 kPa
s'_c = 100 kPa
s'_c = 200 kPa
0
10
20
30
40
50
RAP (%)

(b)

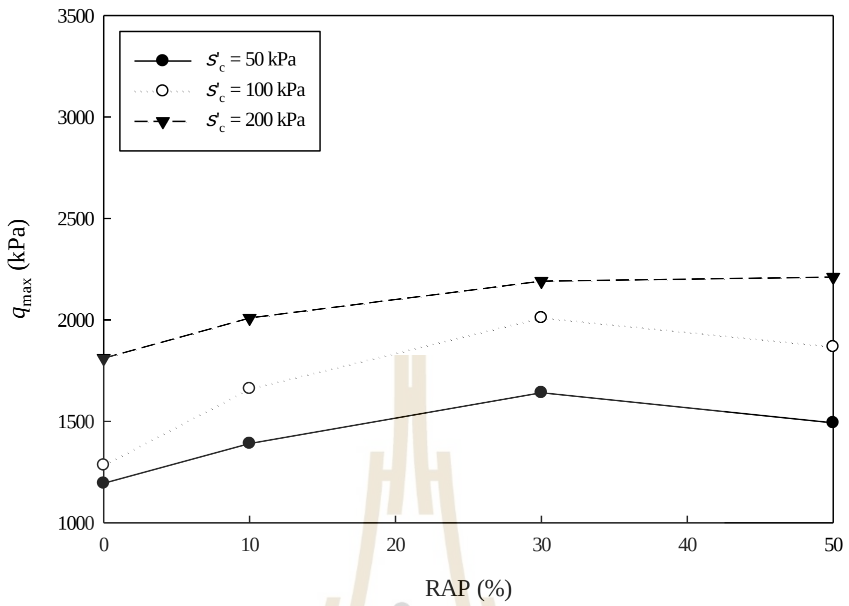

(c)

Figure 4.6 Effect of RAP replacement ratio on maximum deviator stress (a) unstabilized samples (b) cement 1% (c) cement 3%

To evaluate the effect of RAP on the post-failure of cement stabilized RAP-soil samples, the brittleness index, I_B is defined as follows (Consoli, Prietto, & Ulbrich, 1998):

$$I_B = \frac{q_f}{q_u} - 1 \tag{4.1}$$

where q_f is the peak deviator stress, q_u is the ultimate deviator stress. Eq.4.1 suggests that when I_B approaches zero, the values of deviator stress at peak and ultimate states coincide. On the other hand, I_B increase indicates a more brittle response. The variation of I_B calculated from Eq.4.1 with RAP replacement ratios for 3% cement stabilized specimens is presented in Figure 4.7. The result indicated that the brittle index increased with the increased RAP replacement ratio up to 10%. Beyond this, the RAP replacement ratio led to the increased ductility of the blends as indicated by the reduction of I_B with an increased RAP replacement ratio. It might be due to the asphalt binder hindering the rotating or sliding of crushed particles along a localized shear band.

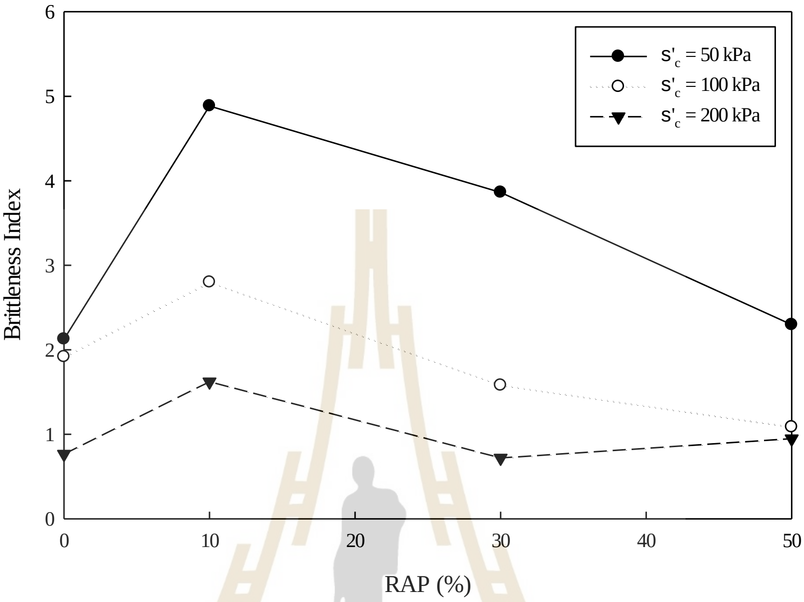

Figure 4.7. Effect of RAP on brittleness index of 3% cement RAP-soil blends

The stress paths of RAP-soil samples are shown in Figure 4.8. The undrained stress path from the specimens tested in the same effective confining pressures (Suksan and Horpibulsuk, 2022) was included for comparison. With the standard drained triaxial compression test, the drained stress path moved along the slope of 3:1 in q vs p' plane. The filled marks representing the state of stress at peak deviator stresses under the drained test were presented. The result showed that the difference in drained and undrained strengths depended on the cement level. Due to the decreased volume during shearing, the drained test provided a higher strength than the undrained test for unstabilized RAP-soil samples.

On the other hand, the initial void ratio of the cement stabilized samples was relatively low. The samples were compressed initially before expanding to a higher void ratio for the drained test. However, the large negative excess pore pressure was generated for the undrained specimen during shearing. The undrained stress path moved to the right side of the drained path and failed at higher strength. The difference in drained and undrained shear strengths in this study is similar to the result of cemented soil reported by Baxter, Sharma, Moran, Vaziri, and Narayanasamy (2011)

The failure envelope was determined by a best fit curve through peak strengths in the drained test. The higher cement content caused a greater peak shear strength. Thus, the intercept of the failure envelope at zero mean effective stress is expected to increase with cement content. The failure envelope for 1% cement samples was more or less parallel to unstabilized samples. Meanwhile, the gradient of the failure envelope significantly increased for 3% cement samples. Typically, the shear strength of cement stabilized soil is composed of two components: interlocking of soil particles and cementation bonding strength (Clough, Sitar, Bachus, & Rad, 1981; Coop & Atkinson, 1993; Horpibulsuk, Miura, & Bergado, 2004; Lo & Wardani, 2002; Schnaid, Prietto, & Consoli, 2001; Sukmak, Sukmak, Horpibulsuk, Arulrajah, & Horpibulsuk, 2023). Cementitious products for 1% cement content significantly increased cohesion but had a marginal effect on friction angle due to they only welding the interparticle contacts. A higher cement of 3%, cementitious products were sufficient to fill the void space, which caused an increase in both friction angle and cohesion. The effect of RAP replacement ratio on the failure envelope is presented in Figure 4.9. The result showed that the gradient of the failure envelope slightly increased with the increased RAP replacement ratio. The steepest slope of the failure envelope was found at RAP replacement ratio of 50%. However, the value of deviator stress at the interception of the failure envelope increased with the increase of RAP replacement ratio up to 30% and decreased when the RAP replacement ratio was 50%. Therefore, the decrease of peak deviator stress at RAP replacement ratio of 50% was only due to the reduction of interparticle bonds.

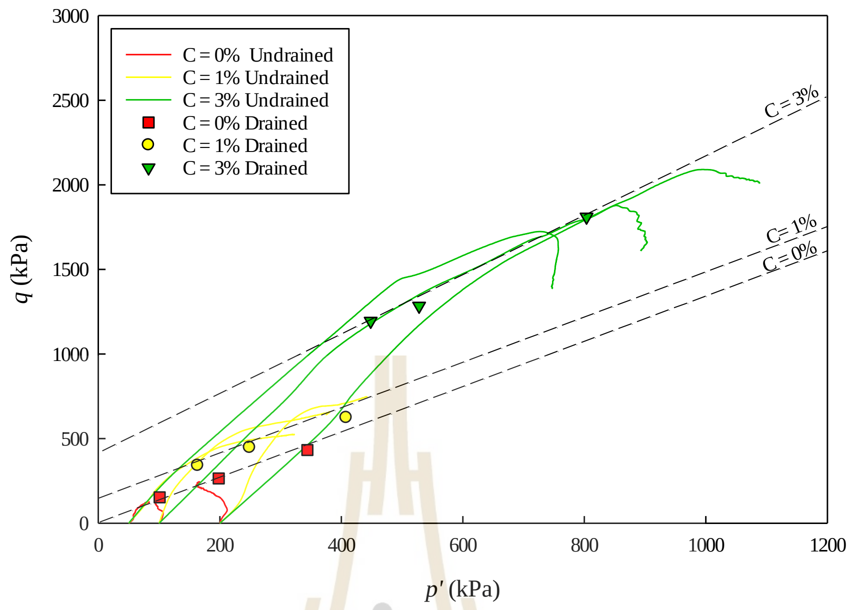

(a)

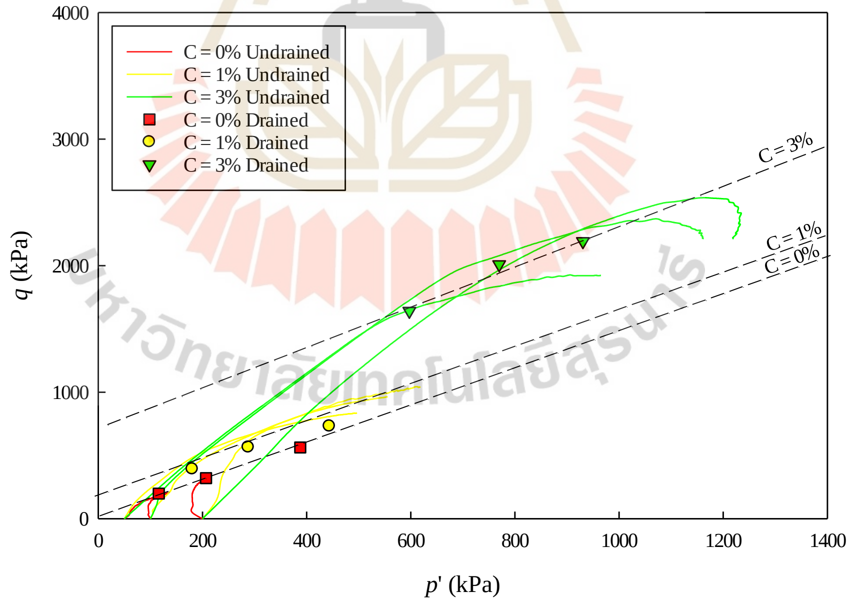

(b)

Figure 4.8 Drained and undrained stress path of RAP-soil blends. (a) Lateritic soil (b) RAP30

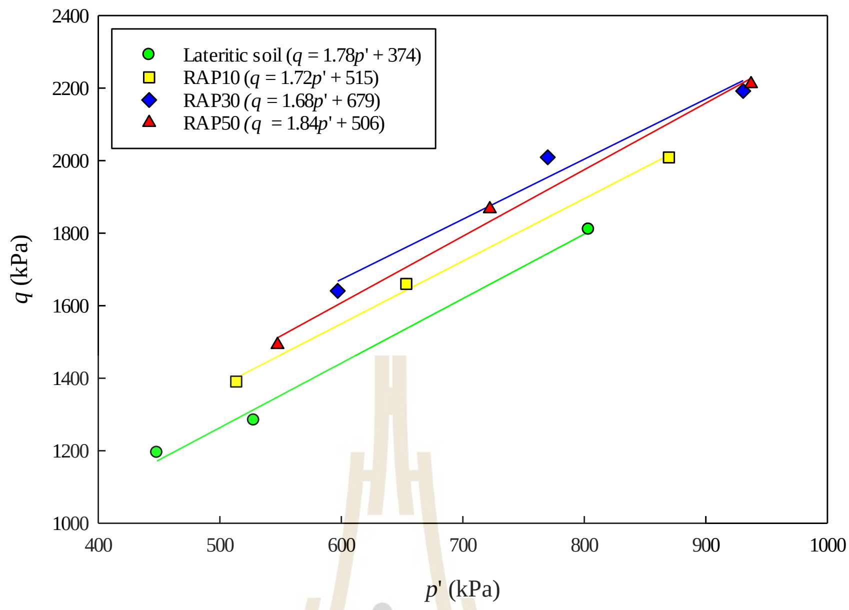

Figure 4.9 Failure envelope of cement stabilized RAP-soil blends cement of 3%

Dilatancy is an essential feature of soil described volume change when granular soil is subjected to shearing. The parameter dilatancy ratio, *d* is defined as follows:

$$d = \frac{\delta\varepsilon_v^p}{\delta\varepsilon_q^p} \tag{4.2}$$

where $\delta\varepsilon_v^p$ is volumetric strain increment, $\delta\varepsilon_q^p$ is deviator strain increment, and superscript *p* denots the plastic component. The dilatancy is often considered in the unique function of the stress ratio, $\eta = q / p'$ (Li & Dafalias, 2000). The reference stress-dilatancy behavior of the lateritic soil is presented in Figure 4.10. To simplify the analysis, the very small elastic strain was ignored, and the total strain was plotted. The stress-dilatancy behavior of unstabilized and cement stabilized lateritic showed differently. For unstabilized lateritic soil, the stress-dilatancy behavior showed a unique linear relationship. The stress ratio increased as the dilatancy ratio decreased. The highest stress ratio at point *A* was associated with a small dilation at the large stain.

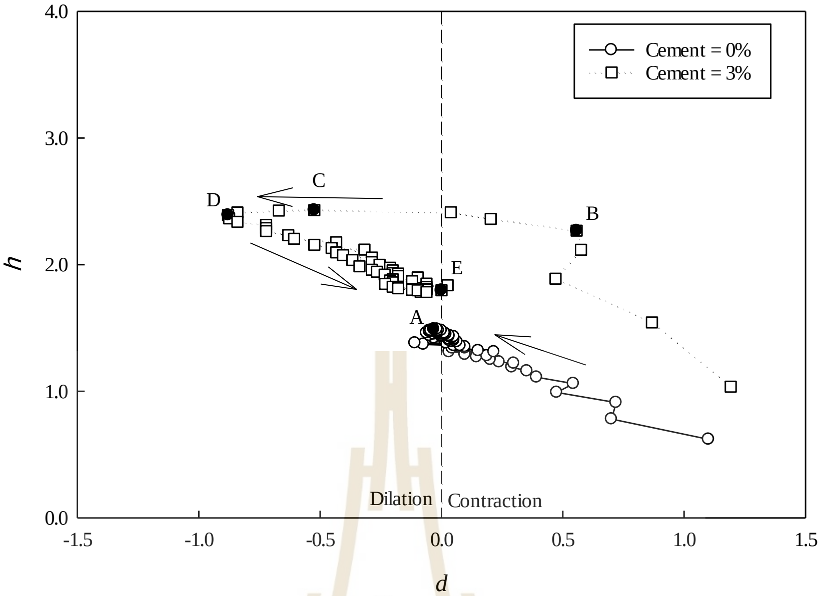

Figure 4.10 Stress-dilatancy relationship of unstabilized and cement stabilized lateritic soil subjected 100 kPa of confining pressure

On the other hand, the cement stabilized samples showed a distinctive hook shape of the stress-dilatancy relationship. After the yield point at point *B*, the dilatancy ratio increased rapidly to the maximum stress ratio at point *C* before reaching the maximum value at point *D*. The different locations at the maximum stress ratio and the maximum dilatancy ratio is similar to result observed in cemented sand reported by Porcino and Marcianò (2017). They revealed that the delay in dilatancy is phenomenally inhibited by the increased confining pressure. Finally, the stress ratio decreased uniquely to zero dilatancy ratio at point *E*. The stress ratio at zero dilation of cement stabilized lateritic soil is relatively higher than that of unstabilized lateritic soil. It is due to the cemented matrix breaking into small pieces after failure. The crushed particles are partially coated by cementitious products, resulting in larger particles than that of unstabilized soil. The stress-dilatancy behavior of cement stabilized lateritic soil in this study agrees well with several studies (Consoli, Cruz, Fonseca, & Coop, 2012; Porcino & Marcianò, 2017; Yu, Tan, & Schnaid, 2007).

The effect of RAP on the stress-dilatancy behavior of RAP-soil samples is presented in Figure 4.12. The stress-dilatancy behavior of RAP-soil samples was similar to that of the lateritic soil. The distinction hook shape of stress-dilatancy behavior can be found in cement stabilized RAP-soil samples. Increased cement content yields a greater stress ratio and dilatancy ratio. For the same cement content, the higher RAP replacement ratio results in a higher stress ratio and dilatancy ratio.

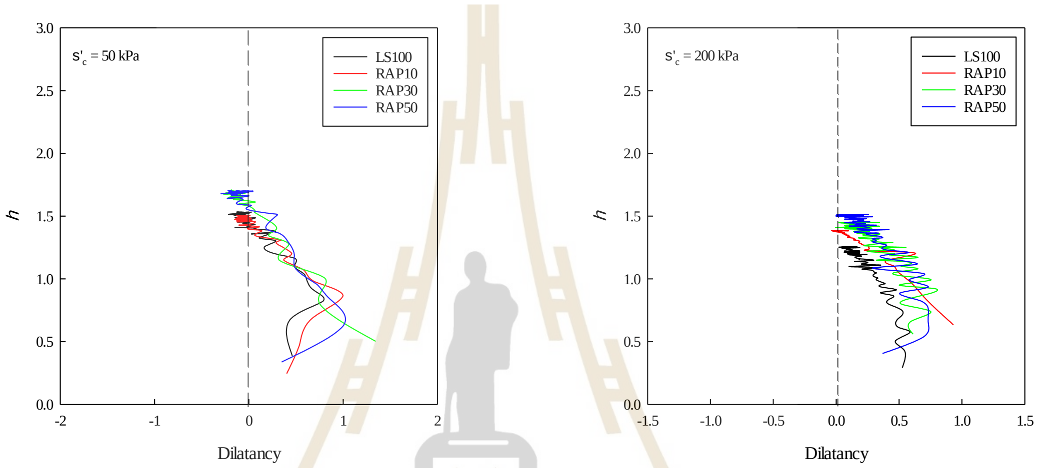

(a)

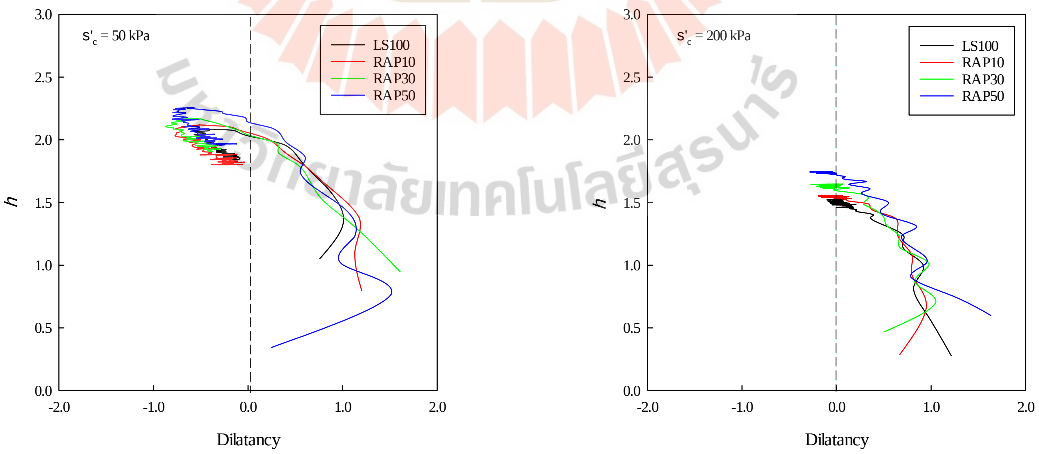

(b)

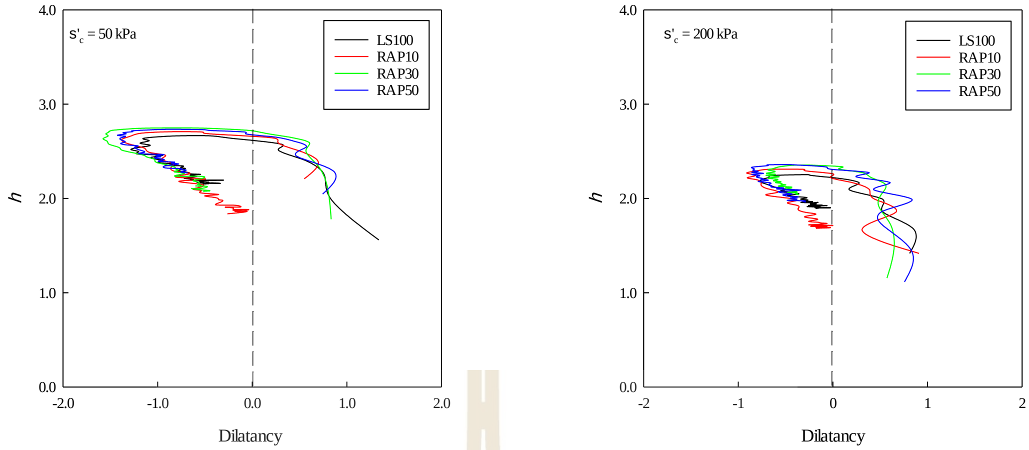

(c)

Figure 4.11 Stress-dilatancy of RAP-soil blends (a) unstabilized (b) cement 1% (c) cement 3%

Following Row's stress dilatancy equation (Rowe, 1962) based on minimum energy considerations, the stress-dilatancy relationship can be expressed as follows:

$$\frac{\sigma'_1}{\sigma'_3}=\left[\tan^2\left(\frac{\pi}{4}+\frac{\phi_f}{2}\right)+\frac{2c}{\sigma'_3}\tan\left(\frac{\pi}{4}+\frac{\phi_f}{2}\right)\right]\left(1-\frac{\delta\varepsilon_v^p}{\delta\varepsilon_1^p}\right) \tag{4.3}$$

where ϕ_f = fiction angle, σ'_1,σ'_3 = major and minor principal stresses, respectively, c = cohesion, $\delta\varepsilon_v^p$ = plastic volumetric strain, $\delta\varepsilon_1^p$ = plastic major strain. Row's stress-dilatancy is usually expressed in terms of the principle stress ratio as follows:

$$R=KD \tag{4.4}$$

where $R=\frac{\sigma'_1}{\sigma'_3}$, $K=\tan^2\left(\frac{\pi}{4}+\frac{\phi_f}{2}\right)+\frac{2c}{\sigma'_3}\tan\left(\frac{\pi}{4}+\frac{\phi_f}{2}\right)$, $D=\left(1-\frac{\delta\varepsilon_v^p}{\delta\varepsilon_1^p}\right)$

Eq. 4.4 suggests that the dilatancy of cohesive granular materials is affected by friction angle and interparticle bonding, and the dilatancy is inhibited by effective confining pressure. The *R*-D_{max} plot of RAP-soil samples is presented in Figure 4.12. The relationship between *R* versus *D* calculated from Eq.4.4 for unstabilized specimens (zero cohesion) is also plotted. With the friction angle of 29° and 33°, *K* = 2.88 and 3.39

for lateritic soil and RAP replacement ratio 50% (RAP50), respectively. It was evident that Row's equation can predict the D_{max} for unstabilized and stabilized RAP-soil samples satisfactory. On the contrary, D_{max} significantly increased with cement contents. Eq. 4.4 suggested that the higher D_{max} of cement-stabilized RAP-soil samples might be attributed to the increased cohesion or friction angle, resulting in the increased K value.

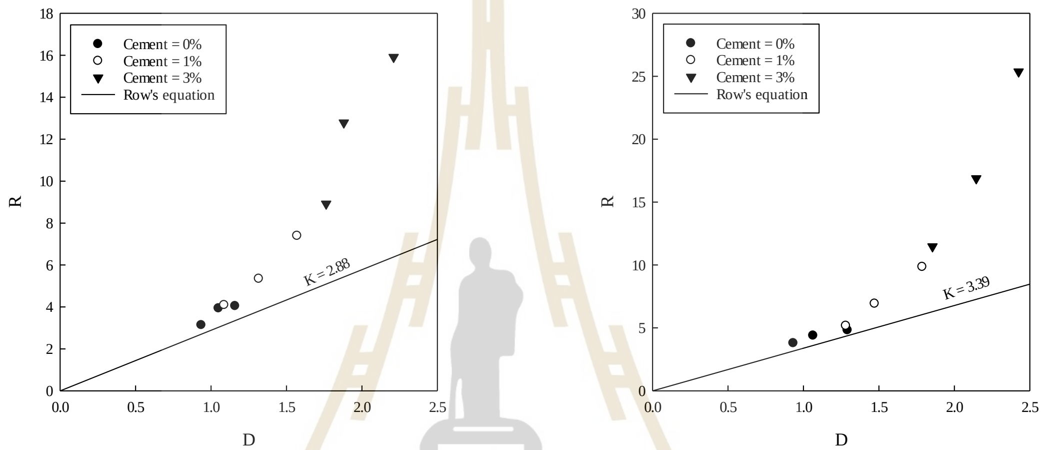

Figure 4.12. The relationship of stress ratio and maximum dilatancy

4.4 Conclusions

The drained shear behavior of RAP-soil samples under three different effective confining pressures is presented in this study. The series of triaxial drained compression tests were performed on unstabilized and cement stabilized RAP-soil samples. The role of RAP replacement ratio and cement content on typical shear response were discussed. The stress-dilatancy behavior of RAP-soil samples was also presented in this study. The conclusions can be drawn as follows:

1) The effect of RAP on the drained shear behavior of RAP-soil samples is highly dependent upon cement content and effective confining pressure level. The strain-hardening response in q-e_a relationship was found for unstabilized RAP-soil samples while the strain-softening behavior was found in cement stabilized

RAP-soil samples. The brittle behavior of cement stabilized RAP-soil samples tended toward the ductile behavior with the increase in the confinement. Higher cement agents induced a more contractive-dilative volumetric response. The maximum volumetric compression of cement stabilized RAP-soil samples increased as the RAP replacement ratio increased.

2) The peak strength increased with the increased cement content and RAP replacement ratio. The brittleness index indicated that the compressible asphalt binder increased the ductility of cement stabilized RAP-soil samples. The 3% cement content improved the cohesion rather than the friction angle. However, 3% cement content could improve both friction angle and cohesion. The excessive RAP replacement ratio caused shear strength to be reduced only due to considerably decrease of cohesion.

3) The stress-dilatancy behavior of RAP-soil samples in this study is similar to that of medium to dense soil. A higher RAP replacement ratio and cement contents caused the increase of stress ratio and dilatancy. However, the dilatancy of RAP-soil samples was suppressed by the increased effective confining pressure. Row's dilatancy equation can model the stress-dilatancy relationship of unstabilized and stabilized RAP-soil samples.

CHAPTER V

LOAD-SETTLEMENT BEHAVIOUR OF SOFT CALY REINFORCED BY STONE COLUMN MADE BY CEMENT STABILIZED RECYCLED ASPHALT PAVEMENT – LATERITIC SOIL BLENDS

5.1 Statement of problems

Compressible soil and low bearing capacity is undesired for infrastructure construction projects. The deep foundation is generally employed to carry load from the superstructure and transfer to hard stratum. For low to medium heavy superstructure, stone column or granular pile is an alternative ground technique. The soft clay layers improved by the stone column can carry a more vertical load and reduce the consolidation settlement and time. The installation of the stone column is more economical than the pile foundation for low to medium heavy superstructure. Typically, the stone column technique can be executed by drilling the hole, then filling the aggregate, and densifying vertically to form the columnar. The soil surrounding the compacted column functions as a confinement against the aggregate movement. The stone column's aggregate is commonly made of quarry stone which is strong and clean with high friction angle.

With the conservation of inadequate natural resources, engineers and researchers looking for alternative materials instead of quarry stone for stone column construction. Tons of waste materials generated from construction and demolition (C&D) annually increased. These waste materials include those such as wood, crushed concrete, crushed brick, glass, and steel slag. Without the suite management, a large volume of these waste were deposited of to the available landfill.

In addition, some kinds of C&D contain toxicity and then affect the soil and groundwater environment in the short or long term (Cabrera, Galvín, & Agrela, 2019) Many researchers evaluated the feasibility of various types of C&D for use as alternative construction materials. Using C&D as sustainable construction materials saves the large extraction of unrenewable virgin resources and is cost-effective.

Regarding stone columns, many type of C&D materials or industry activities were evaluated for the possibility of replacing the traditional stone column aggregate (Zukri & Nazir, 2018). The various type of C&D materials and industrial materials i.e. fly ash aggregate, tire ship, crushed concrete, railway ballast, chased waste glass, were evaluated for possible usage as stone column aggregate (Alkhorshid, Araujo, Palmeira, & Zornberg, 2019; Ayothiraman & Soumya, 2015; Kazmi et al., 2023; Serridge, 2004). The large-scale model of soft ground reinforced by compacted stone column was investigated under both end-bearing and floating type of installation. These studies revealed that recycled aggregate is feasible as an alternative aggregate filler.

Recycled Asphalt Pavement (RAP) is waste debris from asphalt pavement rehabilitation. The properties of RAP are similar to those of original asphalt pavement except for the rheological properties of asphalt binder course by UV exposure and various traffic impacts. RAP may be unsuitably reused for embankment and fill application unless being the treated (i.e. scaping, mixing with aggregate, temperature and confinement) (Dager, Morro, Hubler, & Sample-Lord, 2023). With its well gradation and high friction angle, several engineers and researchers have evaluated the use of RAP in many applications in Civil Engineering, especially in highway work. RAP mixing with aggregate was provided to satisfy the result. The RAP-aggregate blends can meet the strength requirement for road-based materials (Cosentino et al., 2003; Jirayut, Aniroot, & Suksun, 2014). However, the allowable proportion of RAP were reused in construction projects is still limited (Suksan & Horpibulsuk, 2022)

The ground improvement technique using stone column is typically acceptable for soft to medium clay (undrained shear strength, Su >15 kPa) due to the sufficient confinement to against the movement of cohesionless stone column aggregate. The interlocking effect enhancing the strength of stone column aggregate is ineffective when installing in very soft clay. Previous studies were conducted to investigate the feasibility with various methods to extends to extend the limitation of stone column installation (Golait & Padade, 2017; Lin, Maghool, Arulrajah, & Horpibulsuk, 2023; Sushovan, Nadaf, Birali, & Mandal, 2016)

Therefore, this study evaluates cement stabilized Recycled asphalt pavement (RAP) – lateritic soil blends as stone column. The clay model was set up and end-bearing stone column was installed at the center to perform bearing capacity test of the composite ground. With the proper RAP-lateritic soil mixture, the stone column aggregate comprised of the lateritic soil which was replaced by RAP at 30% by dry weight. The ordinary Portland cement was mixed with the lateritic soil and RAP blends at 1% and 3% by dry weight of the blends. In this study, the novelty is the investigation of the feasibility of using cemented RAP-soil blends as stone column in practice. The load-settlement response of the composite ground model was discussed in this chapter. The outcome of this study will promote the usage of RAP and lateritic soil as aggregate in cemented column in sustainable manner

5.2 Materials and specimen preparation

The clay sample was collected from a construction site in Nakhon Ratchasima province, Thailand, at a depth of about 4-5 m below ground level. It liquid and plastic limit of clay of 37% and 28% respectively. The lateritic soil was sourced from a borrow site in Nakhon Ratchasima province, Thailand. Basic properties of the lateritic soil are summarized in Table.5.1. RAP was obtained from rehabilitating the old asphalt pavement of Burial Road No.2 in Nakhon Ratchasima province, Thailand. The graine size distribution curve of RAP and lateritic soil is presented in Figure 5.1. The RAP replacement ratio was fixed at 30% by dry weigh which below the limitation of proper

RAP replacement ratio (<50%) suggestion by previous study that the proper RAP replacement ration should not be excess 50% (Jirayut et al., 2014; Taha, Al-Harthy, Al-Shamsi, & Al-Zubeidi, 2002)

Table 5.1 The basic properties of materials

Properties	Clay	Lateritic soil	RAP
Liquid limit, LL (%)	37	31	
Plastic limit, PL (%)	28	14	
Plasticity Index, PI (%)	9	17	
Coefficient of uniformity, Cc		1.7	1.48
Coefficient of Curvature, Cu		80	8.57
Classification (USCS)	CL	GW	GW

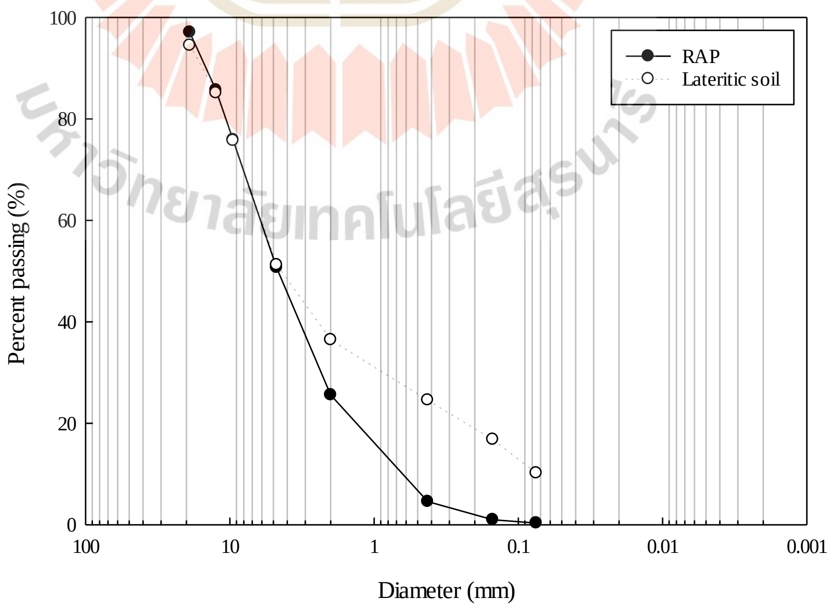

Figure 5.1 Grained size distribution of RAP and lateritic soil

The compaction test was performed to determine the maximum dry density (MDD) and the optimum moisture content (OMC) of RAP-soil blends. The standard Proctor was carried out following the testing procedure of ATSM D698.

The unconfined compression strength (USC) test was conducted to determine the strength of RAP-soil blends. The UCC sample was prepared by screening dry RAP and lateritic soil through sieve No. 4 (sieve opening 4.75 mm) to remove the larger size particle. The lateritic soil was replaced by RAP at 30% by dry weight before cement was admixed. The mixture was mixed thoroughly before the desired amount of water was added and mixed. The mixture was then compacted into a steel mold with dimension of 50 mm and 100 mm high. The specimen's desired dry density and moisture content are according to predetermined MDD and OWC (Figure 5.2). The compacted sample was were extruded and wrapped with a plastic bag. The sample were cured for 28 days. After that the sample were unpacked and submerged under water for 2 hours before USC test.

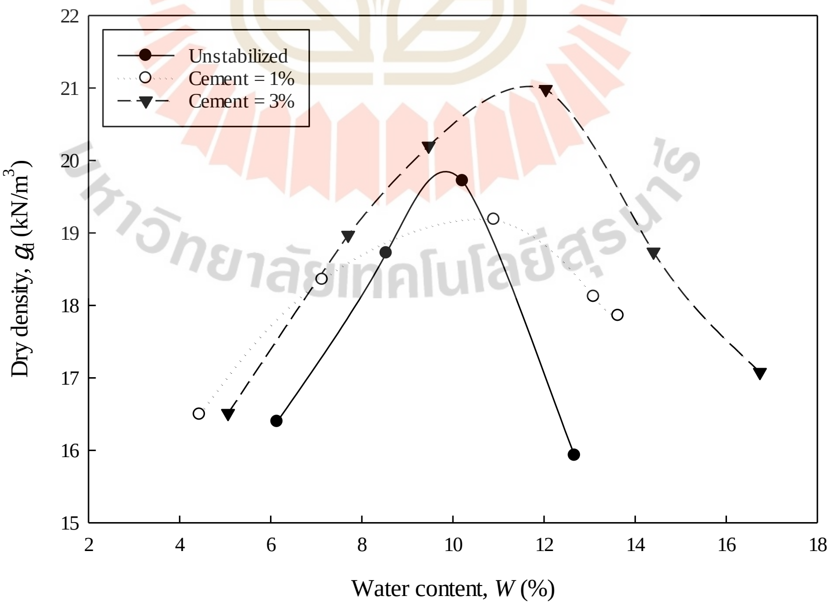

Figure 5.2 Compaction characteristic of RAP-soil blends at various cement contents

The physical model was set up to install cemented RAP-lateritic soil column installation in the middle. The clay was desiccant by oven at 60 C$^{\circ}$ for 48 hours. The dried clay was broken into small particles by light tamping with a rubber hammer. Standard sieve No. 4 was used to screen the larger particle. The distilled water was mixed with clay powder using stirring blade until the water and clay become the paste at 1.5 times liquid limit. The clay paste was then filled in a plastic tank and covered with plastic wrap, letting the clay absorb the water for about 3-4 days. After that, the slurry clay was filled in the PVC mold with a diameter of 150 mm and 300 mm high, connected to a circular steel plate. The vertical drained path was assumed as half of model tank, which required a long period of consolidation. To accelerate consolidation time, the small holes surrounding the surface of the PVC mold was provided to allow the horizontal drained out of water. The filter paper was attached to the drained holes at the inner mold to confine the clay particle. After the clay was filled in PVC mold, the circular steel plate was laid on the clay surface. The plate also had drained holes, allowing the water to drain out vertically. The clay layer was consolidated by applied steel plates starting from a vertical stress at 2.9 kPa. The settlement of the clay layer was measured and the next dead load was applied when the settlement reach 85% primary consolidation approximated suing Asoaka’s method. The stress increment was twice the previous stress. The final stress was 98 kPa and the clay model’s thickness after the end of consolidation was 200 mm (Figure 5.3 (a)).

The dead load on the top of clay model was then removed. The steel casing with a 50 mm diameter was inserted vertically at the center of the clay layer (Figure 5.3 (b)-(c)). As the result, a 50 mm well at the middle of the clay layer was created. The end-bearing cemented RAP-lateritic soil column with a 50 mm diameter and a 200 mm high was installed in the hole (Figure 5.3 (d)) by compaction under standard Procter energy to achieve the 98% MDD. The physical model with the column was next cured in a water tank for 28 days, while the model without column was subjected to the load bearing test immediately.

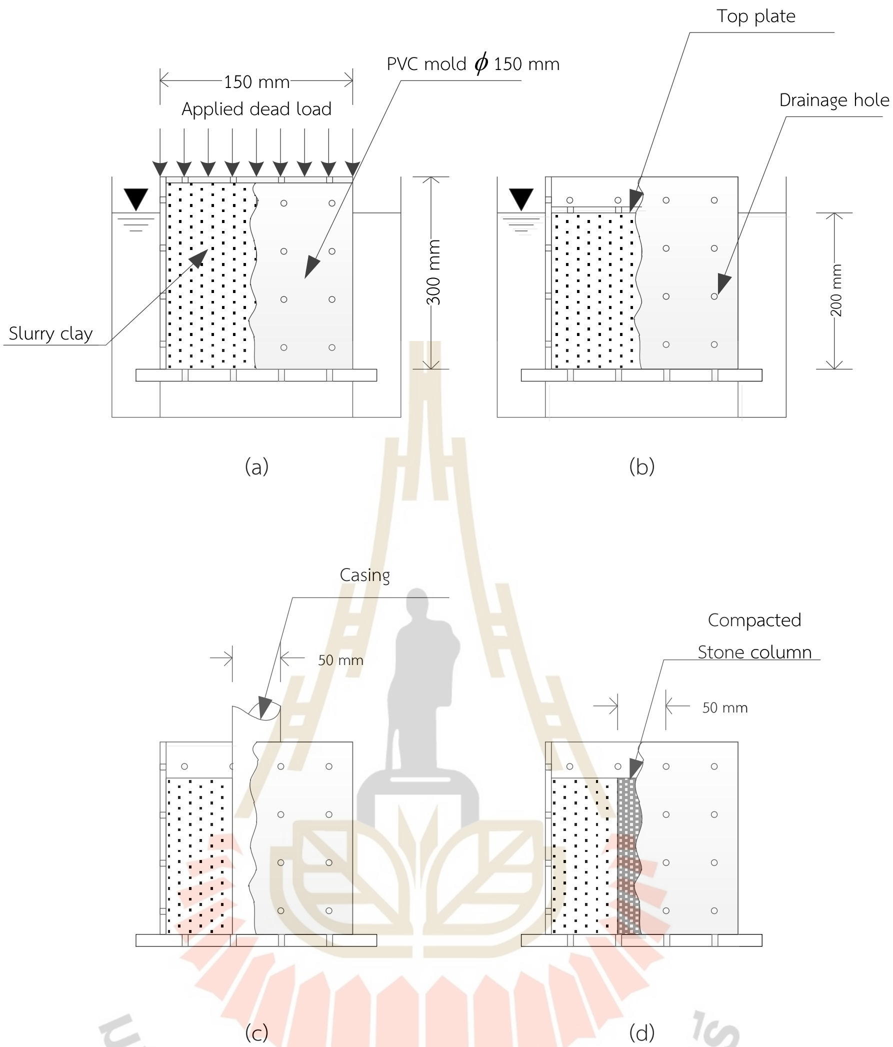

Figure 5.3 Installation of compacted stone column (a) Slurry clay fill in PVC mold and applied dead load (b) Desired high of clay layer (c) Casing perpetrating into clay layer (d) Inserting compacted stone column

After 28 days of curing, the physical model was taken from the water tank and kept in the air for about 30 minutes to allow the clay surface dry. The load bearing test was carries out by placing the circular steel plate with a dimension of 100 mm diameter and 10 mm thick on the top of the physical composite ground. The thickness of the circular plate is sufficient to withstand the applied load, so that the deflection of plate is neglected. A proving ring and two dial gauge were attached to the top plate to measure the vertical load and the settlement, respectively. The schematic of the load bearing test is presented in Figure 5.4. The load was applied by lifting the lower plate of the model vertically against the proving ring with a uniform rate while the load and displacement were recorded. The testing was terminated at 25 mm vertical displacement.

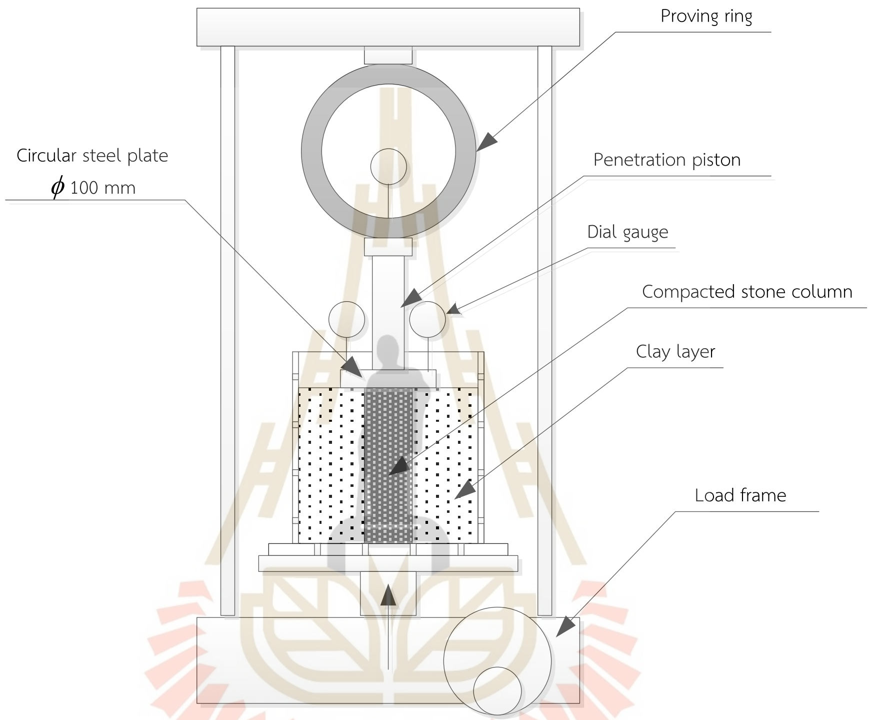

Figure 5.4 Schematic of load-settlement testing

5.3 Result and discussion

The result of the unconfined compressive strength (USC) of RAP-soil blends is presented in Figure 5.5. The unstabilized specimens exhibited strain-hardening behavior. On the other hand, the brittle response was clearly shown with increased cement content. The axial stress increased while the strain at the peak strength decreased with increased cement contents. consistent with a previous study (Schnaid, Prietto, & Consoli, 2001) The higher cement content results in the stronger cementation bonds and hence the higher USC. Rapid reduction of stress after the peak may be expected to be due to broken up of cementation bonds

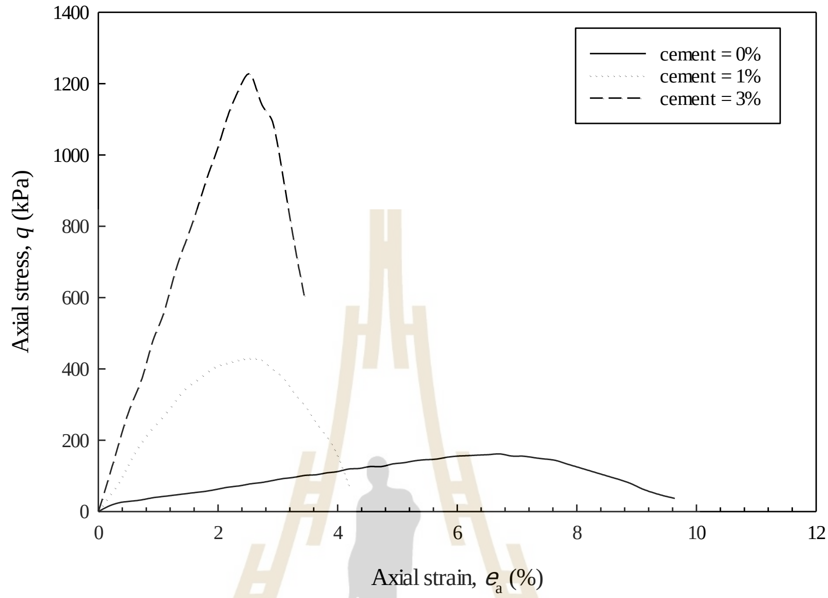

Figure 5.5 Unconfined compressive strength versus axial strain relationship of RAP-soil blends at various cement content

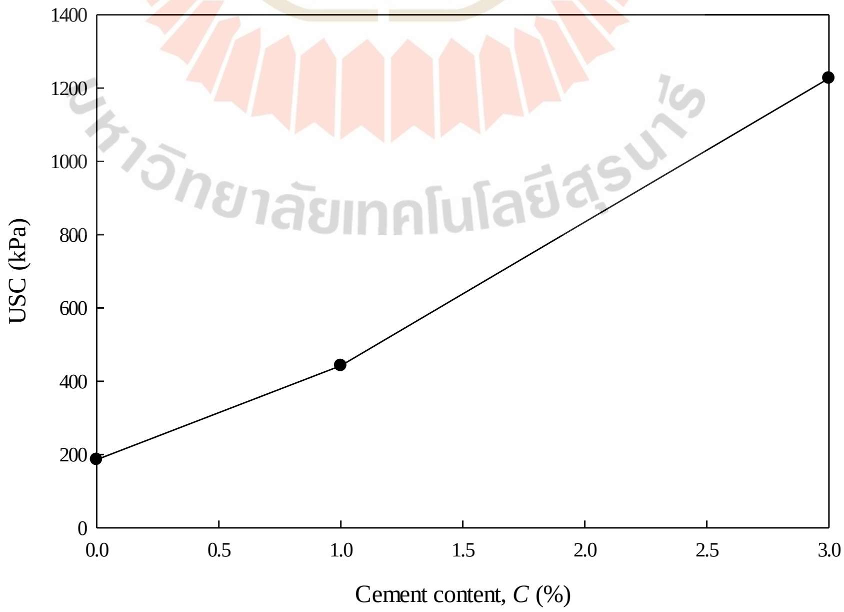

Figure 5.6 The variation of unconfined compressive strength of RAP-soil blends with cement content

The load-settlement curves of composite clay ground are presented in Figure 5.7. For the clay without stone column, the bearing stress increased with displacement linearly up to a certain stress level. Afterward the stress value was constant with further increased in displacement. The load-settlement response of the clay reinforced by an unstabilized stone column was similar to that the clay ground but the bearing stress was higher the same displacement. This implied that higher friction angle of RAP-lateritic soil blends contributes to the enhanced load capacity of the composite ground.

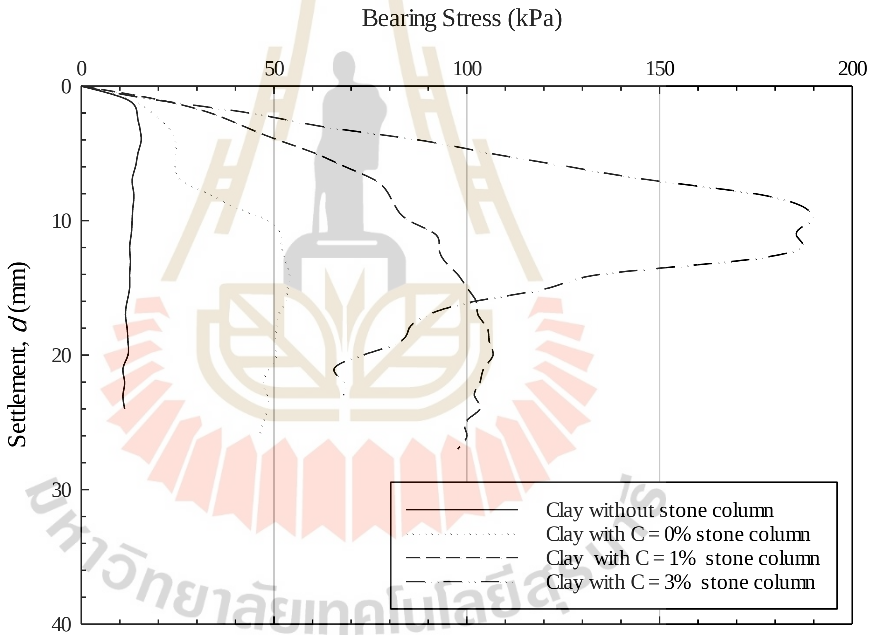

Figure 5.7 Load - settlement curve of clay layer reinforced by stone column

The load-settlement curves of clay ground reinforced with the cement column are dependent upon the level if cement content. The bearing stress was higher for the column with higher cement content for the same vertical displacement. In the other word, settlement decreased with the increased cement content. The load-settlement curve of the 3% cement column showed noticeable peak bearing stress then decreased to the lower value similar to the result obtained from unconfined compressive strength test. However, at the ultimate stress, the bearing stress is higher than that from unreinforced clay ground and composite ground with unstabilized RAP-soil column. It was suggested that the crushed aggregated stone column was further enhancing the bearing stress after failure.

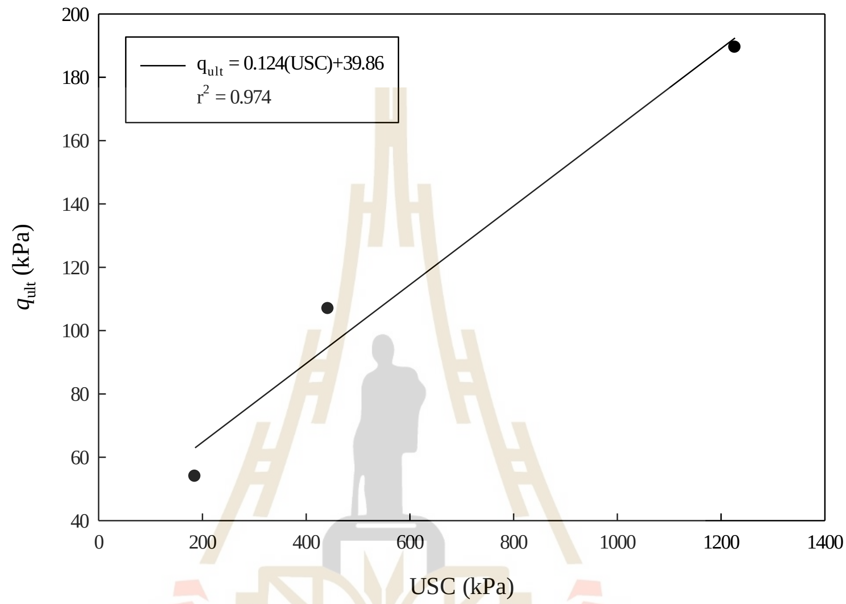

Figure 5.8 Bearing capacity of clay reinforced by stone column

The ultimate bearing capacity of composite ground reinforced by compacted stone column (q_{ult}) suggested by Han (2015) is expressed as follows:

$$q_{ult} = q_{ult,c} as + q_{ult,s}(1 - as) \tag{5.1}$$

where $q_{ult,c}$ = individual bearing capacity of the column, $q_{ult,s}$ = bearing capacity of the clay surrounding the column, and as = the area replacement ratio defined as the cross-sectional area of the column (A_c) to the tributary area (A_e). The as depends upon the pattern of installation layout of the stone column, i.e. rectangular and pattern and triangular. In this study, the physical ground model and the stabilized column were in circular shape. The as is therefore calculated using the following equation:

$$as = \left(\frac{d_c}{D}\right)^2 \tag{5.2}$$

Where d_c = diameter of the column, D = diameter of physical model. As such, the as of 0.11. The $q_{ult,s}$ was obtained from the bearing capacity of unreinforced clay (34.90 kPa) Based on the passive shear failure of the column, $q_{ult,c}$ can be approximately estimated as follows (Han, 2015)

$$q_{ult} = 20Su \tag{5.3}$$

Where Su = undrained shear strength of clay. It is worth noting that **Eq 5.3** was derived for the cohesionless material with typical friction angle of 38°.

Eq. 5.3 suggests that $q_{ult,c}$ only depends on the undrained shear strength of clay and the friction angle of the column. This implies that even with the increase in cement content, the $q_{ult,c}$ remains unchanged. The same is not true for the composite ground with the cement stabilized column Suksan and Horpibulsuk (2022) and Suksan, Horpibulsuk, Mabrathok, and Chinkulkijniwat (In press) revealed that cement stabilization has a marginal effect on the increase in friction angle of cement stabilized RAP-lateritic soil blends but resulted in significant increase in cohesion. In other words, the $q_{ult,c}$ increases significantly with the increased cement content. With the increase in $q_{ult,c}$, the q_{ult} was expected to increase with cement content. The relationship of q_{ult} versus USC of the RAP-soil column for various cement contents was then plotted and is presented in Figure 5.8. The q_{ult} increased proportionally with the increased UCS of the RAP-lateritic soil column.

Based on this finding, the q_{ult} of composite ground with the RAP-lateritic soil column was modified and is expressed as follows:

$$q_{ult} = \beta(USC_{col})as + qult,s(1-as) \tag{4}$$

where the β is constant taking into account the effect of progressive failure. Based on the linear regression analysis, β was calculated as 1.12. The predicted q_{ult} of the composite ground reinforced by the RAP-lateritic soil column via Eq. 5.4 was compared with the measured value as shown in Figure 5.9. It was evident that the predicted q_{ult} was in excellent agreement with the measured q_{ult}. It is concluded that the USC can be used to determine $q_{ult,c}$ and the bearing capacity of composite ground for various compressive strengths of the column.

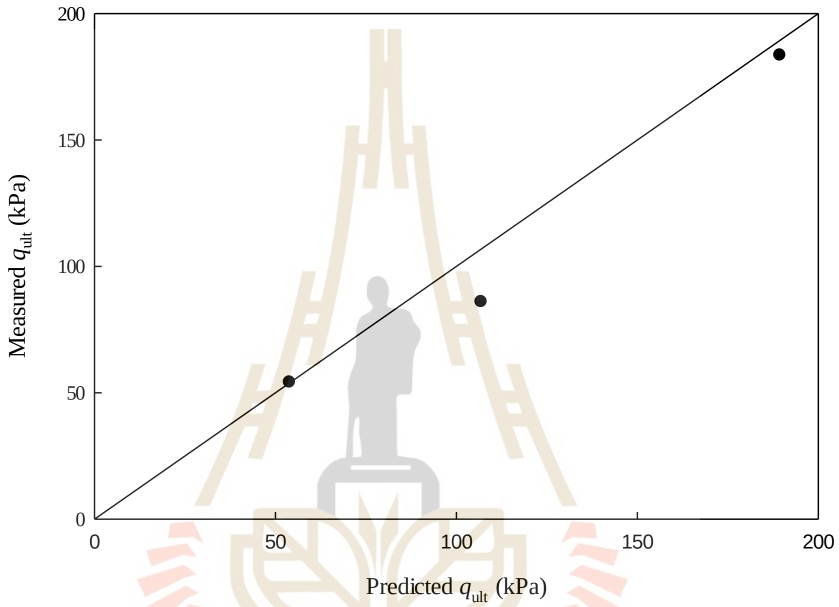

Figure 5.9. The comparison of the laboratory and predicted bearing capacity of the composite ground reinforced by RAP-lateritic soil column.

5.4 Conclusion

This study investigated the load-settlement behavior of soft clay reinforced by RAP-soil columns under static loading condition via the physical model. RAP was replaced with the lateritic soil at 30% and stabilized by Portland cement as a stone column. The evaluation of the effect of cement content on the bearing capacity of the composite ground was discussed. The summary of this study can be drawn as follows:

1) The unconfined compressive strength and stiffness of RAP-soil blends significantly increased with cement content. It was expected that the cementation bond was significantly contributed to the cohesion. The brittle response in stress-strain curves was more pronounced with when cement increased.

2) The load-settlement curve of the clay ground reinforced by the RAP-soil column was dependent upon cement content. At same bearing stress level, the resistance of vertical displacement increased with the increase of cement content.

3) The ultimate load capacity of composite ground significantly increased with cement content. The bearing capacity contributed from RAP-lateritic soil column was strongly governed by the UCS. Based in the proposed bearing capacity equation, the ultimate bearing capacity of the composite ground with of RAP-lateritic soil column can be satisfactory predicted.

CHAPTER VI

CONCLUSION AND RECOMMENDATIONS

6.1 Summary and conclusion

This thesis investigates the performance of the lateritic soil–recycled asphalt pavement mixture improved by cement intended for stone column aggregate. To provide an in-depth understanding of the engineering behavior of RAP-lateritic soil blends, the main study includes three parts. The influence of RAP replacement ratio and cement content on the engineering behavior of RAP-lateritic soil blends was discussed in this study. The shear behavior of RAP-soil blends was investigated through undrained and drained triaxial tests. In addition, the composite ground model was developed to investigate the load-settlement and load-bearing capacity of the soft clay reinforced by stabilized RAP-soil column. The conclusion of each main study can be drawn as follows:

Chapter 3 Evaluation of Cement Stabilized Recycled Asphalt Pavement/Lateritic Soil Blends for Soft Soil Improvement

This study presented the undrained shear response of the blended materials at various RAP replacement ratios and effective confining pressures. The marginal lateritic soil was improved by replacing with RAP contents at 10, 30, and 50% by dry weight with ordinary Portland cement at 1% and 3%. It was found that RAP replacement increased large particles and meanwhile reduced the fine particles resulting in increased compactibility. Under applied effective stress lower than pre-consolidation pressure RAP-soil blends exhibited strain-hardening behavior in which associated with pore pressure decreased. The strain-softening behavior for cement stabilized RAP-soil blends was diminished when RAP replacement ratio increased.

The cementation only affected the cohesion while the friction angle was insignificantly unchanged. The peak strength of cement stabilized RAP-soil blends mainly depends upon the cementation bond strength and interlocking. Shear strength improvement increased with the increased RAP replacement ratio for both unstabilized and cement stabilized RAP-soil blends. Meanwhile, the stiffness of cement stabilized RAP-soil blends decreased due to the high energy absorption of asphalt binder.

Chapter 4 Drained Shear Response of Cement Stabilized Recycled Asphalt Pavement-Lateritic Soil Blends

In this study, the drained shear behavior of cement stabilized recycled asphalt pavement (RAP)-lateritic soil blends is presented. The lateritic soil was replaced by RAP to reduce the fine content and then stabilized by Portland cement for ground improvement and pavement applications. The result indicated RAP replacement ratio, cement content, and effective stress significantly affected the drained shear response of RAP-soil blends. The shear strength increased with cement content and RAP content. However, the excessive RAP replacement ratio resulted in the reduction of peak shear strength. RAP replacement increased the maximum volumetric compression and the dilatation rate. The stress ratio and dilation significantly depended on RAP replacement ratio, and cement content. The dilation was suppressed when effective confining pressure increased. Row's stress dilatancy equation can model the stress-dilatancy behavior of unstabilized and stabilized RAP-soil blends.

Chapter 5 Load-settlement of

This study investigated the influence of cement contents on the load-bearing capacity of soft clay reinforced by stabilized RAP-soil column. The lateritic soil was replaced by RAP at 30% and improved by cement at 1% and 3% to use as stone stabilized column. The physical model of clay ground reinforced by an end-bearing isolated column was set up. The compacted RAP-soil columns were compacted at their maximum dry density via standard Proctor compaction. The result revealed that the load-settlement response of composite ground showed a difference depending upon cement content. The noticeable strain-softening in the load-settlement curve was shown for the composite ground with the cement stabilized RAP-soil column. The load-bearing capacity of composite ground significantly increased in correlation with the increasing unconfined compressive strength of the column. The proposed ultimate bearing equation can estimate the bearing capacity of the composite ground satisfactory.

6.2 Recommendation for further research

6.2.1 The proper fraction of lateritic soil to RAP at 70/30 by dry weight, the excessive RAP over this suggestion will cause a reduction in the strength of the blends.

6.2.2 The maximum dry density and the optimum moisture content of the cement stabilized RAP-soil blends should be specifically determined for each cement content.

6.2.3 The strain-softening behavior in the stress-strain curve of cement stabilized RAP-soil cement suggests that the strain at working load should be limited.

6.2.4 The floating stone column and group pile pattern stone column type may be investigated in further study to clarify the effect of installation type on the load-carry capacity of composite clay.

6.2.6 Further research may investigate the practice of installing RAP-lateritic soil columns in the field.

REFERENCES

REFERENCES

Adhikari, Sambodh, Mohammad J. Khattak, and Bikash Adhikari. "Mechanical Characteristics of Soil-Rap-Geopolymer Mixtures for Road Base and Subbase Layers." *International Journal of Pavement Engineering* 21, no. 4 (2020/03/20 2020): 483-96. https://dx.doi.org/10.1080/10298436.2018.1492131.

Airey, D. W. . "Triaxial Testing of Naturally Cemented Carbonate Soil." *Journal of Geotechnical Engineering* 119, no. 9 (1993): 1379-98. https://dx.doi.org/doi:10.1061/(ASCE)0733-9410(1993)119:9(1379).

Alkhorshid, Nima R., Gregório L. S. Araujo, Ennio M. Palmeira, and Jorge G. Zornberg. "Large-Scale Load Capacity Tests on a Geosynthetic Encased Column." *Geotextiles and Geomembranes* 47, no. 5 (2019/10/01/ 2019): 632-41. https://dx.doi.org/https://doi.org/10.1016/j.geotexmem.2019.103458.

Aniroot, SUKSAN, and HORPIBULSUK Suksun. "Evaluation of Cement Stabilized Recycled Asphalt Pavement/Lateritic Soil Blends for Soft Soil Improvement." *Rock and Soil Mechanics* 43, no. 12 (2022): 3305-15. https://dx.doi.org/10.16285/j.rsm.2022.00111.

Arulrajah, A., Mahdi M. Disfani, S. Horpibulsuk, C. Suksiripattanapong, and N. Prongmanee. "Physical Properties and Shear Strength Responses of Recycled Construction and Demolition Materials in Unbound Pavement Base/Subbase Applications." *Construction and Building Materials* 58 (2014): 245-57.Ayothiraman, Ramanathan, and Sasikala Soumya. "Model Tests on the Use of Tyre Chips as Aggregate in Stone Columns." *Proceedings of the Institution of Civil Engineers - Ground Improvement* 168, no. 3 (2015): 187-93. https://dx.doi.org/10.1680/grim.13.00006.

Ayothiraman, R., and S. Soumya. *Use of /Sheadded Tyre Chips as Aggregate in Stone Column: An Experiment Study*. Proceedings of Indian Geotechnical Conference. Kochi, 2011.

Barksdale, R.D., and R. C. Bachus. *Design and Construction of Stone Columns*. Washington, D.C.: Federal Highway Administration, 1983

Baxter, C. D. P., R. M. S. Sharma, K. Moran, H. Vaziri, and R. Narayanasamy. "Use of a ¯ =0 as a Failure Criterion for Weakly Cemented Soils." *Journal of Geotechnical and Geoenvironmental Engineering* 137, no. 2 (2011): 161-70.

Bejarano, M. O., and J. T. Harvey. "In-Situ Recycling of Asphalt Concrete as Base Material in California." (2003).

Bennert, Thomas, and Ali Maher. *The Development of a Performance Specification for Granular Base and Subbase Material*. New Jersey. Dept. of Transportation, 2005.

Bennert, Thomas, Walter J. Papp, Ali Maher, and Nenad Gucunski. "Utilization of Construction and Demolition Debris under Traffic-Type Loading in Base and Subbase Applications." *Transportation Research Record: Journal of the Transportation Research Board* 1714, no. 1 (2000): 33-39. https://dx.doi.org/10.3141/1714-05.

Bleakley, A. M., P. J. Cosentino, E. H. Kalajian, and M. J. Patel. "Strength and Creep Characteristics of Reclaimed Asphalt Pavement–Sand Blend Backfill in Mechanically Stabilized Earth Walls." *Journal of the Transportation Research Board* 2462 (2014).

BRE. *Br391: Specifying Vibro Stone Columns*. London, UK: CRC Ltd, 2000.

Brown, R. E. "Vibroflotation Compaction of Cohesionless Soils." *Journal of Geotechnical Engineering* 103, no. 12 (1977): 1437-51. https://dx.doi.org/https://doi.org/10.1016/0148-9062(78)90206-1.

Cabrera, Manuel, Adela Pérez Galvín, and Francisco Agrela. "12 - Leaching Issues in Recycled Aggregate Concrete." In *New Trends in Eco-Efficient and Recycled Concrete*. Edited by Jorge de Brito and Francisco Agrela: Woodhead Publishing, 2019.

Chaidachatorn, Komkorn, Jirayut Suebsuk, Suksun Horpibulsuk, and Arul Arulrajah. "Extended Water/Cement Ratio Law for Cement Mortar Containing Recycled Asphalt Pavement." *Construction and Building Materials* 196 (2019/01/30/

2019): 457-67. https://dx.doi.org/https://doi.org/10.1016/j.conbuildmat.2018.11.047.

Chesner, W. H., R. J. Collins, and M. H. MacKay. *User Guidelines for by Products and Secondary Use Materials in Pavement Construction*. McLean, Virginia: Federal Highway Administration, 1998.

Chesner, Warren H., Robert J. Collins, Michael H. MacKay, and John Emery. "User Guidelines for Waste and by-Product Materials in Pavement Construction." Manual (2002). https://rosap.ntl.bts.gov/view/dot/38365.

Chu, J. "An Experimental Examination of the Critical State and Other Similar Concepts for Granular Soils." *Canadian Geotechnical Journal* 32, no. 6 (1995): 1065-75. https://dx.doi.org/10.1139/t95-104.

Clough, G. Wayne, Nicholas Sitar, Robert C. Bachus, and Nader Shafii Rad. "Cemented Sands under Static Loading." *Journal of the Geotechnical Engineering Division* 107, no. 6 (1981): 799-817. https://dx.doi.org/doi:10.1061/AJGEB6.0001152.

Consoli, Nilo Cesar, Rodrigo Caberlon Cruz, António Viana da Fonseca, and Matthew Richard Coop. "Influence of Cement-Voids Ratio on Stress-Dilatancy Behavior of Artificially Cemented Sand." *Journal of Geotechnical and Geoenvironmental Engineering* 138, no. 1 (2012): 100-09. https://dx.doi.org/doi:10.1061/(ASCE)GT.1943-5606.0000565.

Consoli, Nilo C., Pedro D. M. Prietto, and Luciane A. Ulbrich. "Influence of Fiber and Cement Addition on Behavior of Sandy Soil." *Journal of Geotechnical and Geoenvironmental Engineering* 124, no. 12 (1998): 1211-14. https://dx.doi.org/doi:10.1061/(ASCE)1090-0241(1998)124:12(1211).

Coop, M.R., and J.H. Akinson. "The Mechanics of Cemented Carbonate Sands." *Géotechnique* 43, no. 1 (1993): 53-67.

Cosentino, Paul J, Edward H Kalajian, Chih-Shin Shieh, WJK Mathurin, FA Gomez, ED Cleary, and A Treeratrakoon. *Developing Specifications for Using Recycled Asphalt Pavement as Base, Subbase or General Fill Materials, Phase Ii*. 2003.

Dager, Catherine H., Robert H. Morro, Jonathan F. Hubler, and Kristin M. Sample-Lord. "Review of Geotechnical Properties of Reclaimed Asphalt Pavement for Reuse in Infrastructure." *Geotechnics* 3, no. 1 (2023): 21-42. https://www.mdpi.com/2673-7094/3/1/3.

Department of Highway. *Dh-S 205/1989 Strand for of Base Course Aggregate* Thailand, 1989.

Elias, V., J. Welsh, J. Warren, R. Lukas, J.G. Collin, and R.R. Berg. *Ground Improvement Methods*. 2004.

European Asphalt Pavement Association. *Eapa Asphalt in Figures 2020 – Slight Reductions in Total Production after the First Year of the Pandemic*. 2019.

Ghanizadeh, Ali Reza, Morteza Rahrovan, and Kazem Barkhordari Bafghi. "The Effect of Cement and Reclaimed Asphalt Pavement on the Mechanical Properties of Stabilized Base Via Full-Depth Reclamation." *Construction and Building Materials* 161 (2018/02/10/ 2018): 165-74. https://dx.doi.org/https://doi.org/10.1016/j.conbuildmat.2017.11.124.

Golait, Y. S., and A. H. Padade. "Analytical and Experimental Studies on Cemented Stone Columns for Soft Clay Ground Improvement." *International Journal of Geomechanics* 17, no. 4 (2017).

Golait, Y.S., V. Satyanarayana, and S.S.V. Raju. *Concept of under Rammed Cemented Stone Column for Soft Clay Ground Improvement* Vol. 1. Indian Geotechnical Conference Mumbai, India,, 2009.

Guthrie, W. S., D. Cooley, and D. L. Eggett. "Effects of Reclaimed Asphalt Pavement on Mechanical Properties of Base Materials." *Journal of the Transportation Research Board* 2005 (2007): 44-52. https://dx.doi.org/DOI: 10.3141/2005-06.

Han, J. *Principles and Practice of Ground Improvement*. Hoboken, New Jersey: John Wiley & Sons, Inc.,, 2015.

Head, K. H., and R. J. Epps. *Manual of Soil Laboratory Testing : Effective Stress Tests*. Dunbeath: Whittles Publishing, 2014.

Herzog, A., and J.K. Mitchell. "Reaction Accompanying Stabilization of Clay with Cement." In *Cement-Treated Soil Mixtures*.vol. 36: Highway Research Board, 1963.

Horpibulsuk, Suksun, Wanchai Katkan, Wanchai Sirilerdwattana, and Runglawan Rachan. "Strength Development in Cement Stabilized Low Plasticity and Coarse

Grained Soils: Laboratory and Field Study." *Soils and Foundations* 46, no. 3 (2006/06/01/ 2006): 351-66. https://dx.doi.org/https://doi.org/10.3208/sandf.46.351.

Horpibulsuk, S., N. Miura, and D. T. Bergado. "Undrained Shear Behavior of Cement Admixed Clay at High Water Content." *Journal of Geotechnical and Geoenvironmental Engineering* 130, no. 10 (2004): 1096-105.

Horpibulsuk, S., N. Miura, and T. S. Nagaraj. "Assessment of Strength Development in Cement-Admixed High Water Content Clays with Abrams' Law as a Basis." *Ge´otechnique* 53, no. 40 (2003): 439-44.

Hoy, Menglim, Suksun Horpibulsuk, and Arul Arulrajah. "Strength Development of Recycled Asphalt Pavement – Fly Ash Geopolymer as a Road Construction Material." *Construction and Building Materials* 117 (2016/08/01/ 2016): 209-19. https://dx.doi.org/https://doi.org/10.1016/j.conbuildmat.2016.04.136.

Ismail, Mostafa A., Hackmet A. Joer, Wee H. Sim, and Mark F. Randolph. "Effect of Cement Type on Shear Behavior of Cemented Calcareous Soil." *Journal of Geotechnical and Geoenvironmental Engineering* 128, no. 6 (2002): 520-29. https://dx.doi.org/doi:10.1061/(ASCE)1090-0241(2002)128:6(520).

Janbu, N. *Soil Compressibility as Determined by Oedometer and Triaxial Test*. Vol. 1. Proceedings of European Conference on Soil Mechanics and Foundation Engineering (ECSMFE), . Wiesbaden, 1963.

Jirayut, Suebsuk, Suksan Aniroot, and Horpibulsuk Suksun. "Strength Assessment of Cement Treated Soil- Reclaimed Asphalt Pavement (Rap) Mixture." *GEOMATE Journal* 6, no. 12 (06/28 2014): 878-84. Accessed 2022/12/13. https://geomatejournal.com/geomate/article/view/2931.

Juran, I., and O. Riccobono. "Reinforcong Soft Soil with Artificially Cemented Compacted-Sand Column." *Journal of Geotechnical Engineering* 117, no. 7 (1991): 1042-60.

Kallas, B. F. *Flexible Pavement Mixture Design Using Reclaimed Asphalt Concrete*. 1984.

Karlsson, R., and U. Isaacsson. "Material-Related Aspects of Asphalt Recycling — State of the Art." *Journal of Materials in Civil Engineering, American Society of Civil Engineers* 18, no. 1 (2006): 81-92.

Kazmi, Danish, Mehdi Serati, David Williams, Sebastian Olaya, Sadaf Qasim, Yi Pik Cheng, Athina Grizi, and Akbar Javadi. *Shear Strength and Consolidation Behaviour of Kaolin Clay Reinforced with a Granular Column Backfilled with Crushed Waste Glass*, 2023.

Kemp, G. R., and N. H. Predoehl. "A Comparison of Field and Laboratory Environments on Asphalt Durability." *Proceedings of the Association of Asphalt Paving Technologists* 50 (1981): 492-537.

Labaran, Yahaya Hassan, Vivek Shankar Mathur, Shehu Usman Muhammad, and Auwal Alhassan Musa. "Carbon Footprint Management: A Review of Construction Industry." *Cleaner Engineering and Technology* 9 (2022/08/01/ 2022): 100531. https://dx.doi.org/https://doi.org/10.1016/j.clet.2022.100531.

Ladd, R. S. "Preparing Test Specimens Using Undercompaction." *Geotechnical Testing Journal* 1, no. 1 (03/01 1978): 16-23. https://dx.doi.org/10.1520/GTJ10364J.

Laguros, J.G. "Effect of Chemicals on Soil-Cement Stabilization." Iowa State University, 1962.

Leroeil, S., and P.R. Vaughan. "The General and Congruent Effects of Struture Natural Soil and Weak Rocks." *Ge´otechnique* 40, no. 3 (1990): 467-88.

Li, X. S., and Y. F. Dafalias. "Dilatancy for Cohesionless Soils." *Géotechnique* 50, no. 4 (2000): 449-60. https://dx.doi.org/10.1680/geot.2000.50.4.449.

Lo, S R, and S PR Wardani. "Strength and Dilatancy of a Silt Stabilized by a Cement and Fly Ash Mixture." *Canadian Geotechnical Journal* 39, no. 1 (2002): 77-89. https://dx.doi.org/10.1139/t01-062.

Luhr, D. R., W. S. Adaska, and G. E. Halsted. *Guide to Full-Depth Reclamation (Fdr) with Cement*. *Eb234* IL, USA: Portland Cement Association, 2005.

MacKay, M. H. . *Shear Strength of Recyled Construction Materials Intended for Use in Vibro Ground Improvement*. Vol. 6. Proceedings of the Institution of Civil Engineers Ground Improvement 2002.

Marto, A., M. Hasan, M. Hyodo, and A. M. Makhtar. "Shear Strength Parameters and Consolidation of Clay Reinforced with Single and Group Bottom Ash Columns." *Arab J Sci Eng* (2014).

Mckelvey, D., V. Sivakumar, A. Bell, and G. Mclaverty. "Shear Strength of Recycled Construction Materials Intened for Use in Vibro Ground Improvement." *Ground Improvement* 6, no. 2 (2002): 59-68.

McMillan, C., and D. Palsat. "Alberta's Experience in Asphalt Recycling." *Proceedings of the Canadian Technical Asphalt Association* 30 (1985): 148-67.

Nagaraj, TS, and BR Srinivasa. *Analysis and Prediction of Soil Behaviour*: Taylor & Francis, 1994.

National Asphalt Pavement Association. *9 Th Annual Asphalt Pavement Industry Survey*. MD, USA, 2019.

Porcino, Daniela D., and Vincenzo Marcianò. "Bonding Degradation and Stress–Dilatancy Response of Weakly Cemented Sands." *Geomechanics and Geoengineering* 12, no. 4 (2017/10/02 2017): 221-33. https://dx.doi.org/10.1080/17486025.2017.1347287.

Price, G.P. "Fabric of Calcareous Sediments at North Rankin 'a', North Wesr Shelf." Paper presented at the Proceedings of the International Conference on Calcareous Sediments, 1988.

Response, Emergency, and Franklin Associates. *Characterization of Building-Related Construction and Demolition Debris in the United States*. 1998.

Roberts, F. L., P. S. Kandhal, R. E. Brown, D. Lee, and T. W. Kenedy. *Hot Mix Asphalt Materials, Mixture Design, and Construction, 2nd Edition*. Lanham, MD, USA,: Napa Education Foundation, 1996.

Rowe, P. W. "The Stress-Dilatancy Relation for Static Equilibrium of an Assembly of Particles in Contact." *Proceedings of the Royal Society of London. Series A, Mathematical and Physical Sciences* 269, no. 1339 (1962): 500-27. Accessed 2022/11/07/. http://www.jstor.org/stable/2414551.

Schnaid, F., Predo D. M. Prietto, and N.C. Consoli. "Chaeacterization of Cemented Sand in Triaxial Compresion ", *Journal of Geotechnical and Geoenvironmental Engineering* 127, no. 10 (2001): 857-68.

Schnaid, Fernando, Pedro D. M. Prietto, and Nilo C. Consoli. "Characterization of Cemented Sand in Triaxial Compression." *Journal of Geotechnical and*

Geoenvironmental Engineering 127, no. 10 (2001): 857-68. https://dx.doi.org/doi:10.1061/(ASCE)1090-0241(2001)127:10(857).

Serridge, Colin. "The Use of Recycled Aggregates in Vibro Stone Column Ground Improvement Techniques." (01/01 2004): 213-24.

Serridge, C. J. "Achieving Sustainability in Vibro Stone Column Techniques." *Proceedings of the Institution of Civil Engineers, Engineering Sustainability* 1, no. 58 (2005): 211-22.

Shahverdi, M., and A. Haddad. "Use of Recycled Materials in Floating Stone Columns." *Proceedings of the Institution of Civil Engineers – Construction Materials* (2019). https://dx.doi.org/https://doi.org/10.1680/jcoma.18.00086.

Smilikanic, M., J. Stefanovic, H. Neumann, I. Rahimaian, and J. Jovanovic. "Aging of Asphalt on Paved Roads — Characterization of Asphalt Extracted from the Wearing Courses of the Belgrade-Nis Highway." *Journal of Erdol and Kohl* 46, no. 6 (1993).

Soltanabadi, Reza, and Kiachehr Behfarnia. "Evaluation of Mechanical Properties of Concrete Containing Recycled Concrete Aggregate and Recycled Asphalt Pavement." *Journal of Materials in Civil Engineering* 34, no. 12 (2022): 04022348. https://dx.doi.org/doi:10.1061/(ASCE)MT.1943-5533.0004514.

Steels, D.P. *Ground Engineering as Potential End Uses for Recycled and Secondary Aggregates* The Waste & Resources Action Programme 2004.

Stolle, Dieter F.E., Peijun Guo, and John J. Emery. "Mechanical Properties of Reclaimed Asphalt Pavement — Natural Aggregate Blends for Granular Base." *Canadian Journal of Civil Engineering* 41, no. 6 (2014): 493-99. https://dx.doi.org/10.1139/cjce-2013-0009.

Suddeepong, Apichat, Artit Intra, Suksun Horpibulsuk, Cherdsak Suksiripattanapong, Arul Arulrajah, and Jack Shuilong Shen. "Durability against Wetting-Drying Cycles for Cement-Stabilized Reclaimed Asphalt Pavement Blended with Crushed Rock." *Soils and Foundations* 58, no. 2 (2018/04/01/ 2018): 333-43. https://dx.doi.org/https://doi.org/10.1016/j.sandf.2018.02.017.

Suebsuk, J., S. Horpibulsuk, A. Suksan, C. Suksiripattanapong, T. Phoo-ngernkham, and A. Arulrajah. "Strength Prediction of Cement-Stabilised Reclaimed Asphalt

Pavement and Lateritic Soil Blends." *International Journal of Pavement Engineering* (2017): 332-38. https://dx.doi.org/https://doi.org/10.1080/10298436.2017.1293265.

Suebsuk, J., A. Suksan, and S. Horpibulsuk. "Strength Assessment of Cement Treaded Soil-Reclaimed Asphalt Pavement (Rap) Mixture." *Int. J. of GEOMATE* 6, no. 2 (2014): 878-84.

Sukmak, Gampanart, Patimapon Sukmak, Suksun Horpibulsuk, Arul Arulrajah, and Jitwadee Horpibulsuk. "Generalized Strength Prediction Equation for Cement Stabilized Clayey Soils." *Applied Clay Science* 231 (2023/01/03/ 2023): 106761. https://dx.doi.org/https://doi.org/10.1016/j.clay.2022.106761.

Suksan, A., & Horpibulsuk, S. (2022). Evaluation of cement stabilized recycled asphalt pavement/lateritic soil blends for soft soil improvement. *Rock and Soil Mechanics,* 43(12), 3305-3315. doi:10.16285/j.rsm.2022.00111

Suksan, A., Horpibulsuk, S., Mabrathok, M., & Chinkulkijniwat, A. (In press). Drained Shear Response of Cement Stabilized Recycled Aspalt Pavement - Lateritic Soil Blends. *International Journal of Geosynthetics and Ground Engineering*.

T., Huang J., and Airey D. W. "Properties of Artificially Cemented Carbonate Sand." *Journal of Geotechnical and Geoenvironmental Engineering* 124, no. 6 (1998): 492-99. https://dx.doi.org/doi:10.1061/(ASCE)1090-0241(1998)124:6(492).

Taha, Ramzi, Ali Al-Harthy, Khalid Al-Shamsi, and Muamer Al-Zubeidi. "Cement Stabilization of Reclaimed Asphalt Pavement Aggregate for Road Bases and Subbases." *Journal of Materials in Civil Engineering* 14, no. 3 (2002): 239-45. https://dx.doi.org/doi:10.1061/(ASCE)0899-1561(2002)14:3(239).

Taha, R., A.S. Al-Harthy, K. Al-shamsi, and M. Al-Zubeidi. "Cement Stabilization of Reclamed Asphalt Pavement Aggregate for Road Bases and Subbases." *Journal of Masterials in Civil Engineering* 14, no. 3 (2002): 239-45.

Taha, Ramzi, Galal Ali, Adnan Basma, and Omar Al-Turk. "Evaluation of Reclaimed Asphalt Pavement Aggregate in Road Bases and Subbases." *Transportation Research Record* 1652, no. 1 (1999): 264-69. https://dx.doi.org/10.3141/1652-33.

Tarsi, Giulia, Piergiorgio Tataranni, and Cesare Sangiorgi. "The Challenges of Using Reclaimed Asphalt Pavement for New Asphalt Mixtures: A Review." *Materials* 13, no. 18 (2020): 4052. https://www.mdpi.com/1996-1944/13/18/4052.

Tranter, R., I. Jefferson, and G. Ghataora. *The Use of Recycled Aggregate in Vibro-Stone Columns – a Uk Perspective*. GeoCongress. LS, USA, 2008.

Tyrion, F. C. *Asphalt Oxidation*. Vol. 40B. *Asphaltenes and Asphalts*. NY, USA,: Elsevier, 2000.

Vieira, Castorina Silva, and Paulo M. Pereira. "Use of Recycled Construction and Demolition Materials in Geotechnical Applications: A Review." *Resources, Conservation and Recycling* 103 (2015/10/01/ 2015): 192-204. https://dx.doi.org/https://doi.org/10.1016/j.resconrec.2015.07.023.

Williams, Brett, and J. Willis. *Asphalt Pavement Industry Survey on Recycled Materials and Warm-Mix Asphalt Usage 2019 (Information Series 138) 10th Annual Survey*, 2020.

Xueyi, L., A. M. Shubber Ammar, L. Hongsong, and R. Juanjuan. *The Stress Concentrate Ratio of Stone Column under Confined Condition* International Conference on Transportation Engineering 2009 Chengdu, China, 2009.

Yang, Yue Huan, and Ying Biao Wu. "Mix Design for Full-Depth Reclaimed Asphalt Pavement with Cement as Stabilizer." In *Advanced Characterization of Asphalt and Concrete Materials*, 2014.

Yu, H. S., S. M. Tan, and F. Schnaid. "A Critical State Framework for Modelling Bonded Geomaterials." *Geomechanics and Geoengineering* 2, no. 1 (2007/03/20 2007): 61-74. https://dx.doi.org/10.1080/17486020601164275.

Yuan, D. , S. Nazarian, L. R. Hoyos, and A. J. Puppala. *Cement Treated Rap Mixes for Roadway Bases*. 2010.

Yuan, Deren, Soheil Nazarian, Laureano R. Hoyos, and Anand J. Puppala. "Evaluation and Mix Design of Cement-Treated Base Materials with High Content of Reclaimed Asphalt Pavement." *Transportation Research Record* 2212, no. 1 (2011): 110-19. https://dx.doi.org/10.3141/2212-12.

Zhou, C., J.H. Yin, and J.P. Ming. "Bearing Capacity and Settlement of Weak Fly Ash Ground Improved Using Lime – Fly Ash or Stone Columns." *Canadian Geotechnical Journal* 39, no. 3 (2002): 585-96.

Zukri, Azhani, and Ramli Nazir. "Sustainable Materials Used as Stone Column Filler: A Short Review." *IOP Conference Series: Materials Science and Engineering* 342, no. 1 (2018/04/01 2018): 012001. https://dx.doi.org/10.1088/1757-899X/342/1/012001.

APPENDIX A

PULICATIONS

List of Publications

Suksan, A. & Horpibulsuk, S. (2022). Evaluation of cement stabilized recycled asphalt pavement/lateritic soil blends for soft soil improvement[J]. *Rock and Soil Mechanics*, *43*(12): 3305-3315.

Suksan, A., Horpibulsuk, S., Mobkrathok, M., Chinkulkijniwat, A. (2024). Drained Shear Response of Cement-Stabilized Recycled Asphalt Pavement–Lateritic Soil Blends. *Int. J. of Geosynth. and Ground Eng.* **10**, 4 (2024). https://doi.org/10.1007/s40891-023-00518-y

Rock and Soil Mechanics 2022 43(12): 3305–3315
https: //doi.org/10.16285/j.rsm.2022.00111
ISSN 1000–7598
journal homepage: rocksoilmech.whrsm.ac.cn

Evaluation of cement stabilized recycled asphalt pavement/lateritic soil blends for soft soil improvement

SUKSAN Aniroot[1], HORPIBULSUK Suksun[1, 2, 3]

1. School of Civil Engineering, Suranaree University of Technology, Nakhon Ratchasima 30000, Thailand
2. School of Civil Engineering, Center of Excellence in Innovation for Sustainable Infrastructure Development, Suranaree University of Technology, Nakhon Ratchasima 30000, Thailand
3. Academy of Science, The Royal Society of Thailand, Bangkok 10300, Thailand

Abstract: This research evaluates the potential of cement stabilized recycled asphalt pavement (RAP)/marginal lateritic soil blends as stone column aggregate instead of the traditional quarry aggregate. The undrained shear response of the blended materials at various RAP replacement ratios and effective confining pressures are investigated. The RAP replacement ratios were 10%, 30% and 50% by dry weight and ordinary Portland cement contents were 1% and 3%. It was evident that RAP replacement increased large particles and meanwhile reduced fines particles; hence the increased compactibility. Under applied effective stress lower than pre-consolidation pressure, RAP-soil blends exhibited strain-hardening behavior associated with decreased pore pressure. The strain-softening behavior in stress-strain curve for cement stabilized RAP-soil blends was diminished when RAP replacement ratio increased. The role of cementation improved the cohesion while friction angle insignificantly unchanged. The strength and stiffness of cement stabilized RAP-soil blends is mainly dependent upon the cementation bond strength and RAP replacement ratio. Shear strength improvement increased with the increased RAP replacement ratio for both unstabilized and cement stabilized RAP-soil blends while stiffness of cement stabilized RAP-soil blends decreased due to high energy absorption of asphalt binder.

Keywords: soil-cement; ground improvement; recycled asphalt pavement; triaxial; undrained behavior

1 Introduction

Stone column inclusion is a ground improvement technique to improve the impermissible soft soil layer. The main function of stone column is densifying and strengthening of the soft ground. Stone column is also used to accelerate consolidation process of soft soil. There are many installation methods of stone column for various ground condition. These installation methods form unbound backfill aggregate into the composite ground by densification.

The load capacity of the ground reinforced by stone column depends on backfill performance and confining stress[1]. Typically, the quarried stone has been selected as stone column backfill. For the past decades, the environmental impact and sustainable reasons encourage the usage of the alternative materials such as construction and demolition (C&D) materials and industrial by-products as a stone column backfill. Many researchers have ascertained the potential of the crushed concrete, steel slag and artificial cemented soil as a stone column backfill[2–5].

Installing stone columns in very soft ground (undrained shear strength <15 kPa) is not applicable due to the lack of bonding of aggregates and low shear strength of surrounding soil, causing bugling failure[1]. Stabilized aggregates with chemical agents have been applied to overcome this problem. Many researchers proposed the stabilization of fill aggregates to increase their cohesion to withstand bugling failure when installed in the soft ground[5–8].

Recycled asphalt pavement (RAP) is one of C&D materials from rehabilitation of asphalt concrete pavements. RAP is composed of aggregates and binder coating their surface[9]. The amount of RAP has been increasing annually due to the economical growth worldwide, which is generally disposed of to landfill. National Asphalt Pavement Association[10] reported that the total RAP in U.S.A. was about 101.3 million tons in 2018. The estimated 82.2 million tons of RAP were used to construct new asphalt pavements to reduce amount of natural materials. The amount of RAP used for infrastructure construction in 2018 was approximately 46.8% higher than that used in 2009.

RAP has been successfully used in highway and pavement applications[11]. Utilization of RAP in highway construction in particular base courses was achieved

Received: 3 March 2022 Revised: 20 May 2022
First author: SUKSAN Aniroot, male, born in 1989, PhD candidate, focusing on cement stabilized materials. E-mail: aniroot_suk@vu.ac.th
Corresponding author: HORPIBULSUK Suksun, male, born in 1975, PhD, Professor, mainly engaged in the research on pavement geotechnics and ground improvement. E-mail: suksun@g.sut.ac.th

by blending it with conventional aggregates (i.e., crushed rock, lateritic soil) at proper replacement ratio[12]. RAP can also improve the properties of marginal lateritic soil to meet standard specification for stabilized base course[13]. RAP-lateritic soil blends improved by cement provided the satisfactory properties for highway applications[12, 14−15].

The marginal lateritic soil, which is sub-standard for highway application but is abundant in tropical counties including Thailand can be improved by RAP to be used as a stone column backfill. For very soft Bangkok clay, the cement stabilized RAP-lateritic soil can be adopted as stone column alternative to high-quality quarry aggregate, which has an advantage in term of engineering, economic and environmental perspectives.

Therefore, this study evaluates the potential of cement stabilized RAP-marginal lateritic soil blends under compression and shear conditions. The understanding of shear response of the blended materials at various RAP replacement ratios and effective confining pressures are significant for the design of composite ground. Besides, this research outcome will be fundamental for the development of constitutive modeling for numerical simulation.

2 Materials

Lateritic soil sample was collected from a borrow pit in Nakhon Ratchasima, Thailand. The lateritic soil was composed of 15% gravel, 62% sand and 23% fine particle. Following unified soil classification system (USCS), the lateritic soil was classified as clayey sand (SC). The fine content of aggregates for highway applications must be less than 20%[16]. Therefore, this lateritic soil was classified as a marginal material, which cannot be used in highway application.

RAP was obtained from Bureau of Nakhon Ractchasima, Department of Highways, Thailand. RAP was composed of 60−70 penetration grade asphalt binder at approximately 7% by dry weight. RAP was classified as well-graded sand with gravel (SW). Basic and geotechnical properties of the lateritic soil and RAP are summarized in Table 1.

Table 1 Basic properties of lateritic soil and RAP

Materials	Liquid limit (LL) /%	Plastic limit (PL) /%	Plastic index (PI)	Gravel /%	Sand /%	Fine content /%	Specific gravity G_s	Soil classification	Asphalt binder (AS) /%
Lateritic soil	32	16	16	15	62	23	2.58	SC	−
RAP	N/A	N/A	N/A	45	43	1.4	2.35	SW	7

3 Experimental methodology

Extensive laboratory tests were conducted on cement stabilized RAP-soil blends to evaluate the effect of RAP replacement ratio and cement content on their undrained shear behavior. The lateritic soil was replaced by RAP contents at 10%, 30% and 50% by dry weight of lateritic soil to minimize the fine contents (interparticle contact prior to cement stabilization). RAP10, RAP30 and RAP50 herein represented the lateritic soil blended with 10%, 30% and 50% replacement ratio, respectively. Ordinary Portland cement (Type I) was used to stabilize RAP-soil blends at 1% and 3%(C = 1%, 3%) in this research, which is commonly used for soil stabilization in practice[17].

The compaction test was conducted on RAP-soil blends in order to determine the maximum dry density (MDD) and optimum moisture content (OMC) under modified compaction energy (ASTM D1557). Both lateritic soil and RAP were sieved through sieve No. 4 (4.75 mm) and No. 3/8 (9.5 mm), respectively to remove larger particles. The lateritic soil and RAP were air-dried for at least 3 days prior to compaction test. The lateritic soil was replaced by RAP at the target RAP replacement ratios. The RAP-lateritic soil blend was thoroughly mixed and then water was sprayed into the blend for compaction. The sample was compacted in five layers with 25 blows per layer in a standard mold with dimensions of 101.6 mm diameter and 110.68 mm height. In order to obtain complete compaction curve, at least five compaction data points were required.

The compressibility of RAP-soil samples was evaluated via one-dimensional consolidation test following ASTM D2435. The samples were prepared by tamping RAP-soil blends in three layers in a floating-type consolidation ring with dimensions of 20 mm height and 75 mm diameter at MDD and OMC. The sample was submerged under water in a consolidation cell for over 24 hours to ensure saturation before testing. The maximum effective vertical stress applied was 1 500 kPa. Due to very high yield stress of cement stabilized RAP-soil and limitation of equipment, the test was limited to only unstabilized samples.

The cement stabilized RAP-soil samples for triaxial tests were prepared by compaction method suggested by Ladd[18]. The air-dried lateritic soil, RAP and cement were thoroughly mixed by hand to attain uniform mixture prior to mixing with water at the desired quantity. The lateritic soil-RAP-cement mixture was then compacted in a steel mold with a dimension of 50 mm diameter and 100 mm height at MDD and OMC predetermined from the compaction test. After 24 hours, the samples were extruded and sealed by plastic sheet. The unstabilized samples were tested after extrusion while the cement stabilized samples were tested after 28 days of curing to avoid effect of strength development due to hydration during consolidation and shearing processes.

The undrained triaxial compression tests were conducted following the procedure suggested by Head et al.[19]. The method consists of three stages of testing namely saturation, consolidation and shearing. The saturation stage is the process allowing the water through the sample to fill the void by the incremental back pressure technique. The cell pressure and back pressure were increased while the effective stress held constant about 10 kPa until the values of Skempton B parameter reached 0.95 and 0.90 for unstabilized and cemented stabilized samples, respectively. The samples were then subjected to consolidation stage. The desired effective stresses of 50, 100 and 200 kPa were then applied on the samples until the end of consolidation. Finally, the samples were sheared with a rate of 0.1 mm /min while the back pressure valve was closed and excess pore pressure was measured during shear.

The stress-strain variants in this study were calculated as follows:

$$\left.\begin{aligned} q &= \sigma_1' - \sigma_3' \\ p' &= \frac{\sigma_1' + 2\sigma_3'}{3} \\ \varepsilon_q &= \varepsilon_a = \frac{\Delta l}{l_0} \\ \eta &= \frac{q}{p'} \end{aligned}\right\} \tag{1}$$

where σ_1', σ_2', σ_3' are effective principal stresses, q is deviator stress, p' is mean effective stress, η is stress ratio and ε_a is axial stain and ε_q is deviator strain. In the undrained condition, the volume change is not allowed, thus the shear strain and axial strain are identical.

4 Results and discussion

The particle size distribution curves of RAP-soil blends with various RAP replacement ratios are shown in Fig. 1. RAP100 and LS100 are defined as the pure RAP and pure lateritic soil. The RAP contained larger particles than the lateritic soil. The replacement of soil by RAP therefore increased the average particle size (D_{50}) of the blends and reduced fine contents.

The presence of asphalt binder with a low specific gravity of approximately 1.03 caused the RAP having lower specific gravity than the lateritic soil. The specific gravities of RAP-soil blends with different RAP replacement ratios can be approximated by using the following function:

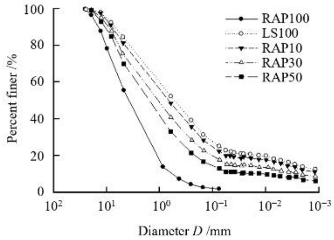

Fig. 1 Particle size distribution of RAP-soil blends

$$G_{\text{blend}} = \frac{1}{\dfrac{\text{LS}}{G_s} + \dfrac{(1-\text{LS})}{G_{\text{RAP}}}} \tag{2}$$

where G_{blend} is specific gravity of blends, G_s is specific gravity of lateritic soil, G_{RAP} is specific gravity of RAP, LS is lateritic soil content in %. The amount of asphalt binder in the blends is determined as follows:

$$A_s = \frac{W_a}{W_s} \times 100 \tag{3}$$

where W_a is weight of asphalt, W_s is weight of solid aggregates. Table 2 summarizes the calculated values of G_{blend} and A_s. The higher RAP content results in a higher asphalt binder adherence and a lower specific gravity of the blends due to lower specific gravity of RAP.

Table 2 Properties of RAP-soil blends

Sample identification	RAP /%	OMC /%	MDD /(kg • m^{-3})	Fine fraction /%	Void ratio	A_s /%
LS100	0	10.8	1 900	23	0.33	0.0
RAP10	10	10.5	1 930	21	0.29	0.7
RAP30	30	10.3	1 970	18	0.24	2.1
RAP50	50	10.3	1 970	15	0.22	3.5

4.1 Compression behavior

The results of compaction test are summarized in Fig. 2 and Table 2. The compaction curve of lateritic soil could be represented by a bell shape, typically found in granular soil. The compaction behavior of pure RAP was found to be insensitive to water (the flat compaction curve) due to high energy absorption of RAP[20]. As such, RAP alone is not suitable as the compacted fill material and must be blended with lateritic soil; the flat compaction curve of RAP tended to diminish when blended with lateritic soil. The MDD of the blends increased with increasing the RAP replacement ratio indicating the higher compactibility of the blends. The compaction curves of RAP30 and RAP50 samples were similar. The OMC of all RAP replacement ratios changed in narrow range and was approximately 10%.

The relationship between void ratio versus effective

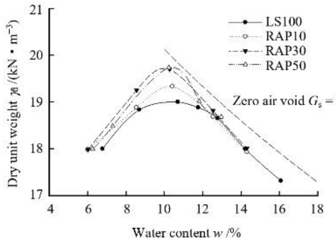

Fig. 2 Compaction characteristic of lateritic soil and RAP blends

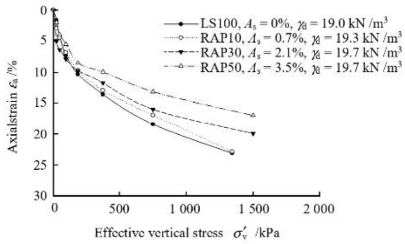

Fig. 4 Relationship between axial strain and effective vertical stress lateritic soil and RAP-soil blends

vertical stress of RAP-soil blends is shown in Fig. 3. The value of C_c reduced from 0.13 to 0.125, 0.071 and 0.076 while C_s reduced from 0.28 to 0.22, 0.16 and 0.177 for 10%, 30% and 50% RAP replacement ratios (RAP10, RAP30 and RAP50), respectively. However, RAP replacement ratio insignificantly affected the yield stress, whereby the yield stress varied between 400 and 500 kPa for all mixtures.

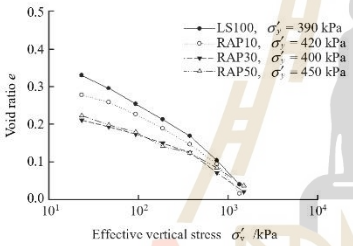

Fig. 3 Consolidation test result of RAP-soil blends

The effect of RAP replacement ratio on the deformation at the same effective vertical stress of all blends is shown in Fig. 4. At post-yield state, the lateritic soil exhibited larger deformation while the RAP50 sample exhibited the lowest deformation at the same effective vertical stress. For example, the axial strain of the RAP50 sample was 13.2% while it was 18.4% for lateritic soil at the same effective vertical stress of 750 kPa. It was noted that the RAP10 sample exhibited the similar axial strain to the lateritic soil at high stress of 1 350 kPa. The RAP replacement increased large particles and meanwhile reduced fines particles as seen by the increase of D_{50}. This improved the resistance to compression at post-yield stress as seen that even though the yield stress and density were practically the same.

4.2 Undrained shear behavior of unstabilized RAP-lateritic soil

The triaxial undrained test results of both unstabilized and stabilized samples at different RAP replacement ratios are summarized in Table 3. The undrained shear response of unstabilized lateritic soil under three confining pressures of 50, 100 and 200 kPa is presented in Fig. 5. The samples exhibited strain-hardening behavior whereby the deviator stress increased with the axial strain without clear peak. The strength and stiffness increased with the increased effective confining pressure. During shearing, the positive excess pore pressure was generated depending upon level of effective confining pressure. The higher effective confining pressure resulted in the higher excess pore pressure.

Assuming that the at-rest lateral earth pressure coefficient K_0 equals 0.5, the yield mean effective stress was calculated to be 300 kPa (the 1D yield stress was found to be 400−500 kPa from consolidation test). This yield mean effective stress was greater than the applied effective confining stresses. In other words, the samples were in over-consolidated state. Typically, over-consolidated clay exhibits negative pore pressure, which was different from the present samples. Even at low effective confining pressure of 50 kPa (the highest over-consolidation ratio, OCR), the negative pore pressure developed very little at the end of test. This might be due to the larger particles of the samples when compared with over-consolidated clay.

The undrained stress paths of unstabilized lateritic soil under 50, 100 and 200 kPa effective confining pressures are shown in Fig. 6. The path of the highest OCR samples (50 kPa of effective confining pressure) initially located close to applied total stress path due to little positive excess pore pressure development. On the other hand, the lowest OCR samples (200 kPa of effective confining pressure) moved more to the left side of the applied total stress path due to high positive excess pore pressure. However, the undrained stress paths of unstabilized lateritic soil for all effective confining pressures were turned to the right side after the peak failure was attained due to the reduction in excess pore pressure.

Table 3 Results of consolidated undrained triaxial compression test on unstabilized and cement stabilized RAP-soil blends

Samples	Cement /%	σ'_c /kPa	ε_a at q_{max} /%	ε_a at Δu_{max} /%	ε_a at η_{max} /%	q_{max} /kPa	Δu_{max} /kPa	η_{max}
LS	0	50	6.25	0.73	5.11	125.13	14.98	1.56
LS	0	100	4.59	2.35	4.16	156.26	48.41	1.46
LS	0	200	6.11	4.31	6.11	246.08	114.77	1.48
LS	1	50	6.32	0.31	0.41	523.82	24.24	2.40
LS	1	100	5.70	0.41	0.41	655.89	58.87	2.37
LS	1	200	4.79	0.62	0.83	748.40	84.34	1.94
LS	3	50	1.67	0.73	0.73	1 722.60	37.95	2.92
LS	3	100	1.56	0.45	0.51	1 875.35	53.70	2.63
LS	3	200	1.86	0.41	0.52	2 090.75	62.04	2.33
RAP10	0	50	6.20	1.14	2.31	143.70	19.14	1.56
RAP10	0	100	6.39	2.73	5.03	175.91	46.84	1.51
RAP10	0	200	6.13	4.97	4.97	265.91	107.33	1.45
RAP10	1	50	1.86	0.41	0.52	644.71	33.15	2.68
RAP10	1	100	6.32	0.52	0.62	813.41	69.01	2.49
RAP10	1	200	5.39	0.52	0.62	742.69	102.48	2.04
RAP10	3	50	1.45	0.52	0.52	1 739.53	36.88	2.91
RAP10	3	100	2.19	0.52	0.52	1 934.31	60.98	2.74
RAP10	3	200	1.46	0.63	0.73	2 192.00	139.13	2.72
RAP30	0	50	5.62	0.62	1.14	201.09	12.47	1.59
RAP30	0	100	5.04	1.26	2.42	205.07	46.30	1.52
RAP30	0	200	4.96	1.90	4.33	338.64	101.49	1.56
RAP30	1	50	7.13	0.62	0.72	835.26	32.88	2.69
RAP30	1	100	6.36	1.04	1.25	962.80	58.47	2.34
RAP30	1	200	5.44	0.84	0.94	1 042.79	117.15	2.17
RAP30	3	50	2.71	0.52	0.62	1 927.04	33.57	2.89
RAP30	3	100	1.97	0.41	0.52	2 368.55	80.75	2.89
RAP30	3	200	2.19	0.73	0.94	2 537.47	100.35	2.56
RAP50	0	50	6.31	0.84	4.21	183.55	19.40	1.73
RAP50	0	100	6.06	1.57	3.87	231.95	51.23	1.70
RAP50	0	200	6.23	3.17	6.23	424.67	95.59	1.68
RAP50	1	50	6.20	0.83	1.14	835.88	30.87	2.61
RAP50	1	100	6.38	0.84	0.94	1 000.68	70.04	2.57
RAP50	1	200	4.91	1.36	1.67	1 088.54	110.59	2.18
RAP50	3	50	3.84	0.62	0.83	1 775.99	37.95	2.92
RAP50	3	100	4.16	0.83	0.93	1 887.30	79.04	2.84
RAP50	3	200	4.16	0.62	0.73	2 381.92	144.47	2.69

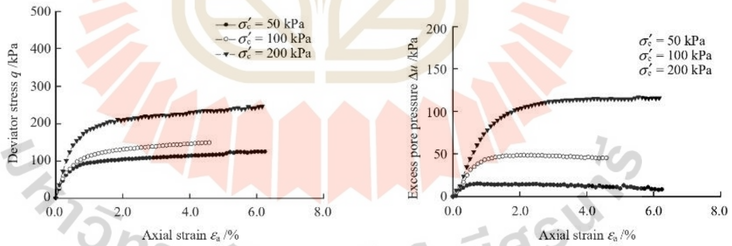

(a) Relationship of deviator stress and axial strain (b) Relationship of excess pore pressure and axial strain

Fig. 5 Undrained behavior of unstabilized lateritic soil

The relationship between stress ratio η versus axial strain of unstabilized lateritic soil is shown in Fig. 7. The η increased with the increased axial stain for all effective confining pressures tested but the slope of relationship was found to be different; i.e. the gentler slope was associated with the higher effective confining pressure. The maximum η was found to be identical for all the effective stresses tested, resulting in the unique failure envelope. This is the distinct undrained shear behavior of compacted lateritic soil which is different from that of normally and over-consolidated clay.

The stress versus axial strain and excess pore pressure versus axial strain relationships of unstabilized RAP-soil blends are shown Fig. 8. It is evident that the strain-hardening behavior in deviator stress versus axial stain relation is associated with the strain-softening behavior

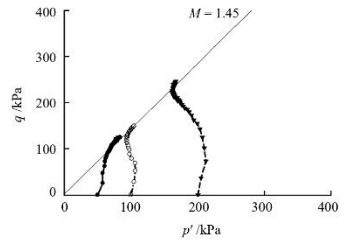

Fig. 6 The undrained stress paths of unstabilized lateritic soil

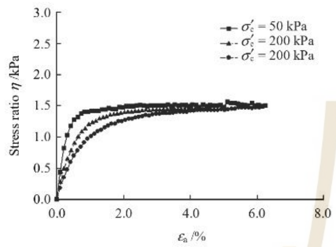

Fig. 7 Relationship between stress ratio versus axial strain of unstabilized lateritic soil

in excess pore water pressure versus axial strain relation in all RAP replacement ratios. The lower strain-softening behavior is associated with the higher effective confining pressure especially at 200 kPa. The maximum deviator stress increased with the increased RAP replacement ratio while the maximum positive excess pore pressure was more or less the same. As such, the failure envelope of RAP-soil blends was steeper than that of the unstabilized soil as shown in Fig. 9. It was evident that the cohesion c' was zero for both unstabilized soil and RAP-soil blends.

4.3 Undrained shear behavior of stabilized RAP-lateritic soil

The undrained shear behavior of cement stabilized lateritic soil at C = 1% and 3% is shown in Fig. 10. Both strength and stiffness significantly increased with increasing the cement content. For the low cement content of 1%, the cement stabilized lateritic soil sample exhibited stain-hardening behavior in deviator stress versus axial strain associated with strain-softening behavior in excess pore water pressure versus axial strain relation. However, with the high cement content of 3%, the strain-softening behavior was found for both deviator stress and excess pore pressure versus axial stain relation. The deviator stress increased to the peak at small axial stain and then decreased to lower value.

The excess pore pressure initially increased to the peak value at small stain (0.5%−1% axial strain) and then decreased to negative value. The rate of reduction in excess pore pressures depended upon degree of cementation and level of effective confining pressures. The cementation bond increased the inter-particle forces, resulting in a higher maximum deviator stress and resistance to deformation. The higher cementation bond strength was associated with the higher negative pore pressure. The strain at peak excess pore pressure was lower than that at the peak

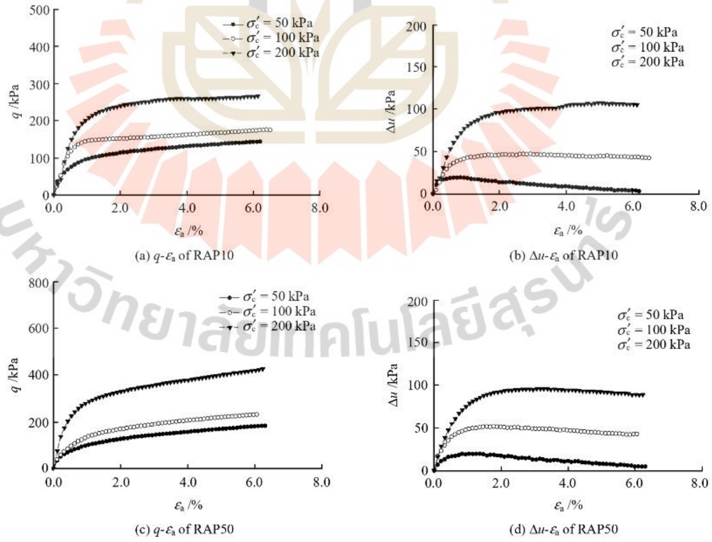

Fig. 8 Undrained behavior of unstabilized RAP10 and RAP50

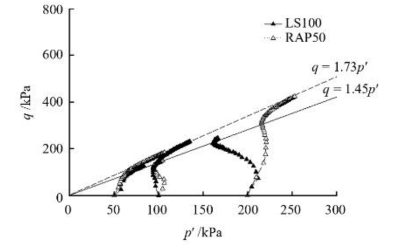

Fig. 9 Effect of RAP replacement ratio on effective stress paths of unstabilized samples

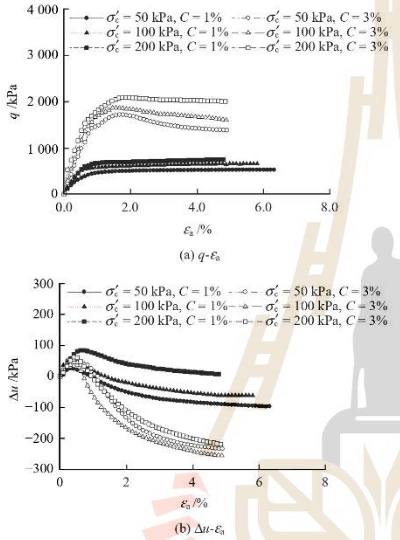

(a) q-ε_a

(b) Δu-ε_a

Fig. 10 Undrained behavior of cement stabilized lateritic soil

deviator stress. This is different from the cement stabilized high water content clay in that the strain at peak excess pore pressure and peak deviator stress is almost identical[21]. This difference is possibly due to the compaction energy effect, which caused the dense package

The undrained stress paths of cement stabilized lateritic soil are presented in Fig. 11. The undrained stress path finally located on the right side of applied total stress path due to negative pore pressure development. The cohesion increased with the increased cement content while the friction angle was insignificantly changed. In other words, the friction angle of cement stabilized was not significantly affected by cementation bonds. This result is in agreement with previous study reported that the friction angle of cement and unstabilized soil are identical[5, 22−23].

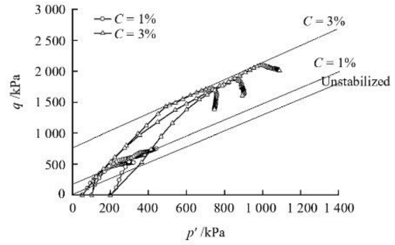

Fig. 11 Undrained stress paths of unstabilized and cement stabilized lateritic soil

The relationship between stress ratio versus axial strain of cement stabilized soil sample compared with that of unstabilized soil samples is shown in Fig. 12. The stress ratio of the stabilized samples increased to the peak at small strain after that tended to decrease to the critical state stress ratio of unstabilized samples. The higher cement content resulted in the higher peak stress ratio. It is of interest to mention that the axial strains at the peak of stress ratio were found to take place before the strain at peak deviator stress (Table 3). Coop et al.[24] revealed that the location of the breakup of the cementation bond took place at peak of stress ratio for cemented sand.

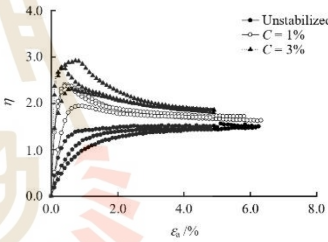

Fig. 12 Stress ratio versus axial stain relationship of unstabilized and stabilized lateritic soil samples

Horpibulsuk et al.[21] reported that the location at peak of stress ratio, peak of deviator stress and peak of excess pore pressure of cement stabilized high-water content clay was practically identical, which is different with the present study. This can be explained that the peak strength of cement stabilized lateritic soil is mainly dependent upon the cementation bond strength and interlocking due to the very low pre-shear moisture content. The cementation bond only influenced the strength until the peak of excess pore pressure.

The undrained shear behavior of cement stabilized RAP-soil blends is shown in the Fig. 13. The cement stabilized RAP-soil blends exhibited similar behavior to the cement stabilized lateritic soil. The strain-softening behavior in deviator stress and axial strain relation was

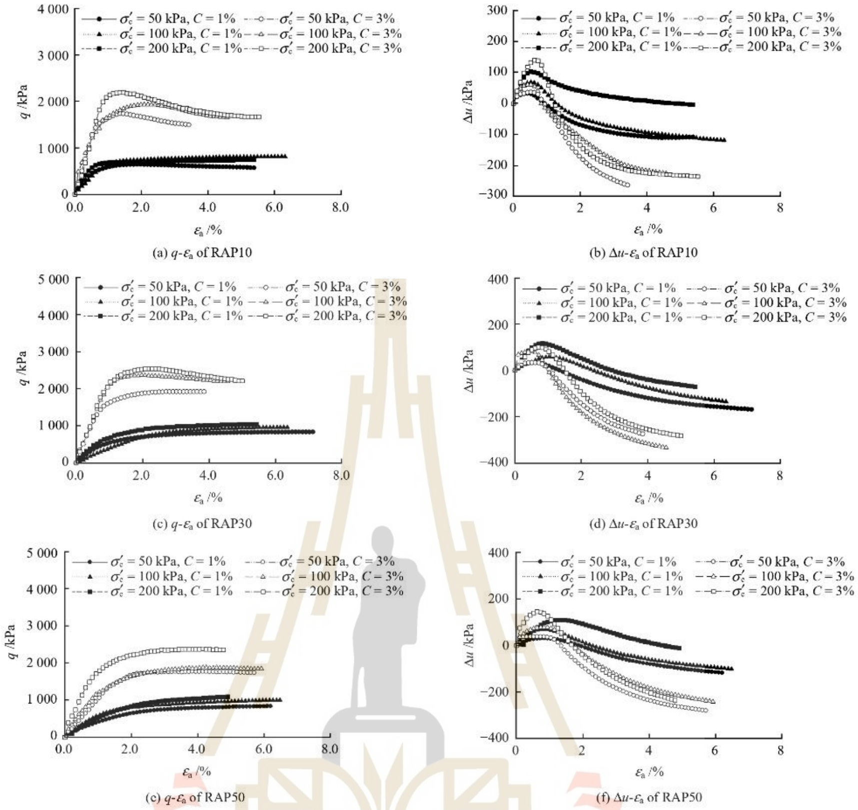

Fig. 13 Undrained behavior of cement stabilized RAP-soil blends

found for the 3% cement stabilized RAP10 and RAP30 samples whereas the cement stabilized RAP50 exhibited stain-hardening behavior in deviator stress and axial strain relation. This is because RAP50 had higher energy absorption due to higher asphalt binder in the blend. However, the cement stabilized RAP10, RAP30 and RAP50 exhibited the strain-softening behavior in excess pore pressure and axial strain relation. In other words, the asphalt binder content did not affect the excess pore pressure development. Similar to the cement stabilized lateritic soil, the peak positive excess pore pressure took place at small stain, which was also observed for cement stabilized RAP-soil blends.

4.4 Strength and ductility improvement due to RAP replacement

The effect of RAP replacement ratio on shear strength improvement Δq is determined as follows:

$$\Delta q = q_{\mathrm{R}} - q_{\mathrm{s}} \tag{4}$$

where q_{R} is the deviator stress of RAP-soil blends samples and q_{s} is the deviator stress of the lateritic soil at the same axial strain level in similar test conditions. The relationship of Δq versus axial strain of both unstabilized and cement stabilized RAP-lateritic soil samples under 200 kPa confining pressure is shown in Fig. 14. For unstabilized samples, Δq was higher for higher RAP replacement ratio because the increased RAP replacement ratio caused denser particle package and lower void ratio. For low cement content of 1%, except RAP10 sample, Δq decreased initially to the lowest value and then increased sharply to the peak value before levelling off.

The decrease of Δq at the initial stage is because the slope of stress-stain curve of cement stabilized RAP-soil blends was lower than that of cement stabilized lateritic soil. In other words, the gentle strength development at the initial stage was found for RAP10 while the significant

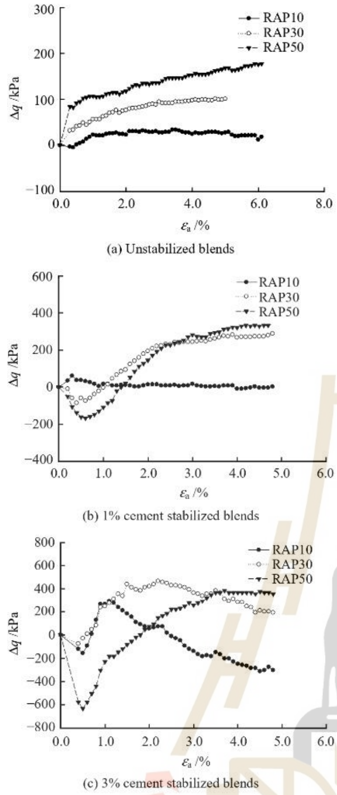

(a) Unstabilized blends

(b) 1% cement stabilized blends

(c) 3% cement stabilized blends

Fig. 14 Strength improvement under 200 kPa confining pressure

strength development associated with lower stiffness was found for RAP30 and RAP50 samples. The shear strength improvement at larger strain was more with the increased RAP replacement ratio for both the unstabilized and stabilized RAP-soil samples. With strain-softening behavior in deviator stress and axial strain relation for 3% cement samples, Δq of RAP10 and RAP30 samples decreased after the peak value. On the other hand, Δq of RAP50 sample increased gradually even with the increase in strain due to strain-hardening behavior. It is clear that Δq increased with the increased RAP replacement ratio for both unstabilized and cement stabilized RAP-soil blends. Due to high energy absorption of asphalt binder, the more delay in Δq of cement stabilized RAP-soil blends was found at initial stage as the RAP replacement ratio increased. Eventually, the strength development of cement stabilized RAP-soil was mobilized at larger strain due to interlocking.

The variation in shear improvement as discussed early indicated the lower slope of stress-stain curve of cement stabilized samples when RAP replacement ratio increased. To evaluate the effect of RAP replacement on stiffness of cement stabilized RAP-soil blends, the initial tangent modulus E_i of the blends with various RAP replacement ratios and cement contents was compared. The E_i of stabilized materials is typically steeper with an increase of confining pressure. The normalized initial tangent modulus by atmosphere pressure (P_a = 101.3 kPa) is employed to evaluate the stiffness of the cement stabilized RAP-soil blends. The relationship between E_i versus confining pressure normalized by P_a in log-log scale is shown Fig. 15 and can be expressed in term of power function[25] as follows:

$$E_i = kP_a\left(\frac{\sigma_c'}{P_a}\right)^n \tag{5}$$

where k is the intercept at $\frac{\sigma_c'}{P_a}=1$ and n is slope.

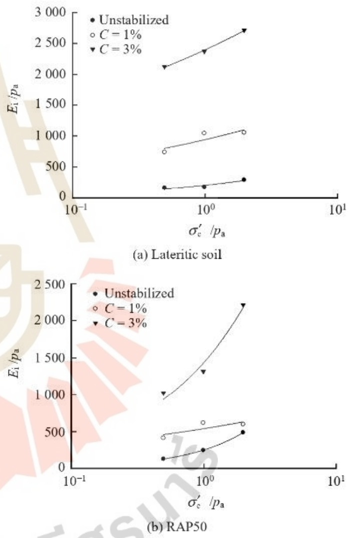

(a) Lateritic soil

(b) RAP50

Fig. 15 Normalized initial stiffness versus normalized effective confining pressure

Table 4 summarizes the result of E_i for unstabilized and cement stabilized RAP-soil blends. The relationship of the coefficient of k versus RAP replacement ratios is shown in Fig. 16. As expected, k of unstabilized samples gradually increased with RAP replacement ratio associated with the increased shear improvement. With higher cement content, at the same RAP replacement ratio, k increased because the higher cementation bond strength induced more resistance to deformation during shear (higher slope stress-strain curve).

The increase of k value with cement content is in agreement with the result of cement stabilized sand reported by previous studies[26−27]. However, k of cement stabilized RAP-soil blends decreased with the increased RAP replacement ratio. Hoy et al.[28] investigated the microstructure of RAP using scanning electron microscope and indicated that asphalt binder partly coated the surface of aggregate and hence resulted in lower stiffness.

Table 4 Values of stiffness parameter

Sample name	RAP content /%	Cement C /%	k	n
LS100	0	0	201.14	0.418 1
		1	975.26	0.258 1
		3	2 397.10	0.176 7
RAP10	10	0	229.56	0.445 0
		1	945.07	0.237 8
		3	2 922.90	0.231 0
RAP30	30	0	247.98	0.675 3
		1	611.50	0.148 1
		3	2 315.40	0.124 0
RAP50	50	0	219.80	0.967 9
		1	534.89	0.267 7
		3	1 405.00	0.568 7

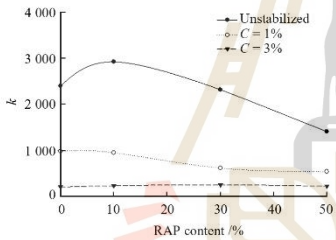

Fig. 16 Effect of RAP on k value

In this research, the role of cementation bonds and compaction energy on the undrained shear response of cement stabilized RAP-lateritic soil was illustrated. Due to the break-up of cementation bonds, the strain-softening in both deviator stress-axial strain and excess pore pressure-axial strain is detected. The RAP replacement was found to prevent the sudden break-up of the cementation bonds as seen by the smaller reduction in deviator stress after the peak state with a higher RAP replacement ratio. The understanding of the different shear responses of this material in stabilized and unstabilized states is vital for development of constitutive models based on the soil structure concept such as Structured Cam Clay model[29−33].

The stabilized RAP-lateritic soil can be used as the stone columns in soft Bangkok clay whose undrained shear strength is low. The apparent cohesion of the RAP-lateritic soil can reduce the lateral earth pressure, which prevents the failure of the surrounding clay during the installation of RAP-lateritic soil. The RAP replacement can improve the ductility of the composite ground during the service state especially under cyclic and earthquake conditions.

5 Conclusions

This research evaluates the undrained shear response of cement stabilized recycled asphalt pavement/marginal lateritic soil blends at various RAP replacement ratios and effective confining pressures. The RAP replacement improved the gradation and maximum dry density of lateritic soil; hence the resistance to compression at post-yield stress. The unstabilized RAP-soil blends exhibited strain-hardening behavior in deviator stress versus axial stain relation associated strain-softening behavior in excess pore water pressure versus axial strain relation.

For cement stabilized RAP-soil blends at low cement of 1%, RAP-soil blends exhibited stain-hardening behavior in deviator stress versus axial strain. But with the high cement content of 3%, the strain-softening behavior was found for both deviator stress and excess pore pressure versus axial stain relation. The high RAP replacement ratio of 50% can prevent the strain softening in deviator stress versus axial stain relation due to high energy absorption of asphalt.

The failure envelope of unstabilized RAP-soil blends was steeper with the increased RAP replacement ratio while the cohesion c' was zero. For cement stabilized samples, the undrained stress paths located the right side of applied stress path total stress path due to negative pore pressure development. The cohesion increased with the increased cement content while the friction angle was insignificantly changed.

The RAP replacement was found to improve the shear strength in both unstabilized and stabilized states. Due to high energy absorption of asphalt binder, the higher RAP replacement led to a more delay in shear strength improvement but a lower initial stiffness (more ductile behavior) of cement stabilized RAP-soil blends.

References

[1] HAN J. Principles and practice of ground improvement[M]. Hoboken, New Jersey: John Wiley & Sons, Inc., 2015.

[2] MCKELVEY D, SIVAKUMAR V, BELL A, et al. Shear strength of recycled construction materials intended for use in vibro ground improvement[J]. Ground Improvement, 2002, 6(2): 59−68.

[3] SHAHVERDI M, HADDAD A. Use of recycled materials in floating stone columns[C]//Proceedings of the Institution of Civil Engineers - Construction Materials. [S. l.]: [s. n.],

2019.

[4] ZUKRI A, NAZIR R. Sustainable materials used as stone column filler: a short review[C]//IOP Conference Series: Materials Science and Engineering. [S. l.]: [s. n.], 2018.

[5] JURAN I, RICCOBONO O. Reinforcong soft soil with artificially cemented compacted-sand column[J]. Journal of Geotechnical Engineering, 1991, 117(7): 1042−1060.

[6] GOLAIT Y S, PADADE A H. Analytical and experimental studies on cemented stone columns for soft clay ground improvement[J]. International Journal of Geomechanics, 2017, 17(4): 0401616100.

[7] GOLAIT Y S, SATYANARAYANA V, RAJU S S V. Concept of under rammed cemented stone column for soft clay ground improvement[C]//Indian Geotechnical Conference. Mumbai, India: [s. n.], 2009: 356−360.

[8] ZHOU C, YIN J H, MING J P. Bearing capacity and settlement of weak fly ash ground improved using lime – fly ash or stone columns[J]. Canadian Geotechnical Journal, 2002, 39(3): 585−596.

[9] CHESNER W H, COLLINS R J, MACKAY M H. User guidelines for byproducts and secondary use materials in pavement construction[M]. McLean, VA: Federal Highway Administration, 2008.

[10] National Asphalt Pavement Association. 9th Annual Asphalt Pavement Industry Survey, IS-138 Appendix B: State-by-State Use of Recycled Materials and Warm-Mix Asphalt In Asphalt Pavement Mixtures[M]. Greenbelt, MD: NAPA, 2019.

[11] BENNERT T, PAPP M, MAHER A, et al. Utilization of construction and demolition debris under traffic-type loading in base and subbase applications[J]. Transportation Research Record: Journal of the Transportation Research Board, 2000, 1714(1): 33−39.

[12] TAHA R, AL-HARTHY A S, AL-SHAMSI K, et al. Cement stabilization of reclaimed asphalt pavement aggregate for road bases and subbases[J]. Journal of Masterials in Civil Engineering, 2002, 14(3): 239−245.

[13] SUEBSUK J, HORPIBULSUK S, SUKSAN A, et al. Strength prediction of cement-stabilised reclaimed asphalt pavement and lateritic soil blends[J]. International Journal of Pavement Engineering, 2017: 332−338.

[14] SUEBSUK J, SUKSAN A, HORPIBULSUK S. Strength assessment of cement treaded soil-reclaimed asphalt pavement (RAP) mixture[J]. International Journal of GEOMATE, 2014, 6(2): 878−884.

[15] GUTHRIE W S, COOLEY D, EGGETT D L. Effects of reclaimed asphalt pavement on mechanical properties of base materials[J]. Journal of the Transportation Research Board, 2007, 2005: 44−52.

[16] Department of Highway. DH-S 205/1989 Strand for of base course aggregate Thailand[S]. Bangkok: Department of Highway, 1989.

[17] HORPIBULSUK S, KATKAN W, SIRILERDWATTANA W, et al. Strength development in cement stabilized low plasticity and coarse grained soils: laboratory and field study[J]. Soils and Foundations, 2006, 46(3): 351−366.

[18] LADD R S. Preparing test specimens using undercompaction[J]. Geotechnical Testing Journal, 1978, 1(1): 16−23.

[19] HEAD K H, EPPS R J. Manual of soil laboratory testing: effective stress tests[M]. Dunbeath: Whittles Publishing, 2014.

[20] ARULRAJAH A, DISFANI M M, HORPIBULSUK S, et al. Physical properties and shear strength responses of recycled construction and demolition materials in unbound pavement base/subbase applications[J]. Construction and Building Materials, 2014, 58: 245−257.

[21] HORPIBULSUK S, MIURA N, BERGADO D T. Undrained shear behavior of cement admixed clay at high water content[J]. Journal of Geotechnical and Geoenvironmental Engineering, 2004, 130(10): 1096−1105.

[22] CLOUGH G W, SITRA N, BACHUS R C. Cemented sand under static loading[J]. Journal of the Geotechnical Engineering Division, 1981, 100(6): 799−817.

[23] SCHNAID F, PRIETTO P D M, CONSOLI N C. Chaeacterization of cemented sand in triaxial compression[J]. Journal of Geotechnical and Geoenvironmental Engineering, 2001, 127(10): 857−868.

[24] COOP M R, ATKINSON J H. The mechanics of cemented carbonate sands[J]. Geotechnique, 1993, 43(1): 53−67.

[25] JANBU N. Soil compressibility as determined by oedometer and triaxial test[C]//Proceedings of European Conference on Soil Mechanics and Foundation Engineering (ECSMFE). Wiesbaden: [s. n.], 1963: 19−25.

[26] SCHNAID F, PRIETTO P D M, CONSOLI N C. Characterization of cemented sand in triaxial compression[J]. Journal of Geotechnical and Geoenvironmental Engineering, 2001, 127(10): 857−868.

[27] CLOUGH G W, SITAR N, BACHUS R C, et al. Cemented sands under static loading[J]. Journal of the Geotechnical Engineering Division, 1981, 107(6): 799−817.

[28] HOY M, HORPIBULSUK S, ARULRAJAH A. Strength development of recycled asphalt pavement – fly ash geopolymer as a road construction material[J]. Construction and Building Materials, 2016, 117: 209−219.

[29] HORPIBULSUK S, LIU M D, LIYANAPATHIRANA D S, et al. Behavior of cemented clay simulated via the theoretical framework of the Structured Cam Clay model[J]. Computers and Geotechnics, 2010, 37: 1−9.

[30] SUEBSUK J, HORPIBULSUK S, LIU M D. Modified structured Cam Clay: a constitutive model for destructured, naturally structured and artificially structured clays[J]. Computers and Geotechnics, 2010, 37: 956−968.

[31] SUEBSUK J, HORPIBULSUK S, LIU M D. A critical state model for overconsolidated structured clays[J]. Computers and Geotechnics, 2011, 38(5): 648−658.

[32] SUEBSUK J, HORPIBULSUK S, LIU M D. Finite element analysis of the non-uniform behavior of structured clay under shear[J]. KSCE Journal of Civil Engineering, 2016, 20(4): 1300−1313.

[33] SUEBSUK J, HORPIBULSUK S, LIU M D. Compression and shear responses of structured clays during subyielding[J]. Geomechanics and Engineering, 2019, 18(2): 121−131.

BIOGRAPHY

Mr. Aniroot Suksan was born in 1989 in Khon Kaen, Thailand. In 2012, he graduated with a bachelor’s degree in Civil engineering from the Rajamangkala University of Technology Isan, Nakhon Ratchasima, Thailand. Two years later he obtained his master’s degree in Civil Engineering from the School of Civil Engineering, Suranaree University of Technology in 2014. Subsequently, he entered a Ph.D. student in Civil Engineering at the School of Civil Engineering, Suranaree University of Technology. During his Ph.D. study, he worked as a research assistant for the Department of Civil Engineering, at Rajamangkala University Isan. Since 2017, he has been a lecturer for the Department of Civil Engineering at Vongchavalitkul University, Nakhon Ratchasima, Thailand. In 2021, he was appointed as the Head of the Department of Civil Engineering, at Voungchawalitkul University.